

*Technical University of Crete*  
*School of Electrical and Computer Engineering*



*Diploma Thesis*

**Optimal Operation Scheduling of Microgrids of Large  
Building Complexes**

*Kyriakou Dimitra*

**EXAMINING COMMITTEE**

Associate Professor Kanellos Fotios (Supervisor)

Professor Stavrakakis Georgios

Associate Professor Koutroulis Eftychios

Chania, Crete, September 2021

## **Acknowledgements**

I would like to express my sincere thanks to my supervisor, Prof. Kanellos Fotios, for assigning me this interesting project, as well as, for his valuable assistance, continuous support and guidance throughout the preparation of my diploma thesis.

I would also like to especially thank my family and friends for their love, support, encouragement and trust.

## **Abstract**

Microgrids constitute a developing area of the energy industry, representing a paradigm shift from centralized power plants to more localized, distributed generation, particularly in cities, communities and campuses. Microgrids provide efficient and low-cost energy, improve the local robustness and the regional electric grid operation and stability. Moreover, plug-in vehicles (PEVs) are expected to play an important role in the operation of electric power systems as electric vehicle technology is rapidly developing.

In this thesis, a method for optimal operation scheduling of microgrids of large building complexes is proposed. It is based on a hierarchical multi-agent system (MAS) comprising a group of large office buildings, considering their thermal and electrical loads, and plug-in electric vehicles (EVs). A significant advantage of the proposed algorithm is that at the time periods of the day that the electric grid is not available, the microgrid is able itself to supply a satisfactory percentage of the buildings' electric power demand exploiting only the hosted PEVs. The main target of the method is to minimize the total operation cost of the microgrid while satisfying at the same time a large number of technical and operation constraints. The examined optimization problem is solved using the particle swarm optimization (PSO) method. The efficiency of the method is proved by detailed simulation results of different operation scenarios, showed that cost savings in range of 27% can be achieved.

## Περίληψη

Τα μικροδίκτυα αποτελούν έναν αναπτυσσόμενο τομέα της ενεργειακής βιομηχανίας, αντιπροσωπεύοντας ένα παράδειγμα απομάκρυνσης από τις κεντρικές μονάδες παραγωγής ηλεκτρικής ενέργειας προς μια πιο τοπική, κατανομημένη παραγωγή, ιδίως σε πόλεις, κοινότητες και πανεπιστήμια. Τα μικροδίκτυα παρέχουν αποδοτική και χαμηλού κόστους ενέργεια, βελτιώνουν την τοπική ευρωστία και τη λειτουργία του περιφερειακού ηλεκτρικού δικτύου. Επιπλέον, τα διασυνδεδεμένα ηλεκτρικά οχήματα (PEVs) αναμένεται να διαδραματίσουν σημαντικό ρόλο στη λειτουργία των συστημάτων ηλεκτρικής ενέργειας, καθώς η τεχνολογία των ηλεκτρικών οχημάτων αναπτύσσεται με ταχείς ρυθμούς.

Στην παρούσα διατριβή προτείνεται μια μέθοδος για τον βέλτιστο προγραμματισμό λειτουργίας μικροδικτύων μεγάλων κτιριακών συγκροτημάτων. Βασίζεται σε ένα ιεραρχικό σύστημα πολλαπλών πρακτόρων (MAS) που περιλαμβάνει μια ομάδα μεγάλων κτιρίων αποτελούμενα από γραφεία, λαμβάνοντας υπόψη τα θερμικά και ηλεκτρικά φορτία τους, καθώς και ηλεκτρικά οχήματα (EVs). Ένα σημαντικό πλεονέκτημα του προτεινόμενου αλγορίθμου είναι ότι στις χρονικές περιόδους της ημέρας που το ηλεκτρικό δίκτυο δεν είναι διαθέσιμο, το μικροδίκτυο είναι σε θέση να καλύπτει το ίδιο ένα ικανοποιητικό ποσοστό της ζήτησης ηλεκτρικής ενέργειας των κτιρίων του με μοναδική μονάδα παραγωγής τα διασυνδεδεμένα ηλεκτρικά οχήματα. Ο βασικός στόχος της μεθόδου είναι η ελαχιστοποίηση του συνολικού κόστους λειτουργίας του μικροδικτύου και η ταυτόχρονη ικανοποίηση ενός μεγάλου αριθμού τεχνικών και λειτουργικών περιορισμών. Το πρόβλημα βελτιστοποίησης που εξετάζεται, επιλύεται με τη χρήση του αλγορίθμου particle swarm optimization (PSO). Η αποτελεσματικότητα της μεθόδου αποδεικνύεται από λεπτομερή αποτελέσματα προσομοίωσης διαφορετικών σεναρίων λειτουργίας, τα οποία έδειξαν ότι μπορεί να επιτευχθεί εξοικονόμηση κόστους της τάξης του 27%.

## Nomenclature

### Abbreviations

EC	Electric Chiller
SoC	State of Charge
EV	Electric Vehicle
MAS	Multi-Agent System
PB	Parking Battery
PMS	Power Management System
EMS	Energy Management System

### Sets and indices

B, b	Set of the building of the microgrid, index indicating the number of the building
P, p	Set of the parking garages of the microgrid, index indicating the number of the parking
k	index indicating the type of electrical devices
nz	symbol denoting neighboring thermal zone
j	denotes the jth thermal zone of the building
z	denotes the number of zones of each floor
f	denotes the total number of building's floors

### Parameters, constants and variables

$N_{people, j}$	Forecasted number of people in the jth building thermal zone
$EP$	The forecasted electricity price
$p_j, C_j, V_j$	the density, specific heat capacity and volume of the air of the jth thermal zone
$T_{in, j}$	indoor temperature set-point (°C) of the jth thermal zone
$T_{out}$	outdoor temperature (°C)
$a_w$	absorbance coefficient of the external surface of the wall
$R_{se}$	the external surface heat resistance for convection and radiation of the external wall
$\tau_{win}$	the glass transmission coefficient of the windows
$SC$	the shading coefficient of the windows
$p_g$	ground reflectance
$\beta_z$	surface slop
$\theta, \theta_z$	incidence, zenith angle, respectively
$U_{wall, y}, U_{win, y}$	heat transfer coefficient of the yth wall/window of the thermal zone
$F_{wall, y}, F_{win, y}$	the area of the total wall/window surface at the yth wall/window orientation
$\dot{Q}_{ex, wall, j}$	heat transfer through the external walls of the jth thermal zone (kW)

$\dot{Q}_{win, j}$	heat transfer across the windows of the jth thermal zone (kW)
$\dot{Q}_{sw, j}$	heat contribution due to the solar radiation on the surface of the external walls of the jth thermal zone (kW)
$\dot{Q}_{sg, j}$	the whole solar radiation transmitted across the windows of the jth thermal zone (kW)
$Q_{EC, j}$	cooling power generated by the EC of the ith thermal zone (kW)
$\dot{Q}_{in, wall, j}$	heat exchange between a thermal zone and its neighboring zones
$Q_{in, j}$	internal heat gains from people, appliances and lighting of the jth thermal zone (kW)
$Q_{j, k}$	heat gains of the kth type of electrical device of the jth thermal zone
$Q_{EC, total}$	total cooling power of the building (kW)
$T_{in, nz}$	indoor temperature of the neighbor thermal zone (°C)
$I_b, I_d, I$	beam, diffuse and total radiation on horizontal surface, respectively
$T_{max, j}, T_{min, j}$	the maximum and minimum values of the indoor temperature set-point of the jth thermal zone (°C)
$P_{parking, max}$	maximum power transfer rate of the equivalent battery of the EV parking lot
$P_{parking, min}$	minimum power transfer rate of the equivalent battery of the EV parking lot
$SoC_{parking, max}$	maximum stored energy (kWh) of the equivalent battery of the EV parking lot
$SoC_{parking, min}$	minimum stored energy (kWh) of the equivalent battery of the EV parking lot
$SoC_{PB}$	SoC of the equivalent battery (kWh) of the EV parking lot
$SoC_{0, parking}$	initial SoC (kWh) of the equivalent battery of the EV parking lot
$SoC_{t, parking}$	target energy (kWh) of the equivalent battery of the EV parking garage
$n_{ch}, n_{disc}$	charging (discharging) efficiency coefficients of the PEV battery
$n_{aut}$	Load percentage that should be supplied by the equivalent battery in autonomous operation.

# Contents

<b>1. INTROUCTION .....</b>	<b>8</b>
1.1. General .....	8
1.2. Thesis Overview .....	8
<b>2. MICROGRID .....</b>	<b>9</b>
2.1. Microgrid Operational Configurations .....	9
2.1.1. Conceptual Configuration for Distribution Systems .....	9
2.1.2. Distributed Generation .....	9
2.2. Benefits of Microgrids .....	11
2.3. Challenges of Microgrids .....	12
2.4. Microgrid Energy Production .....	13
2.5. Microgrid Energy Storage .....	13
2.5.1. Batteries .....	14
2.5.2. Flywheels .....	14
2.5.3. Pumped Hydroelectric Energy Storage .....	14
2.5.4. Fuel Cells-Hydrogen Energy Storage .....	15
2.5.5. Compressed Air Energy Storage Systems .....	15
2.5.6. Ultracapacitors .....	15
2.6. Electric Vehicles .....	15
2.6.1. Benefits of Electric Vehicles .....	15
2.6.2. Types of electric Vehicles .....	16
2.6.3. Operation mode of Electric Vehicles .....	17
2.7. Load Management .....	17
2.8. Microgrid Control .....	18
2.8.1. Centralized Control .....	18
2.8.2. Decentralized Control .....	18
2.8.3. Hierarchical Control .....	19
<b>3. MAS STRUCTURE AND OPERATION .....</b>	<b>20</b>
3.1. Load Agents .....	21
3.2. Optimization Level 1 (Energy Management System 1 – EMS1) .....	21
3.3. Optimization Level 2 (Energy Management System 2 – EMS2) .....	21

<b>4. MICROGRID COMPONENT’S MODELS.....</b>	<b>22</b>
4.1. Model of a Building Thermal Load Agent (TLA) .....	22
4.1.1. Building Thermal Model .....	22
4.1.2. Thermal Zones Power Dispatch.....	26
4.2.3. Discrete Time Building Thermal Model .....	26
4.2. Model of a Building Electrical Load Agent (ELA) .....	27
4.3. Parking Dynamic Aggregated Battery Agent Model (PDABA) .....	28
<b>5. MICROGRID COMPONENT’S MODELS.....</b>	<b>32</b>
5.1. Particle Swarm Optimization Algorithm .....	32
5.2. Optimization Level 1 .....	34
5.3. Optimization Level 2 .....	35
5.4. Algorithm Overview .....	35
<b>6. RESULTS.....</b>	<b>36</b>
6.1. Case Study .....	36
6.2. Scenarios for a 24-hour period .....	46
6.2.1. Scenario I.....	46
6.2.2. Scenario II.....	54
6.2.3. Scenario III .....	57
<b>7. CONCLUSION.....</b>	<b>67</b>
<b>8. REFERENCES .....</b>	<b>68</b>

# 1. INTRODUCTION

---

## 1.1. General

In recent years, the rapid increase in energy consumption by large commercial buildings has immediate negative environmental consequences, such as enormous amounts of greenhouse gases and pollutants emissions from the burning of fossil fuels for power generation. As a result, innovative technologies are required for the development of a smart building energy management system.

Microgrid is a small electrical system consisting of at least one distributed generation, local loads and storage devices. The microgrid concept has shown to be quite effective in utilizing complexes of various types of buildings. Except for the interconnected operation with the power system can also operate autonomously, known as “island mode”. This means that local generation units will be able to serve the local load on their own. Therefore, microgrids should comprise the appropriate algorithms for the control and operation of these units.

Electric Vehicles (EVs) have been experiencing considerable development in recent years. Their increasing penetration promises a challenging future full of new opportunities for the microgrid energy management. The use of current EVs in microgrids is recommended as a way to improve the resilience of microgrids in the face of grid outages without having to spend more money in order types of generation units. In the event of a contingency, under specific conditions, they have the ability to supply energy to islanded microgrids provided that they provided charging facilities enable them for V2G operation.

## 1.2. Thesis Overview

Chapter 2 focuses on the microgrid definition and all microgrid related important information.

Chapter 3 gives a description of the structure and the operation of the proposed energy management system.

Chapter 4 presents the models of the examined microgrid components.

Chapter 5 gives the objective functions and constraints used in the adopted optimization levels, the optimization method exploited to solve the examined optimization problems and finally the overview proposed algorithm.

Chapter 6 presents the results obtained by the simulation of different operation scenarios and analyses them.

Chapter 7 gives general conclusions derived from the obtained results and some aspects for the future expansion of the present work.

## **2. MICROGRID**

---

### **2.1. Microgrid Operational Configurations**

#### **2.1.1. Conceptual Configuration for Distribution Systems**

Electrical utility distribution systems can be categorized into three types: centralized, decentralized, and distributed. A simple connection of nodes to a central source of electricity production defines a centralized system. This is prevalent in utility configurations where the electricity produced by central power plants is delivered directly to individual users via transmission links. Multiple generator units in the central power plants ensure that power is available at all times e.g. the reliability of the system is increased. However, if the configuration at the central station fails, the entire system may fail.

In a decentralized design, multiple spatially dispersed points of electrical generation are connected to their loads a number of remote stations. Decentralized systems offer a higher level of robustness than centralized systems.

In a web-like structure, distributed configurations provide both generation and loads at each node and are linked to all other generation and load points. Because a failure at any station or link may be handled by rerouting transmission to assure reliability, distributed networks are the most resilient. Decentralized or distributed network architectures are common in microgrids. When single transmission pathways or specific nodes are compromised, distributed configurations are the most resilient.

The centralized and the distributed generation are presented in the following figure and some additional information is provided in the following paragraph.

#### **2.1.2. Distributed Generation**

The "distributed generation" (DG) term generally refers to the production of electricity near the consumption. Combined heat and power or cogeneration (CHP) units and renewable energy sources (RES) are among the most widespread distributed generation resources. Renewable energy is energy produced from natural resources such as wind, sunlight, tides, waves, geothermal heat and biomass. DGs can be used in an isolated way, supplying the consumer's local demand, or integrated into the grid supplying energy to the electric power system, or a combination of these. These generating units are generally connected to the power systems at the low voltage distribution level.

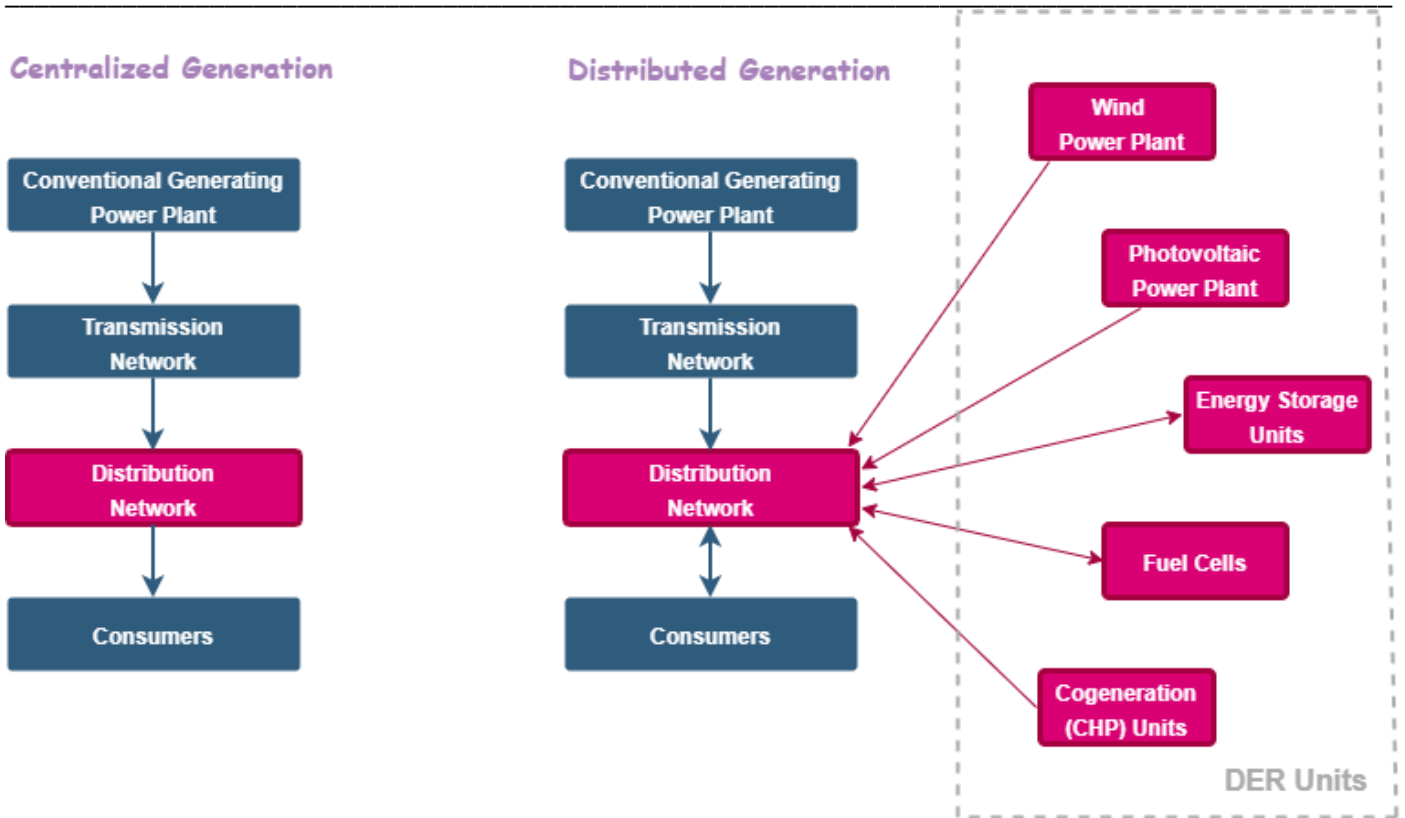


Fig. 1. A unidirectional centralized (left) and a bidirectional distributed (right) generation system

Distributed generation is characterized by some features which are not present in centralized systems:

- the power generated is relatively small and has variations dependent on the availability and variability of primary energy source
- the power flow is bidirectional, in comparison with the central generation system where the power flow is unidirectional
- location in the network area dependent of the presence of the primary energy source.

Distributed generation is the key to meet growing power demand, provide benefits to consumer by improving the quality of life, relieves utility to supply additional loads and opens the opportunities for power trading in a competitive environment. They can play an important role in:

- reducing the transmission losses
- improving the power quality
- improving the reliability of the grid
- providing better voltage support
- reducing the greenhouse emissions

The major obstacle for the distributed generation has been the need to control a large number of dispersed energy sources and loads. This problem is mainly solved through microgrids and advanced control techniques and supervisory systems.

## **2.2. Benefits of Microgrids**

Microgrids are a continuously growing sector of the energy industry, representing a paradigm shift from remote central station power plants toward more localized, distributed generation—especially in cities, communities and campuses. Their capability to isolate from the larger grid makes microgrids resilient while their ability to conduct flexible, parallel operations makes the grid more competitive.

By “islanding” from the grid in emergencies, a microgrid can both continue serving its load when the grid is down and serve its surrounding community by providing a platform to support critical services—allowing safe and reliable operation in a wide extend of activities and services.

Microgrids have several benefits to the environment, to utility operators, and to customers [15].

- Microgrids offer the opportunity to deploy more zero-emission electricity sources, thereby reducing greenhouse gas emissions. The microgrid manager (e.g., local energy management system) can balance generation from non-controllable renewable power sources, such as solar, with distributed, controllable generation, such as natural gas-fueled combustion turbines. They can also use energy storage and the batteries of electric vehicles to balance power production and consumption within the microgrid.
- Microgrids can make use of on-site energy that would otherwise be lost through transmission lines and heat that would otherwise be lost on pipes. When power has to travel long distances (e.g., from a centralized power station), electrical line losses occur, requiring additional generation to ensure that the distant demand is met. Since microgrid electricity is generated next to where it will be used (also known as distributed generation), line losses are minimized and less power is required to meet the same level of demand while system stability is enhanced. Also, when electricity is generated from certain centralized power sources (e.g., fossil fuels and nuclear power) a great amount of heat energy is created and typically released – unused – into the atmosphere. When power is generated close to the end users, it becomes economically feasible to use this heat energy productively, such as heating water or space in nearby homes and businesses, reducing greenhouse gas emissions.
- Microgrids can improve local management of power supply and demand, which can help defer costly investments by utilities in new power generation. When sited strategically within the electricity system, microgrids help reduce or manage electricity demand and alleviate grid congestion, thereby lowering electricity prices and reducing peak power requirements. In this manner, microgrids may support system reliability, improve system efficiency, and help delay or avoid investment in new electric capacity (e.g., “peaker” plants, substations, transmission lines, energy storage or other infrastructure). When connected to the local distribution network or transmission system, microgrids can also export excess electricity or import imbalances from the surrounding system from a single node.

- Microgrids can enhance grid resilience to more extreme weather or cyber-attacks. Microgrids can continuously power individual buildings, neighborhoods, or entire cities, even if the surrounding macrogrid suffers an outage. This concept of a microgrid functioning independently from the surrounding system is known as islanding. Microgrids can also help the macrogrid recover from a system outage, either indirectly, by sustaining services needed by restoration crews, or directly, by helping to re-energize the grid.

### **2.3. Challenges of Microgrids**

Irrespective of their numerous advantages, implementing microgrids faces serious challenges not only on a federal and state level, but also on a technological level. On a federal level, we have microgrids contributing to distributed systems that provide power on a wholesale basis. Microgrids have the ability to provide multiple benefits like load abating and resource provision. However, market regulations do not allow for such multiple utilities [14].

Technological challenges faced in the operation and deployment of microgrids are mentioned below.

- The fault current in microgrids can be much higher than those faced in distributed systems. It can severely affect protection methods and damage safety devices. This is a major concern during island operation. Blindly implementing microgrids on feeders without careful analysis of the various protective measures can lead to serious damages to the grid.
- Issues during start-up of island mode- During the initial stages of island mode start-up can cause a sudden intake of current which can affect the frequency of the system and voltages. This can cause the generators to trip and go offline during the initial phase. In order to combat this, an analysis is needed on energy generation control methods during island mode and specialized controls need to be developed.
- Balancing between generation and load in island mode- This is one of the most common challenges faced by microgrids. The balance between load and power generation needs to be constantly maintained. Sudden or large change in loads can introduce instability into the island system.

## 2.4. Microgrid Energy Production

Microgrids generate electricity using distributed energy resources. Electrical generation and storage systems are combined in DERs, which can be deployed in a large number of units. Distributed fossil-fuel generators, batteries, and renewable resources such as solar panels and wind turbine generators can all be used to power microgrids. It's worth noting that when batteries are discharging, the system perceives them as a source of power generation.

Microgeneration is the local distribution of power generated by residences and small businesses. Despite the granularity of the generation, the contribution from microgeneration sources has a significant impact. The option to choose from a variety of generation sources, usually in complementing combinations, is a benefit of microgrid architecture. The aim is to maximize electricity generation depending on available resources, efficiency, and costs.

In a microgrid, it is essential to maintain the power supply-demand balance because the generation of the intermittent distributed sources such as photovoltaic and wind turbines is difficult to be predicted and their generation may fluctuate significantly depending on the availability of the primary sources (solar irradiation and wind). The supply-demand balancing problem becomes even more important when the microgrid is operating in island mode where only limited supply is available to balance the demand [17].

## 2.5. Microgrid Energy Storage

Storage units have a very important role in microgrids, especially in their autonomous operation, since they can substitute the generation units or regulate the loads. Energy can be stored either directly or indirectly, as shown in the following diagram. Energy storage technologies that are suitable for microgrids are batteries, flywheels and hydrogen storage technologies.

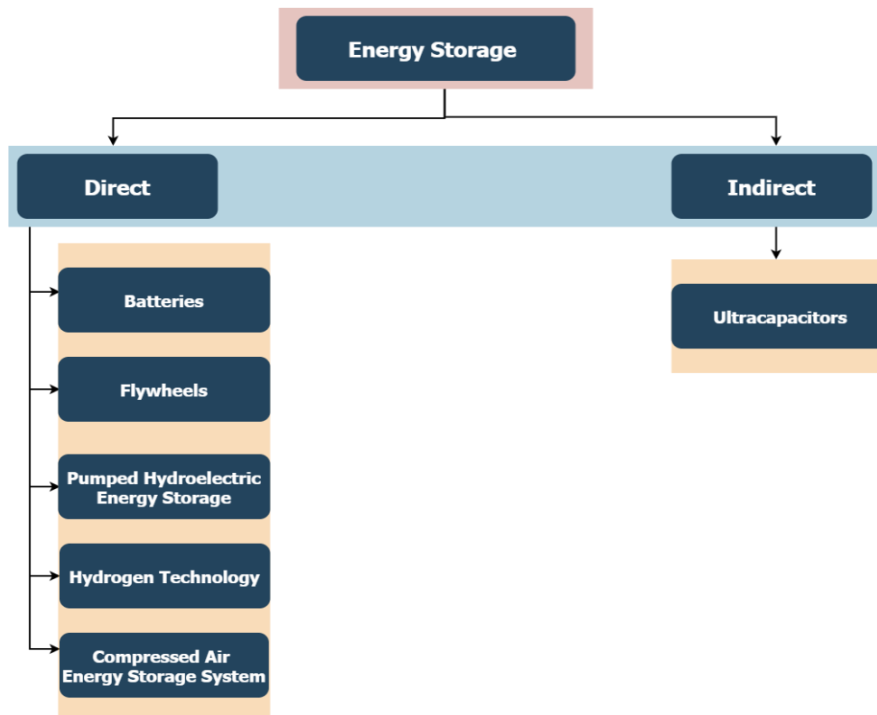


Fig. 2. Classification of Storage Units

### 2.5.1. Batteries

Batteries are devices that store electricity in electrochemical form. Nowadays, there is a wide variety of rechargeable batteries available commercially and many more under design. The most prominent types are mentioned below.

- **Lithium-Ion**

A Lithium-Ion (Li-Ion) battery is an advanced battery technology that uses lithium ions as a key component of its electrochemistry. These batteries have one of the highest energy densities of any battery technology today. Li-ion batteries have no memory effect, a detrimental process where repeated partial discharge/charge cycles can cause a battery to ‘remember’ a lower capacity. Li-Ion batteries have displaced Ni-Cd batteries as the market leader in portable electronic devices, such as smartphones and laptops [9].

- **Lead-Acid**

Lead-Acid batteries have the distinct benefit of being the most widely utilized type of battery for the most rechargeable battery application, such as starting vehicle engines. Despite their low energy density, moderate efficiency and high maintenance requirements, lead-acid batteries have a long lifetime and low costs when compared to other battery types [10].

- **Flow Batteries**

A flow battery is a rechargeable battery in which electrolyte flows through one or more electrochemical cells from one or more tanks. With a simple flow battery, it is straightforward to increase the energy storage capacity by increasing the quantity of electrolyte stored in the tanks. Flow batteries have been installed in several places for a wide range of applications. They are a reliable, low cost and an environmentally friendly method for electrical energy storage. [11].

### 2.5.2. Flywheels

They are rapidly rotating disks or cylinders used to store kinetic energy, which is easily converted into electrical energy by coupling them to a generator. It is an expensive, very efficient and flexible technology.

### 2.5.3. Pumped Hydroelectric Energy Storage

It is a widespread large-scale energy storage technique. It consists of two large tanks, which are located at points with a significant difference in altitude, and a pump and hydro turbine arrangement. During the period of low electricity consumption, water is pumped from the lower to the upper tank, where it is stored until needed. During periods of high demand, water from the upper tank is released through the pipes and flows into the hydro turbine, so that it works like a classic hydroelectric project, generating energy.

## 2.5.4. Fuel Cells – Hydrogen Energy Storage

A fuel cell uses the chemical energy of hydrogen to cleanly and efficiently produce electricity. Fuel cells can be used in a wide range of applications, providing power for applications across multiple sectors, including transportation, industrial/commercial/residential buildings, and long-term energy storage for the grid in reversible systems. Fuel cells have several benefits over conventional combustion-based technologies currently used in many power plants and vehicles. Fuel cells can operate at higher efficiencies than combustion engines and can convert the chemical energy in the fuel directly to electrical energy with efficiencies capable of exceeding 60%. Fuel cells have lower or zero emissions compared to combustion engines [12].

## 2.5.5. Compressed Air Energy Storage System

Energy is stored with the form of compressed air. Compressed air is used to rotate turbines that are the prime movers of electric generators.

## 2.5.6. Ultracapacitors

Ultracapacitors, or supercapacitors as they are also known, are an energy storage technology that offers high power density, almost instant charging and discharging, high reliability, and very long lifetimes. Ultracapacitors are now delivering significant economic benefits across a wide range of markets including automotive, grid and renewables, transportation and industrial applications [13].

## 2.6. Electric Vehicles

In recent times, Electric Vehicles (EVs) are rapidly increasing around the world, mainly, due to the fact that they have significant advantages in environmental protection. Therefore, electric vehicles present new opportunities and challenges to the operation of the electric power systems.

### 2.6.1. Benefits of Electric Vehicles

The most significant advantages of EVs are the following [5],[8]:

- Reduce car emissions to help the environment: Carbon dioxide emissions from traditional vehicles contribute to greenhouse gases in the atmosphere and accelerate climate change. All electric vehicles do not release carbon dioxide into the atmosphere and hybrid electric cars use their battery to greatly improve the maximum covered distance with a gasoline-powered engine ensuring higher efficiency and lower emissions than conventional vehicles. Electric Vehicles can be fueled by electricity from renewable sources, such as wind, hydropower and solar. They are also built to be more environmentally friendly than conventional vehicles, as the large battery inside the electric car can be recycled.
- Electric motors are more efficient and have a much better response than conventional motors.

- Lower operating and maintenance costs: Any type of fully electrically powered vehicle has a significant difference on the consumption cost compared to the cost of any gasoline or diesel car. Not only electricity is less expensive than gasoline but it is also much more, meaning that rapid fuel price swings are all but eliminated by going electric. Moreover, conventional engines require expensive maintenance over their lifetimes, while electric vehicles do not.
- Reduction of noise caused by the traffic, since the electric vehicles’ motor running is significantly quieter, thanks to the missing exhaust.

### 2.6.2. Types of Electric Vehicles

The term “electric vehicle” actually includes three types of electric cars. Each type of vehicle has its advantages and disadvantages regarding range, emissions and affordability [7]. The types of EVs are:

#### 1. Hybrid Electric Vehicles (HEVs)

They are powered by both gasoline/diesel and electricity. The vehicle alternates between the two to maximize efficiency. They contain a fuel tank and a classic engine along with an electric battery and motor. The battery is only recharged by the conventional engine and by the energy generated when decelerating and braking (regenerative braking).

#### 2. Plug-In Hybrid Electric Vehicles (PHEVs)

Versatile hybrids in which the electric battery can be recharged both by the electricity grid and by the combustion engine. They are similar to HEVs with the difference being that they are mostly powered by electricity instead of classic fuel. Like hybrids, PHEVs offer greater range than fully electric vehicles.

#### 3. Battery Electric Vehicles (BEVs)

Also known as “plug-in” electric vehicles, they exclusively use battery power, which needs to be recharged by connecting to the electricity grid or by a process known as regenerative braking in which the car’s motor slows down the vehicle to recover energy. They do not emit pollutants and are ideal for short urban journeys.

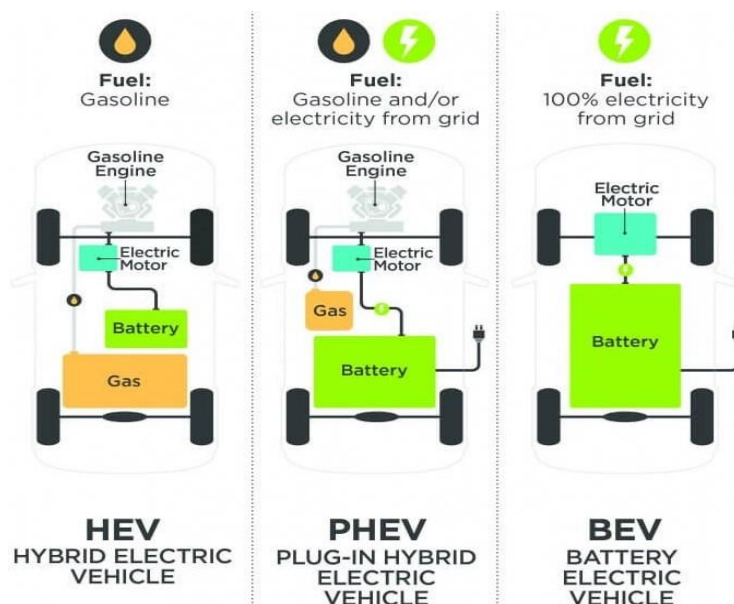


Fig. 3. The three types of Electric Vehicles [7]

### 2.6.3. Operation mode of Electric Vehicles

The charging points of the parking lot considered in this study are able to provide bidirectional power flow which comprises two operation modes.

- Grid to Vehicle (G2V) operation mode

PEV draws power from the network and charges its battery packs. The power drawn from the network can be appropriately adjusted according to electricity price and loading of the network.

- Vehicle to Grid (V2G) operation mode

PEV injects power to the network. Hence, the electricity can be transferred from the PEV batteries back to the grid at periods that transmission system is overloaded or electricity price is high.

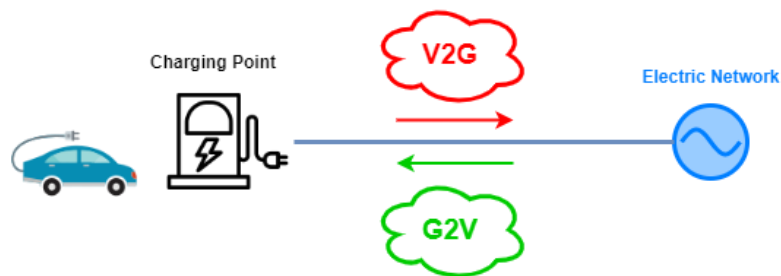


Fig. 4. V2G and G2V operation mode of Electric Vehicles

## 2.7. Load Management

Depending on the amount of electricity required and their operation characteristics and constraints, loads can be classified into groups. Sensitive, adjustable and shedable are the most typical classifications.

### a) Sensitive Loads

Sensitive loads consist of all devices that must operate continuously without fail, hence the nominal power has always to be guaranteed. These might include elevators, emergency lighting, computers and TVs. It is assumed that the algorithm does not have any control on these loads.

### b) Adjustable Loads

Adjustable loads can operate at lower power levels than their nominal power. These loads can reduce their power consumption during peak periods due to high energy prices. Examples include mainly Heating, Ventilation and Air Conditioning (HVAC).

### c) Shedable / Shiftable Loads

Shedable and shiftable loads are those whose power consumption can be shed or shifted to a different time slot so that they can use electricity in the appropriate electricity price time period. The microgrid can shift this load from the peak period of power consumption to another period, thereby reducing the operation cost. This type of loads might include kitchen equipment, interior lighting, washing machines etc.

## 2.8. Microgrid Control

Energy management in Microgrid systems must be done properly in order to improve the system's overall efficiency, reduce the cost of the electricity, and lengthen the life of its components (e.g., converters, batteries, fuel cells). The exploited control strategies can be classified into three main categories: Centralized, decentralized, and hierarchal control. These control strategies are presented in the rest of this paragraph [18].

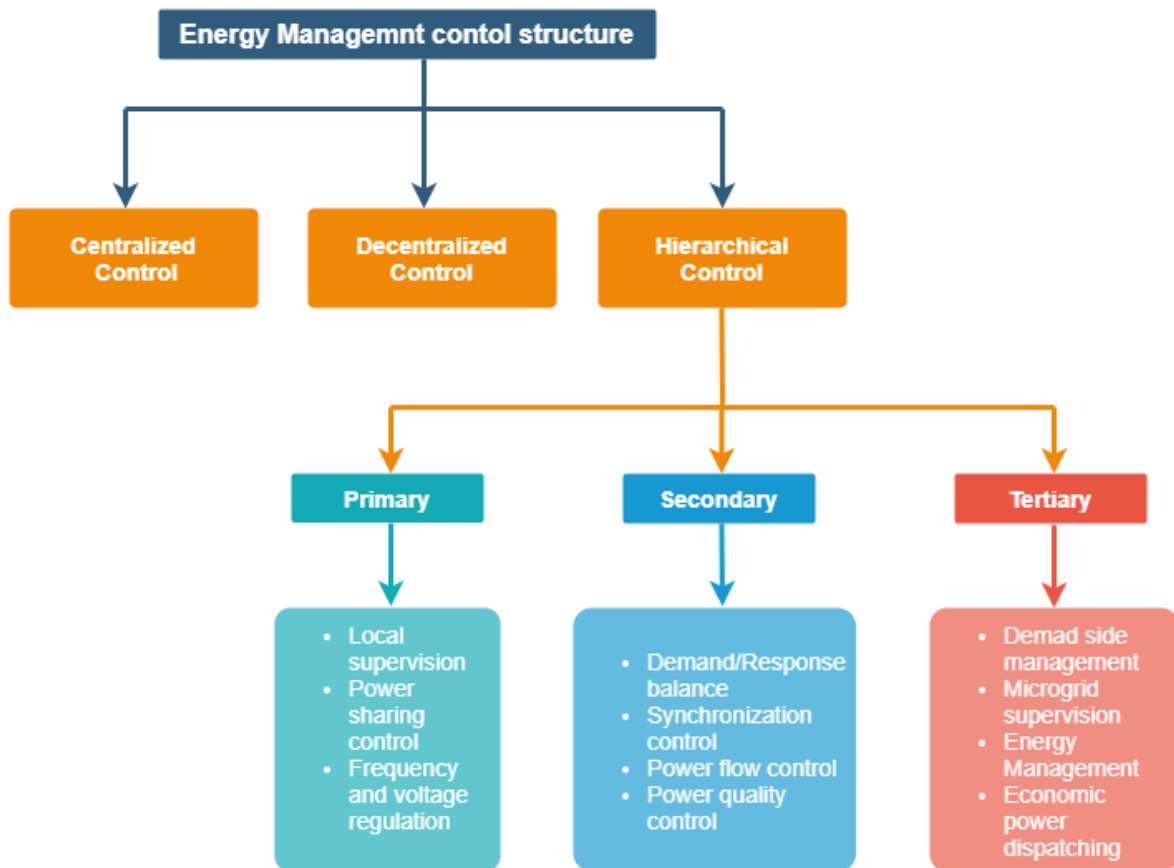


Fig. 5. Control structure for energy management in microgrid systems

### 2.8.1. Centralized Control

In order to manage different entities of the system, centralized control approaches use a single central controller, which is characterized by a high-performance processing unit and a secure communication architecture. To communicate and interact directly with the central controller, each entity needs a local controller. Furthermore, the central control may monitor, gather and analyze real-time data using contemporary communication and computing technologies. This enables all entities to collaborate with the central controller while maintaining microgrid's operation flexibility in both grid-connected and island mode. The central controller gathers data such as RES energy production, energy consumption patterns, market operator energy prices, and weather conditions, and then implements the most optimal and efficient system control.

## 2.8.2. Decentralized Control

Unlike centralized strategies, decentralized control considers each entity autonomous with the use of a local controller. This signifies that a leader is in charge of various groupings of entities. The phrases "decentralized" and "distributed controls" are often used in place of each other in the literature. The distributed control can be considered as a decentralized control in which local controllers use local measurements, such as frequency and voltage values. They are also allowed to share information with neighbors. For a distributed control, local controllers do not only use local measurements but also are able to send and receive required information to other local controllers. Limited local connections are necessary in decentralized control approaches, and control decisions are based only on local measurements.

## 2.8.3. Hierarchical Control

A compromise between the fully centralized and decentralized control structures is realized by providing hierarchical control structures according to three control levels: Primary, secondary, and tertiary.

### 1) Primary Control

The primary control level stabilizes the voltage and frequency generated from each source in order to satisfy the limits required by the standards. Moreover, the active and reactive power is divided. In addition, the primary control level detects the operating mode of the microgrid, offering the ability to operate in grid-connected and island modes.

### 2) Secondary Control

In secondary control level, the microgrid voltage and frequency are restored after system's load variation and the changes introduced by renewable energy sources are offset. The aim is to ensure and enhance the power quality within the limits required by the standards, allowing the synchronization between the microgrid systems and the main electrical network.

### 3) Tertiary Control

In tertiary control, optimal operation scheduling of the operation of the microgrid over a given time horizon takes place. In addition, the cost of operating the system is minimized, taking into account load forecasts, renewable energy production and the price of electricity.

### 3. MAS STRUCTURE AND OPERATION

The structure of the microgrid examined in this paper is shown in Fig. 6. It includes a group of large office buildings, considering their thermal and electrical loads, and a cluster of EVs plugged in the charging points of the parking lots. In the microgrid, the electricity supplier is the external power grid.

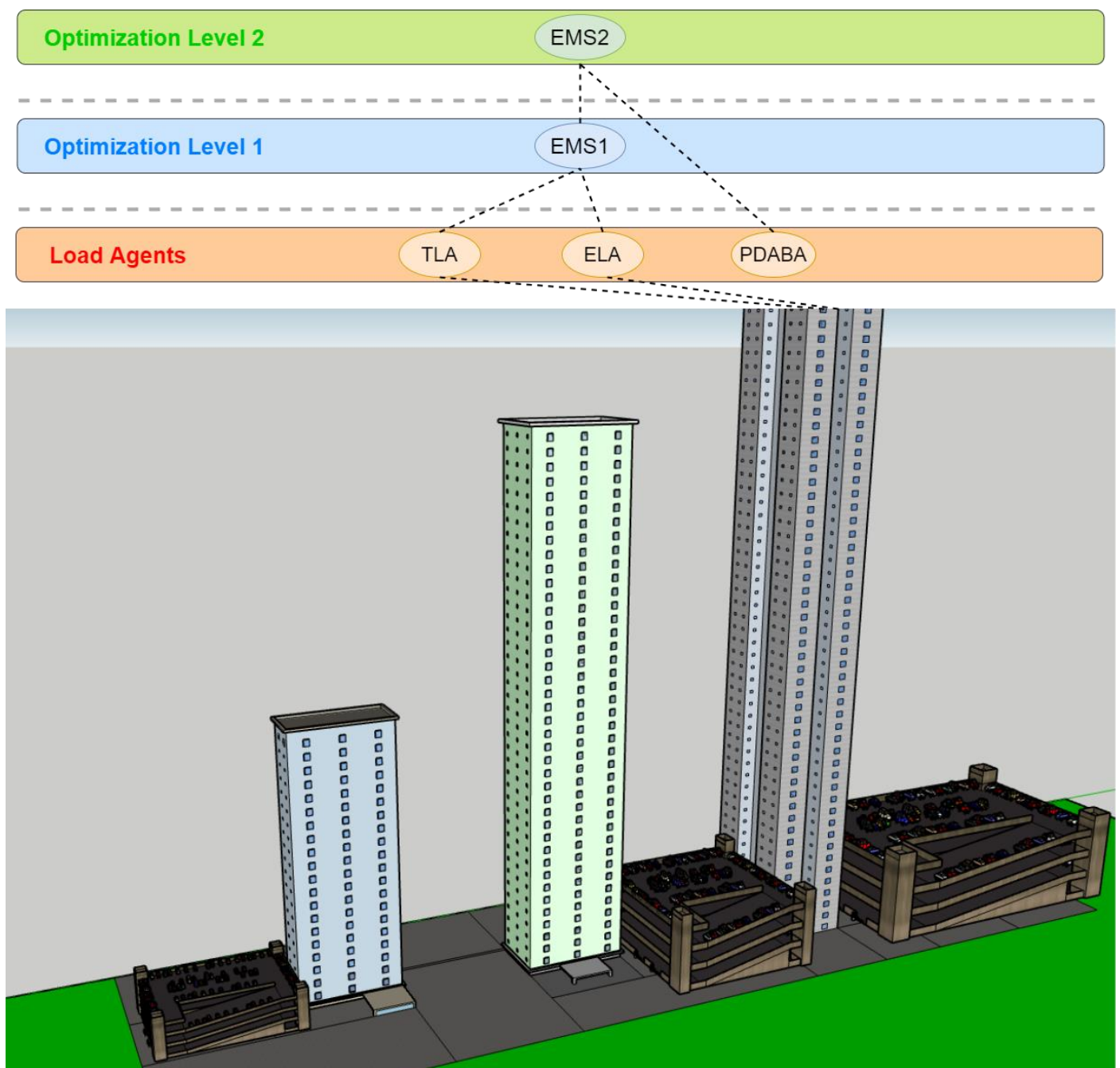


Fig. 6. Configuration of the proposed Microgrid management system

The proposed hierarchical MAS for the optimal operation scheduling of microgrids of large building complexes is shown in Fig. 6. It consists of different types of agents which are briefly described next, whereas their mathematical models are given in Chapter 4 [1].

### **3.1. Load Agents**

Thermal Load Agent (TLA), Electrical Load Agent (ELA) and Parking Dynamic Aggregated Battery Agent (PDABA) are included in the category of Load Agents. TLA and ELA aim to estimate the thermal and electrical loads of the microgrid's buildings, regarding the forecasted work schedule and activity of the people present in each thermal zone. The PDABA develops a dynamic equivalent battery model for the cluster of PEVs hosted by the charging points of the parking lots. The proposed model requires data like EV arrival/dwell times and their technical characteristics. These quantities are estimated using the probability density functions (PDFs) [6]. It is a necessary requirement to ensure that each PEV will reach the target energy the driver has defined at its disconnection time without violating any constraint of the PEVs and the distribution network. Despite the fact that PDABA is considered as a load agent i.e., PEVs absorb power from the network and charge their battery packs, they also have the ability to operate in V2G mode i.e., they inject power to the grid in specific time periods.

### **3.2. Optimization Level 1 (Energy Management System 1 – EMS1)**

It determines the optimal operation of each building thermal zone HVAC systems, as well as the buildings' electrical systems within the optimization period. Building specifications, conditioned space (outdoor temperature, solar radiation, occupancy, activity level, various types of appliances used) and the electricity price forecasts are considered. Specifically, EMS1 provides the optimal electric power demand of the HVAC systems and it optimally shifts the non-critical electrical loads with the purpose of minimizing their use during peak demand. The main goal of EMS1 is to minimize the total daily energy cost, while satisfying all the operational and technical characteristics of the system e.g., maintaining a certain thermal comfort for the occupants of each thermal zone of the building during the day and enforcing the electric power demand to be between its minimum and maximum values.

### **3.3. Optimization Level 2 (Energy Management System 2 – EMS2)**

It performs the second stage of the optimization process. It estimates the optimal scheduling of the power exchanged by the cluster of PEVs with the electric network based on the forecasted electricity price. The primary goal of the proposed optimization strategy is to minimize the daily microgrid operation cost with satisfying all the constraints of the PEVs and the distribution network.

## 4. MICROGRID COMPONENT'S MODELS

---

### 4.1. Model of a Building Thermal Load Agent (TLA)

#### 4.1.1. Building Thermal Model

In this work, each building is divided in thermal zones. The definition of zones is the division of the heating and cooling systems of a building into the sections that allow independent control of temperatures from one area to another.

Using the following thermal equilibrium equation, a mathematical relationship between the interior temperature set-point, cooling demand, and external temperature is developed to analyze the thermal performance of each thermal zone [2].

$$p_j \cdot C_j \cdot V_j \cdot \frac{dT_{in,j}}{dt} = \dot{Q}_{ex,wall,j} + \dot{Q}_{in,wall,j} + \dot{Q}_{win,j} + Q_{in,j} + \dot{Q}_{sw,j} + \dot{Q}_{sg,j} - Q_{EC,j} \quad (1)$$

The heat exchange between a thermal zone and its outdoor environment is described by the Eqs. (2)-(5).

$$\dot{Q}_{ex,wall,j} = \sum_y U_{wall,y} \cdot F_{wall,y} \cdot (T_{out} - T_{in,j}) \quad (2)$$

$$\dot{Q}_{win,j} = \sum_y U_{win,y} \cdot F_{win,y} \cdot (T_{out} - T_{in,j}) \quad (3)$$

$$\dot{Q}_{sw,j} = \sum_y a_w \cdot R_{se} \cdot U_{wall,y} \cdot F_{wall,y} \cdot I_{T,j} \quad (4)$$

$$\dot{Q}_{sg,j} = \sum_y \tau_{win} \cdot SC \cdot F_{win,y} \cdot I_{T,j} \quad (5)$$

Eq. (6) estimates the heat exchange between a thermal zone and its neighboring zones.

$$\dot{Q}_{in,wall,j} = \sum_y U_{wall,y} \cdot F_{wall,y} \cdot (T_{in,nz} - T_{in,j}) \quad (6)$$

By appropriately modifying the equations (1)-(6) and considering as output the internal temperature of each thermal zone, a system for the building thermal performance of the following form is obtained. We assume that there is no heat transfer from one floor to another due to insulation.

$$\frac{dT_{in,j}(t)}{dt} = A_b \cdot T_{in,j}(t) + B_b \cdot U \quad (7)$$

$$T_{in,j}(t) = C_b \cdot T_{in,j}(t) + D_b \cdot U \quad (8)$$

Initially, the tables  $A_1, B_1, C_1, D_1$  corresponding to the first floor of the building are constructed as in the following.

$$A_{1(z \times z)} = \begin{bmatrix} A_{1,1} & A_{1,2} & \cdots & A_{1,z} \\ A_{2,1} & A_{2,2} & \cdots & A_{2,z} \\ \vdots & \vdots & \ddots & \vdots \\ A_{z,1} & A_{z,2} & \cdots & A_{z,z} \end{bmatrix} \quad (9)$$

$$B_{1(z \times (2 \cdot z + 2))} = \frac{1}{p_z \cdot C_z \cdot V_z} \cdot \begin{bmatrix} -1 & 0 & \cdots & 0 \\ 0 & -1 & \cdots & 0 \\ \vdots & \vdots & \ddots & \vdots \\ 0 & \cdots & \cdots & -1 \\ B_{ex,w} & B_{ex,w} & B_{ex,w} & B_{ex,w} \\ 1 & 0 & \cdots & 0 \\ 0 & 1 & \cdots & 0 \\ \vdots & \vdots & \ddots & \vdots \\ 0 & \cdots & \cdots & 1 \\ B_{rad} & B_{rad} & B_{rad} & B_{rad} \end{bmatrix} \quad (10)$$

$$C_{1(z \times z)} = \begin{bmatrix} 1 & & & \\ & 1 & & \\ & & \ddots & \\ & & & 1 \end{bmatrix} \quad (11)$$

$$D_{1(z \times z)} = \begin{bmatrix} 0 & 0 & \cdots & 0 \\ 0 & 0 & \cdots & 0 \\ \vdots & \vdots & \ddots & \vdots \\ 0 & \cdots & \cdots & 0 \end{bmatrix} \quad (12)$$

The following equation applies to the diagonal elements of the matrix  $A_1$ .

$$A_{j,j} = - \sum_y U_{wall,y} \cdot F_{wall,y} - \frac{1}{p_z \cdot C_z \cdot V_z} \cdot \sum_y U_{win,y} \cdot F_{win,y} \quad (13)$$

For the remaining elements of the matrix  $A_1$ , the following equation applies:

$$A_{j,i} = \begin{cases} \frac{1}{p_z \cdot C_z \cdot V_z} \cdot U_{wall,y} \cdot F_{wall,y}, & j, i \in N_z \\ 0, & j, i \notin N_z \end{cases} \quad (14)$$

The following are the equations that calculate the elements  $B_{ex,w}$  and  $B_{rad}$  of matrix  $B_1$ .

$$B_{ex,w} = \sum_y U_{wall,y} \cdot F_{wall,y} + \sum_y U_{win,y} \cdot F_{win,y} \quad (15)$$

$$B_{rad} = \sum_y a_w \cdot R_{se} \cdot U_{wall,y} \cdot F_{wall,y} + \sum_y \tau_{win} \cdot SC \cdot F_{win,y} \quad (16)$$

Let assume that the tables  $A_1 \dots A_f, B_1 \dots B_f, C_1 \dots C_f, D_1 \dots D_f$  corresponding to the 1<sup>st</sup>...f<sup>th</sup> floor of the building, respectively. Then the respective tables  $A_b, B_b, C_b, D_b$  of the building are calculated as it follows.

$$A_{b_{(f \cdot z) \times (f \cdot z)}} = \begin{bmatrix} A_{1(z \times z)} & 0_{(z \times z)} & \dots & 0_{(z \times z)} \\ 0_{(z \times z)} & A_{2(z \times z)} & \dots & \vdots \\ \vdots & \vdots & \ddots & 0_{(z \times z)} \\ 0_{(z \times z)} & \dots & \dots & A_{f \times z(z \times z)} \end{bmatrix} \quad (17)$$

$$B_{b_{(f \cdot z) \times (2 \cdot z + 2)}} = \begin{bmatrix} B_{1(z \times (2 \cdot z + 2))} \\ B_{2(z \times (2 \cdot z + 2))} \\ \vdots \\ B_{f(z \times (2 \cdot z + 2))} \end{bmatrix} \quad (18)$$

$$C_b_{(f \cdot z) \times (f \cdot z)} = \begin{bmatrix} 1 & & & \\ & 1 & & \\ & & \ddots & \\ & & & 1 \end{bmatrix} \quad (19)$$

$$D_b_{(f \cdot z) \times (f \cdot z)} = \begin{bmatrix} 0 & 0 & \dots & 0 \\ 0 & 0 & \dots & 0 \\ \vdots & \vdots & \ddots & \vdots \\ 0 & \dots & \dots & 0 \end{bmatrix} \quad (20)$$

The input vector  $U$  is given below.

$$U = \begin{bmatrix} Q_{EC,1}(t) \\ \vdots \\ Q_{EC,f \times z}(t) \\ T_{out}(t) \\ Q_{in,1}(t) \\ \vdots \\ Q_{in,f \times z}(t) \\ I_T(t) \end{bmatrix} \quad (21)$$

with

$$Q_{in,j} = N_{people,j} \cdot \sum_k Q_{j,k} \quad (22)$$

$$I_{T,j} = I_b \cdot R_b + I_d \cdot \left( \frac{1 + \cos\beta_z}{2} \right) + I \cdot p_g \cdot \left( \frac{1 - \cos\beta_z}{2} \right) \quad (23)$$

$$\underline{P}_{EC,total} \leq P_{EC,total}(t) \leq \overline{P}_{EC,total} \quad (24)$$

$$R_b = \frac{\cos\theta}{\cos\theta_z} \quad (25)$$

### 4.1.2. Thermal Zones Power Dispatch

Considering a summer cooling scenario, we assume that the thermal power required to be provided to the  $j$  thermal zone of the building is as follows.

$$Q_{EC,j}(t) = \frac{T_{in,j}(t) - T_{min,j}}{T_{max,j} - T_{min,j}} \cdot Q'(t) \cdot V_j \quad (26)$$

Furthermore, the sum of the thermal power of all thermal zones should be equal to the total thermal power of the building according to the following equation.

$$\sum_j Q_{EC,j}(t) = Q_{EC,total}(t) \Rightarrow \sum_j \left\{ \frac{T_{in,j}(t) - T_{min,j}}{T_{max,j} - T_{min,j}} \cdot Q'(t) \cdot V_j \right\} = Q_{EC,total}(t) \Rightarrow$$

$$Q'(t) = \frac{Q_{EC,total}(t)}{\sum_j \left\{ \frac{T_{in,j}(t) - T_{min,j}}{T_{max,j} - T_{min,j}} \cdot V_j \right\}} \quad (27)$$

According to equations (26)-(27), the thermal model dispatch is implemented, and the thermal power required to be provided to each thermal zone is a function of the total thermal power of the building, thermal zone volume and its internal temperature as described in the Eq. (28).

$$Q_{EC,j}(t) = \frac{\frac{T_{in,j}(t) - T_{min,j}}{T_{max,j} - T_{min,j}} \cdot V_j}{\sum_j \left\{ \frac{T_{in,j}(t) - T_{min,j}}{T_{max,j} - T_{min,j}} \cdot V_j \right\}} \cdot Q_{EC,total}(t) \quad (28)$$

Constraint (29) enforces the temperature of each zone to be between its minimum and maximum allowed values.

$$T_{min,j} \leq T_{in,j}(t) \leq T_{max,j} \quad (29)$$

### 4.1.3. Discrete Time Building Thermal Model

Finally, the system of continue time equations (7-8) is transformed to discrete time equations, with  $\Delta t$  time step, as in the following.

$$T_{in,j}(k + 1) = A_{b,d} \cdot T_{in,j}(k) + B_{b,d} \cdot U(k) \quad (30)$$

$$T_{in,j}(k) = C_{b,d} \cdot T_{in,j}(k) + D_{b,d} \cdot U(k) \quad (31)$$

## 4.2. Model of a Building Electrical Load Agent (ELA)

There are different types of electrical loads in each thermal zone of the building. The classification of the loads is helpful for energy management and dispatch. Specifically, buildings comprise critical and non-critical loads. Critical loads consist of devices, such as lighting, personal computers, TVs, whose power consumption cannot be modified. Non-critical loads are comprised of devices, such as washing machines, that have a certain flexibility to shift their electricity consumption into different time slots of the day.

The power consumed by the electrical loads of the  $j^{\text{th}}$  building thermal zone is calculated taking into account the forecasted number of people and each type of device they use, as it follows:

$$P_{el\_load,j} = N_{people,j} \cdot \sum_k P_{j,k} \quad (32)$$

The total electric power consumption of the building is calculated as in the following:

$$P_{el,b} = \sum_j P_{el\_load,j} \quad (33)$$

In this work it is considered that the electrical power consumption of non-critical loads constitutes a fixed percentage ( $n_{non\_cr}$ ) of the total power consumed by the electrical loads of the building as it follows.

$$P_{non\_cr} = n_{non\_cr} \cdot P_{el,b} \quad (34)$$

The optimal load sifting algorithm is allowed to transfer a specific percentage of each hour's non-critical loads to a different time slot on condition that sum of time-shiftable loads over the examined time period remains the same. The time period where the non-critical loads can be shifted is denoted with  $[T_{shift} \bar{T}_{shift}]$ .

Non-critical load's shifting should satisfy the following constraints:

$$P_{non\_cr}^*(t) = \begin{cases} n_{shift}(t) \cdot P_{non\_cr}(t), & \forall t \in [T_{shift} \bar{T}_{shift}] \\ P_{non\_cr}(t), & otherwise \end{cases} \quad (35)$$

$$P_{non\_cr}^*(t) \geq \underline{n}_{shift} \cdot P_{non\_cr}(t) \quad (36)$$

$$P_{non\_cr}^*(t) \leq \bar{n}_{shift} \cdot P_{non\_cr}(t) \quad (37)$$

$$\underline{P}_{HVAC} \leq P_{el,b} \leq \bar{P}_{HVAC} \quad (38)$$

$$\sum_{t=T_{shift}}^{\bar{T}_{shift}} P_{non\_cr}(t) \cdot \Delta t = \sum_{t=T_{shift}}^{\bar{T}_{shift}} P_{non\_cr}^*(t) \cdot \Delta t \quad (39)$$

Where,  $n_{shift}$  is a coefficient estimated by the optimal load shifting algorithm and  $P_{non\_cr}^*(t)$  is the optimal electric power consumed by the non-critical loads of a building. Eq. (39) guarantees that the energy of the shifted load will be equal to the initial one by the end of the day.

### 4.3. Parking Dynamic Aggregated Battery Agent Model (PDABA)

A dynamic equivalent battery model is developed for the cluster of PEVs hosted by microgrid's parking lots. It is based on forecasts of PEVs plug-in and dwell time, their initial state of charge and their technical characteristics. The main goal of this model is to obtain the dynamic upper and lower limits of the state of charge (SoC) or stored energy equivalently and the active power of the battery for the purpose of scheduling optimally the power that the EVs should exchange with the electric network. This power depends on forecasted electricity price and the state of charge of PEV'-s' equivalent battery. The operation area of an individual EV is shown in Fig. 7.

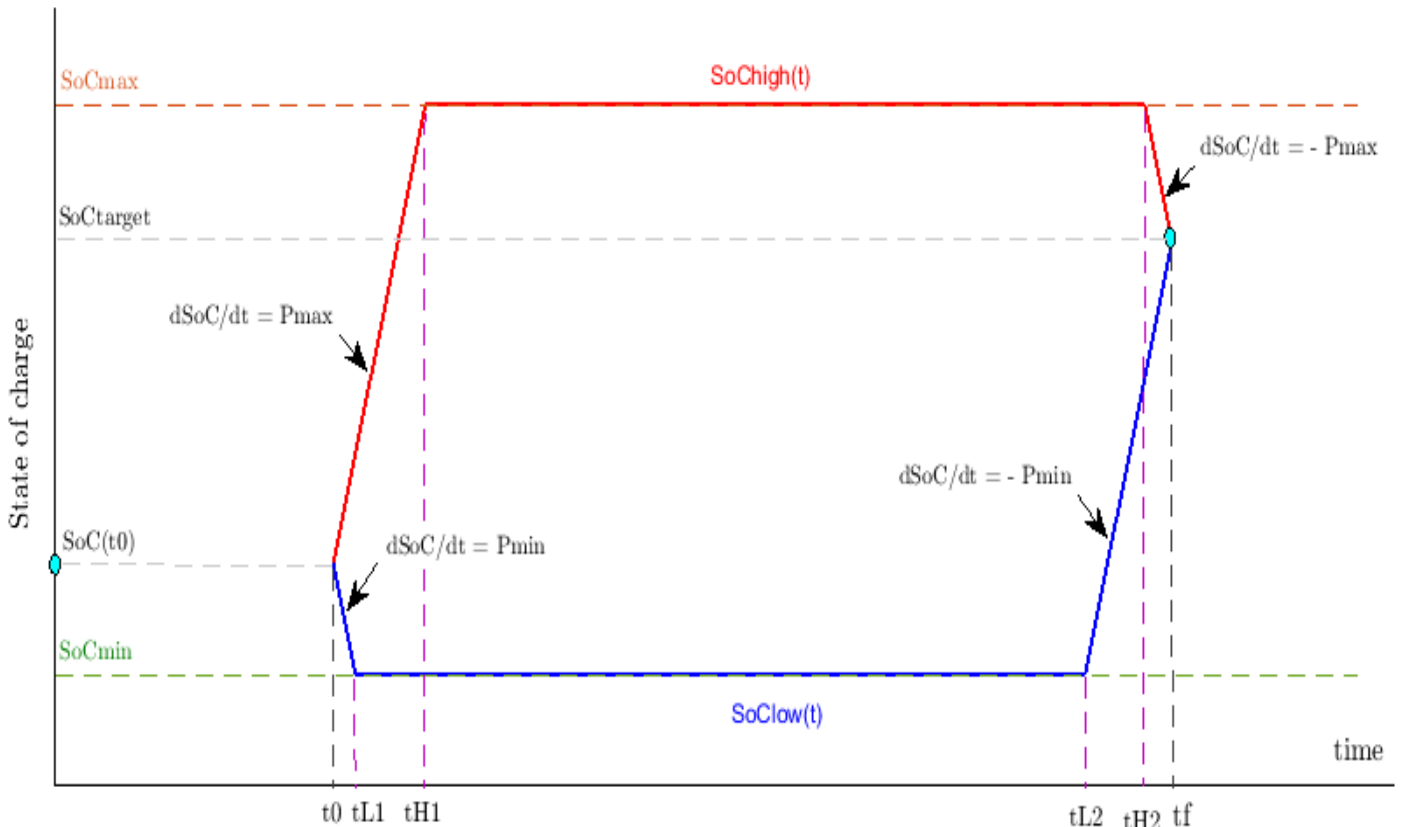


Fig. 7. State of charge bounds of a PEV

The time that the electric vehicle is plugged to the network and unplugged from it is denoted with  $t_0$  and  $t_f$ , respectively.  $SoC_{max}$  and  $SoC_{min}$  are the maximum and the minimum values of PEV's battery state of charge (in kWh).  $SoC_0$  is the initial state of charge (kWh) of each electric vehicle.  $P_{max}$  and  $P_{min}$  are the maximum and minimum power transfer rate of the PEV's battery, respectively.  $SoC_{target}$  is the target energy that driver has defined and each PEV should reach at its disconnection time. The dynamic lower and upper bounds of the SoC,  $SoC_{low}$  and  $SoC_{high}$ , are defined by 4 points. These points are  $(t_0, SoC(t_0))$ ,  $(t_{L1}, SoC_{min})$ ,  $(t_{L2}, SoC_{min})$ ,  $(t_f, SoC_{target})$  for  $SoC_{low}$  and  $(t_0, SoC(t_0))$ ,  $(t_{H1}, SoC_{max})$ ,  $(t_{H2}, SoC_{max})$ ,  $(t_f, SoC_{target})$  for  $SoC_{high}$ .

$t_{L1}$  and  $t_{H1}$  for the  $i^{th}$  charging point denote the time points that  $SoC_{low}$  and  $SoC_{high}$  start to decrease and increase with a constant rate of change  $P_{min}$  and  $P_{max}$ , respectively. They are estimated as in the following:

$$t_{L1}(i) = t_0(i) + \frac{SoC_{min}(i) - SoC_0(i)}{P_{min}(i)} \quad (40)$$

$$t_{H1}(i) = t_0(i) + \frac{SoC_{max}(i) - SoC_0(i)}{P_{max}(i)} \quad (41)$$

$t_{L2}$  and  $t_{H2}$  for the  $i^{th}$  charging point denote the time points that  $SoC_{low}$  and  $SoC_{high}$  start to increase and decrease with a constant rate of change  $-P_{min}$  and  $-P_{max}$ , respectively. They are estimated as in the following:

$$t_{L2}(i) = t_f(i) + \frac{SoC_{target}(i) - SoC_{min}(i)}{P_{min}(i)} \quad (42)$$

$$t_{H2}(i) = t_f(i) + \frac{SoC_{target}(i) - SoC_{max}(i)}{P_{max}(i)} \quad (43)$$

$SoC_{low}$  and  $SoC_{high}$  limits of the electric vehicle connected to the  $i^{th}$  charging point are estimated at time  $t$  as:

$$SoC_{low}(i, t) = \begin{cases} SoC_{min}(i), & t_{L1}(i) \leq t \leq t_{L2}(i) \\ SoC_{min}(i) + P_{max}(t - t_{L2}(i)), & t_{L2}(i) < t < t_f(i) \\ SoC_0(i) - P_{max}(t - t_0(i)), & t_0(i) < t < t_{L1}(i) \end{cases} \quad (44)$$

$$SoC_{high}(i, t) = \begin{cases} SoC_{max}(i), & t_{H_1}(i) \leq t \leq t_{H_2}(i) \\ SoC_{max}(i) - P_{max}(t - t_{H_2}(i)), & t_{H_2}(i) < t < t_f(i) \\ SoC_0(i) + P_{max}(t - t_0(i)), & t_0(i) < t < t_{H_1}(i) \end{cases} \quad (45)$$

The technical characteristics of the equivalent battery are given by the following equations:

$$P_{parking,max}(t) = \sum_i P_{max}(i, t) \quad \forall t \in [T_{initial} T_{final}] \quad (46)$$

$$P_{parking,min}(t) = \sum_i P_{min}(i, t) \quad \forall t \in [T_{initial} T_{final}] \quad (47)$$

$$SoC_{parking,max}(t) = \sum_i SoC_{high}(i, t) - SoC_{diff}(t), \quad \forall t \in [T_{initial} T_{final}] \quad (48)$$

$$SoC_{parking,min}(t) = \sum_i SoC_{low}(i, t) - SoC_{diff}(t), \quad \forall t \in [T_{initial} T_{final}] \quad (49)$$

The dynamic change of SoC of the parking equivalent battery due to the plugging and unplugging of EVs (kWh) is calculated as shown in following equation:

$$SoC_{diff}(t) = \sum_{T_{initial}:\Delta t:t} SoC_{0,parking}(t) - SoC_{t,parking}(t) \quad (50)$$

with

$$SoC_{0,parking}(t) = \sum_i SoC_0(i) \quad \forall t \in [T_{initial} T_{final}] \quad (51)$$

$$SoC_{t,parking}(t) = \sum_i SoC_{target}(i) \quad \forall t \in [T_{initial} T_{final}] \quad (52)$$

Where  $T_{initial(final)}$  is the initial(final) time point of the optimization period.

Let us assume that  $P_{opt}(t)$  is the optimal active power the equivalent battery exchanges with the electric network. Its SoC (in kWh) at the end of the next time interval is calculated as it follows:

$$SoC_{PB}(t + \Delta t) = \begin{cases} SoC_{PB}(t) - P_{opt}(t) \cdot n_{ch} \cdot \Delta t, & P_{opt}(t) < 0 \\ SoC_{PB}(t) - \frac{P_{opt}(t)}{n_{disch}} \cdot \Delta t, & P_{opt}(t) \geq 0 \end{cases} \quad (53)$$

Moreover, the equivalent battery should satisfy the following constraints.

$$SoC_{PB}(T_{initial}) = SoC_{PB}(T_{final}) \quad (54)$$

$$SoC_{parking,min}(t) \leq SoC_{PB}(t) \leq SoC_{parking,max}(t) \quad \forall t \in [T_{initial} T_{final}] \quad (55)$$

$$P_{parking,min}(t) \leq P_{opt}(t) \leq P_{parking,max}(t) \quad \forall t \in [T_{initial} T_{final}] \quad (56)$$

The following additional constraints should be applied for each building in case that the microgrid should operate autonomously within a specific time period  $[T_{auto} \bar{T}_{auto}]$ , such as during an electric grid power supply interruption.

$$Q_{EC,total}(t) + n_{aut} \cdot P_{el,b}(t) = P_{opt}(t) \quad \forall t \in [T_{auto} \bar{T}_{auto}] \quad (57)$$

$$SoC_{parking,min,aut}(t) = SoC_{parking,min}(t) + \sum_t^{\bar{T}_{auto}} (Q_{EC,total}(t:\bar{T}_{auto}) + 0.2 \cdot P_{el,b}(t:\bar{T}_{auto})) \cdot \Delta t \quad (58)$$

$$\forall t \in [T_{auto} \bar{T}_{auto}]$$

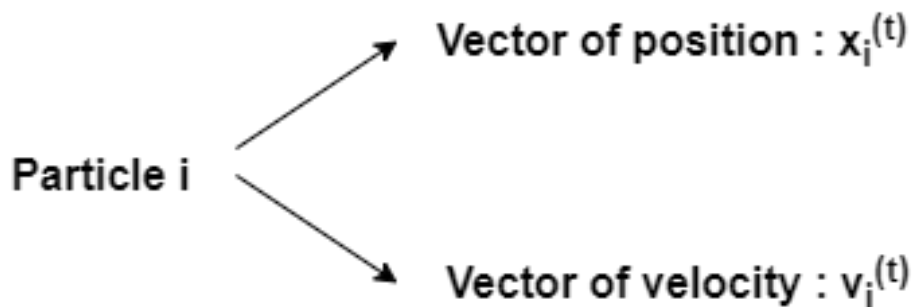
# 5. OPTIMIZATION OF MICROGRID OPERATION

---

## 5.1. Particle Swarm Optimization Algorithm (PSO)

In this work, an optimization technique, known as Particle Swarm Optimization (PSO), is applied to optimally schedule the operation of the Microgrid. This algorithm is based on a simple mathematical model to describe the social behavior of birds and fish. In these swarms, each member gains knowledge from the whole and in turn contributes its individual knowledge back to the swarm. It is one of the most useful and highly efficient heuristic methods and it has been successfully applied to various optimization problems. It finds the global maximum or minimum for non-convex and non-linear optimization problems and it offers solutions of fairly high accuracy. Another advantage of the method is that it is remarkably simple to implement.

PSO contains a population of candidate solutions called a swarm of particles. Every particle has a position in the search space of the optimization problem. The search space is the set of all possible solutions of the optimization problem and we would like to find the best one.



- $x_i^{(t)} \in X$  : Describes the position of the particle  $i$  in the search space  $X$ .
- $v_i^{(t)} \in X$  : Describes the movement of the particle  $i$  in the sense of direction and distance. It is in the same space as the position. Dimensions of  $v$  and  $x$  are the same.
- $t$  : discrete time expressing the iteration number of the algorithm.

Particles are learning from each other, obeying some simple rules to find the best solution for an optimization problem by defining the mathematical model of motion of particles. In addition to position and velocity particle has a memory of its own best position. This is denoted by personal best position.

The mathematical model of PSO is very simple. In each iteration of PSO, position and velocity of every particle is updated according to a simple mechanism. The particle moves to a new position. The new position is created according to the previous velocity, to its personal best and global best. Hence, it aims to move to a better location as it uses the previous decision about the movement of the particle and it uses the previous experience of the particle self and the swarm. Obeying these rules by every particle of the swarm, particles will collaborate to find the best location in the search space and therefore the best solution for the optimization problem.

A classic PSO method can be described as in the following:

$$\begin{cases} v_i^{(t+1)} = w \cdot v_i^{(t)} + c_1 \cdot r_1 \cdot (P_i - x_i^{(t)}) + c_2 \cdot r_2 \cdot (G - x_i^{(t)}) \\ x_i^{(t+1)} = x_i^{(t)} + v_i^{(t+1)} \end{cases}$$

- $P_i$  : the best previous solution corresponding to the  $i^{\text{th}}$  particle
- $G$  : the best global solution
- $w$  : the inertia weight factor
- $c_1, c_2$  : acceleration constants
- $r_1, r_2$  : random numbers varying between 0 and 1

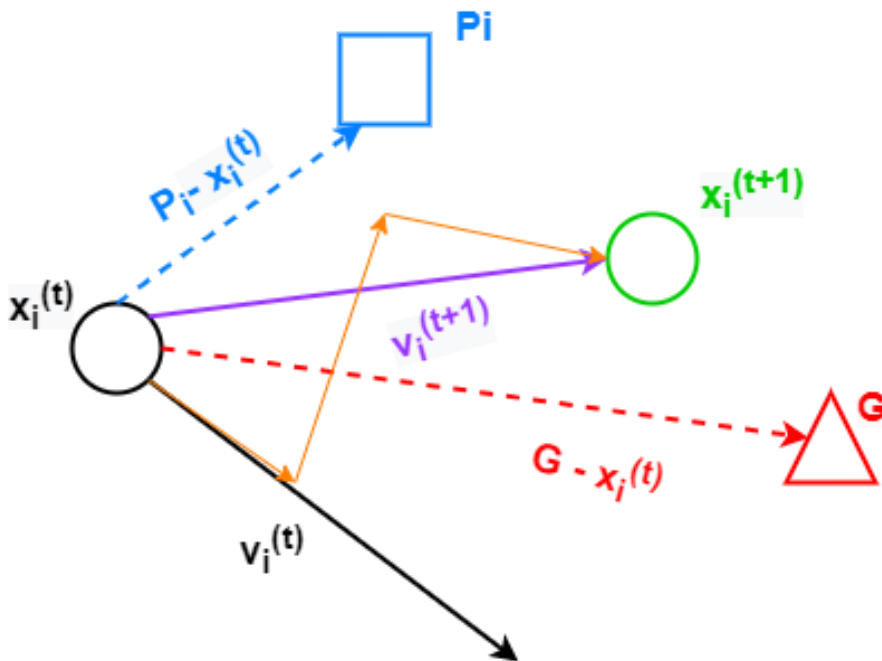


Fig. 8. Iteration scheme of the particles

In the examined problem, the building thermal model's differential equations should be solved within the optimization procedure, making its formulation difficult if classical optimization techniques are applied. However, using PSO algorithm, this problem does not appear since the building thermal model, regardless of its complexity, can be included in the objective function.

### 5.2. Optimization Level 1

In the first level of optimization, the algorithm minimizes the operation cost of the thermal and non-critical electrical loads for every building of the microgrid, while maintaining the required temperature comfort range.

The augmented objective cost function of the examined optimization problem is formulated in Eq. (59) and it is used in order to apply the PSO method.

$$\min \left\{ \sum_t (Q_{EC,total}(t) + P_{non\_cr}^*(t)) \cdot EP(t) \cdot \Delta t + Pen_{PMS} \right\} \tag{59}$$

The first term in Eq. (59) represents the total operation cost of HVAC system and the non-critical electrical loads. The building energy system is subject to technical and operational constraints which are defined by Eqs. (24), (29), (36)-(39). The second term comprises suitably formed penalty terms ( $Pen_{PMS}$ ) in order to take into account the above constraints.

PSO is applied to each building of the microgrid. A vector of variables is appropriately defined and assigned to each particle. In the first section of the particle, each particle contains the total HVAC power consumption of the building at every time slot of the optimization period. The second section of the particle comprises the adjustment coefficients of the non-critical electrical loads of the building over each time interval. The structure of each particle of the swarm is shown in Fig. 9.

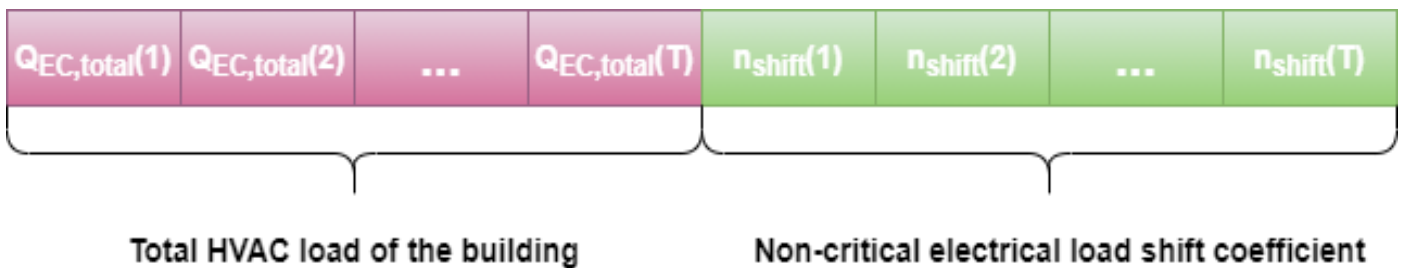


Fig. 9. PSO particle structure in EMS1

### 5.3. Optimization Level 2

In the second level of the optimization, the algorithm estimates the optimal active power of the equivalent aggregate battery of each EV parking lot of the microgrid for the purpose of scheduling optimally and minimizing the total cost of the electric power that the microgrid should exchange with the electric network.

The augmented objective cost function of the examined optimization problem is formulated in Eq. (60) and it is used in order to apply the PSO method.

$$\min \left\{ \sum_t \left( \sum_p P_{opt,p}(t) + \sum_b Q_{EC,total,b}^* + P_{non_{cr},b}^* + P_{el,b}(t) \right) \cdot EP(t) \cdot \Delta t + Pen_{EMS} \right\} \quad (60)$$

Where  $B$  and  $P$  are the sets comprising the buildings and the EVs parking garages of the microgrid, respectively.

The first term in Eq. (60) represents the cost of the total power exchanged by the buildings and their EV parking lots and the electric grid. The electric vehicles are subject to technical and operational constraints which are defined by Eqs. (54)-(56). The second term comprises suitably formed penalty terms ( $Pen_{EMS}$ ) in order to take into account the respective constraints.

PSO is applied in order to solve the above optimization problem. A vector of variables is appropriately defined and assigned to each particle. Each section of the particle comprises the respective electric power exchanged by each EV parking lot of the microgrid and the electric grid. The structure of each particle of the swarm for the examined system is shown in Fig. 10.



Fig. 10. PSO particle structure in EMS2

### 5.4. Algorithm Overview

The flowchart of the proposed hierarchical microgrid energy management is shown in Fig. 11. Initially, the forecasts of work schedule, activity of people, outdoor temperature, EVs' and their arrival/dwell times, solar radiation and electricity price are received for the next 24-hour period.

TLA and ELA take into account these daily forecasts to estimate the thermal and electrical loads of the microgrid's buildings, while PDABA to develop a dynamic equivalent battery model for the cluster of PEVs hosted by the charging points of the parking lots of the buildings.

In the first level of optimization, the profiles outlined in the previous step of the algorithm are used by algorithm to determine the optimal operation of each building thermal zone HVAC systems, as well as the buildings' electrical systems within the optimization period.

In the second level of optimization, the optimal electric power consumption profiles of the buildings are used to estimate the optimal scheduling of the power exchanged by the cluster of PEVs with the electric grid in order to minimize the daily total operation cost of the microgrid.

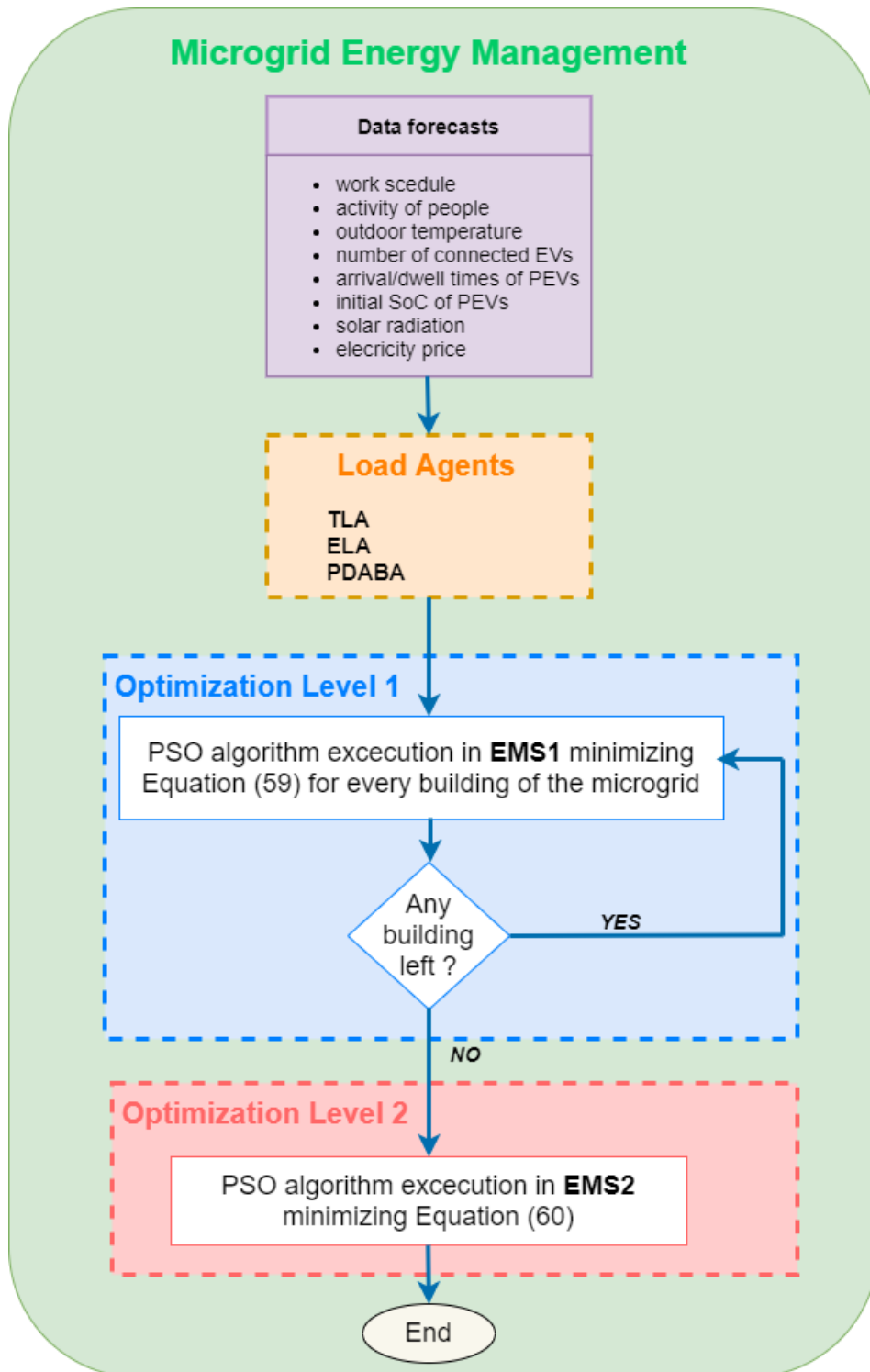


Fig. 11. Flowchart of the microgrid energy management algorithm

## 6. RESULTS

---

The optimization algorithm described above has executed for a number of operation scenarios. The case study and the results for these different scenarios are represented in this chapter.

### 6.1. Case Study

The time series used of the electricity price (EP) which has been used in all considered scenarios is shown in Fig. 12. It is observed that the electricity price takes the lowest values during 13:00 – 16:00.

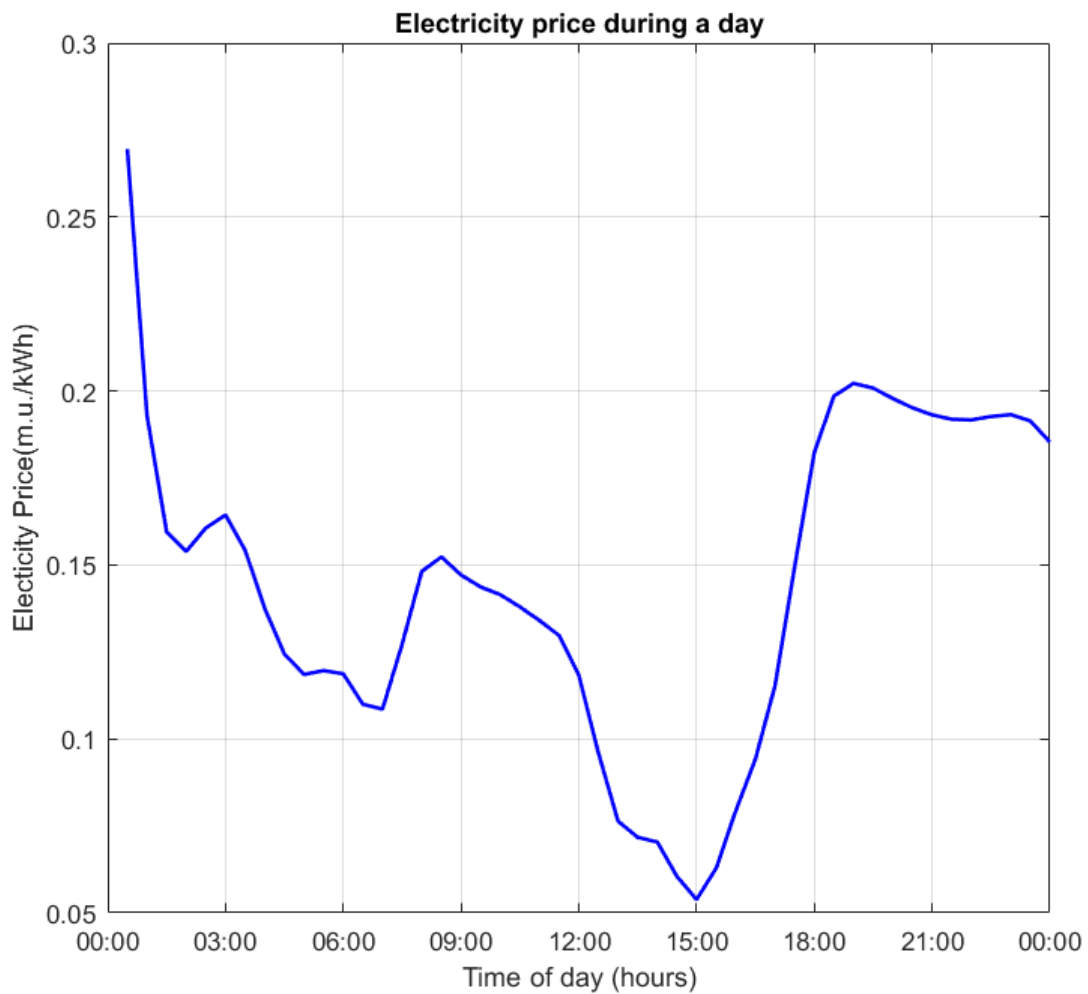


Fig. 12. Electricity price during the day

The forecasted outdoor temperature  $T_{out}$  is presented in Fig. 13.

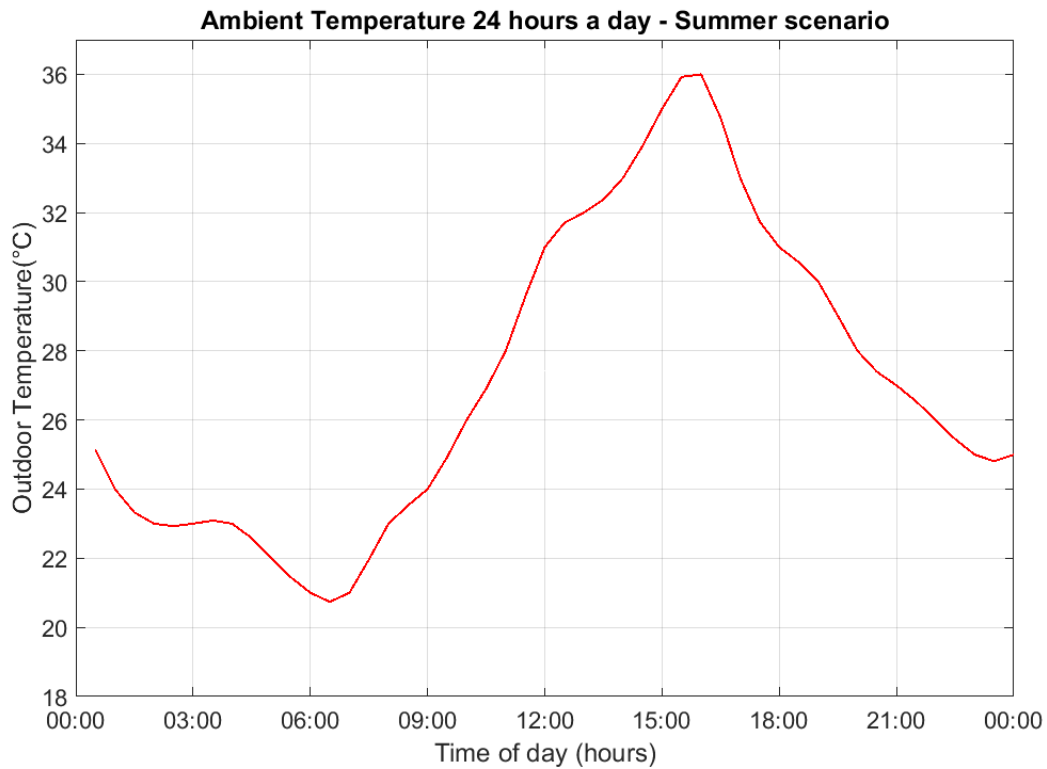


Fig. 13. Outdoor temperature ( °C )

The beam ( $I_b$ ), diffuse ( $I_d$ ) and total ( $I$ ) radiation forecasts on horizontal surface, respectively ( $\text{kW}/\text{m}^2$ ), are shown in Fig. 14. In Fig. 15, total solar radiation on a tilted surface ( $\text{kW}/\text{m}^2$ ) is given.

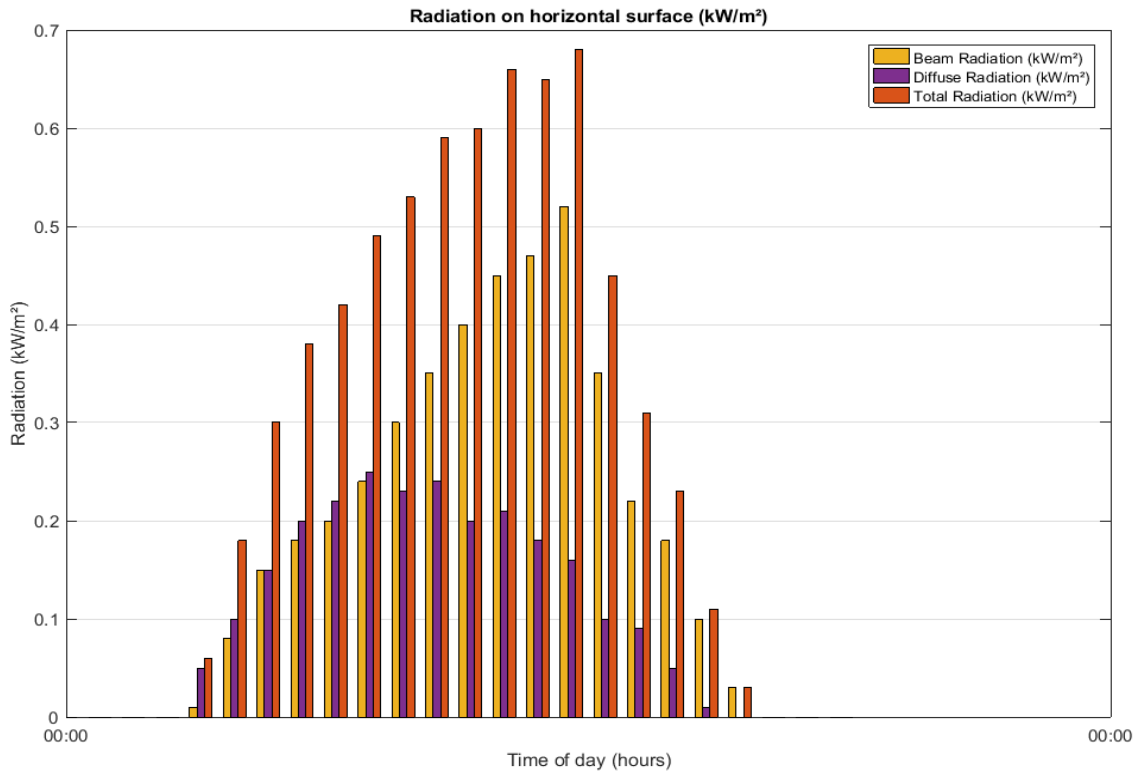


Fig. 14. Beam, Diffuse and Total Radiation ( $\text{kW}/\text{m}^2$ )

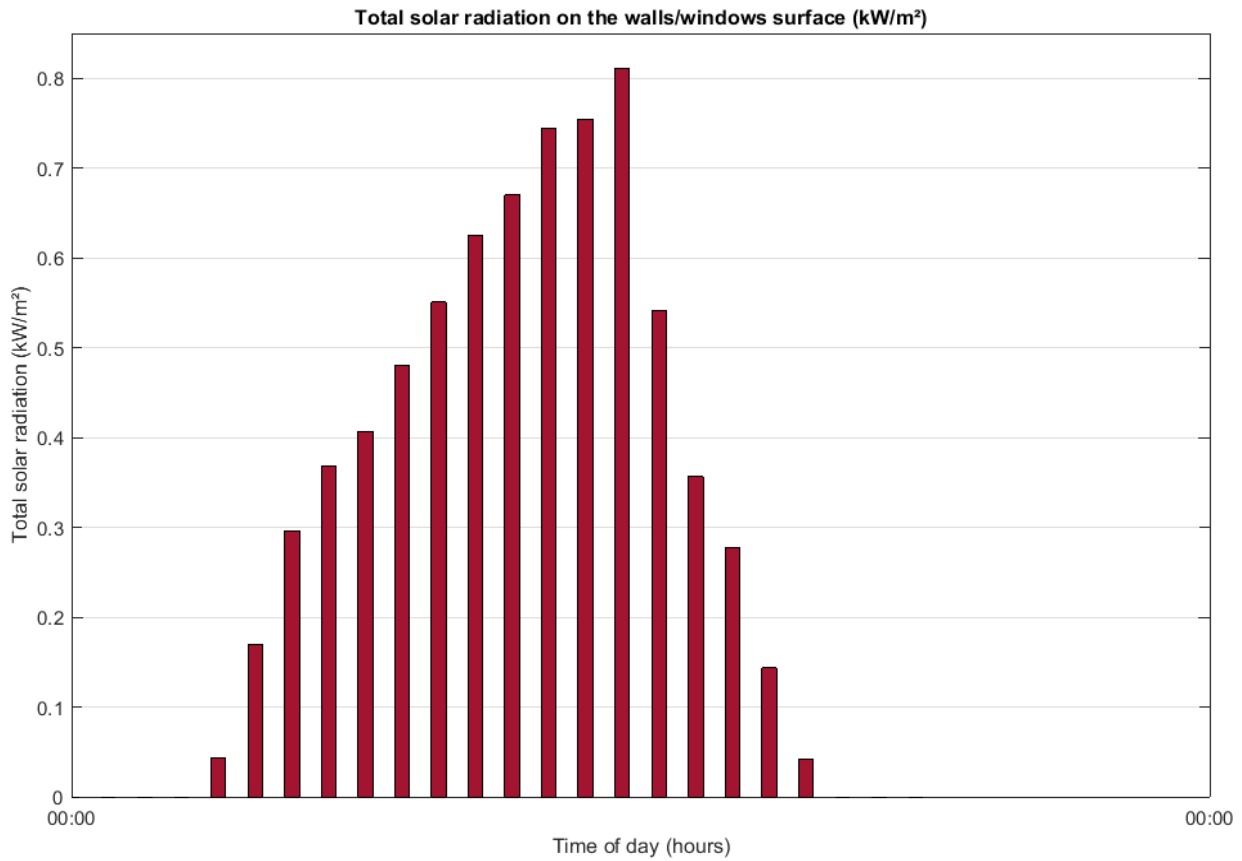


Fig. 15. Total Solar Radiation on tilted surface (kW/m<sup>2</sup>)

The connection and the dwell times of the plug-in electric vehicles depend on the different type of activities (home, work, shop, social) that their drivers have and they are estimated using probability density functions, as shown in Fig. 16 and in Fig. 17, respectively [4].

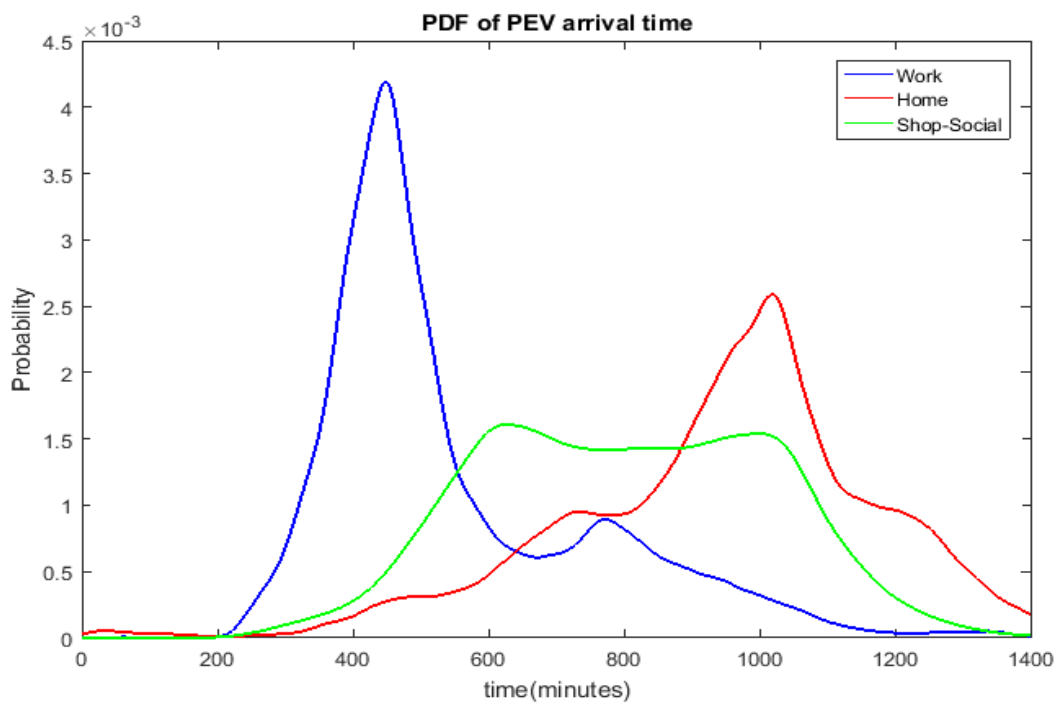


Fig. 16. PDF of electric vehicles connection time

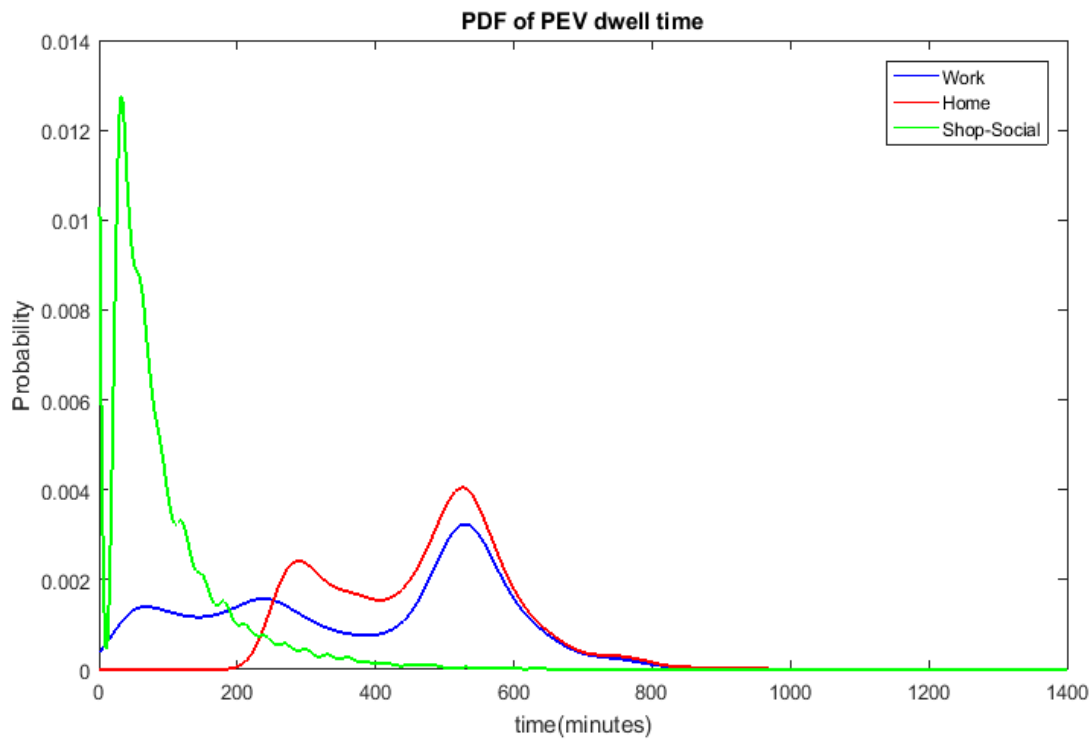


Fig. 17. PDF of electric vehicles dwell time

For instance, as it can be observed, the connection rate for PEVs of citizens being at work peaks at 450<sup>th</sup> min (7.5 h), whereas their dwell time peaks approximately at 510<sup>th</sup> min (8.5 h).

In this case study, the microgrid operator is assumed to have three different buildings under its surveillance. The considered buildings represent commercial buildings which are large offices. Each of the microgrid buildings has its own parking lot for EVs with different characteristics each one.

The structure and the floor plan of each building, as well as the number of people and the number of electric vehicles connected to the respective parking lot in a 24-hour period, are shown in the following figures.

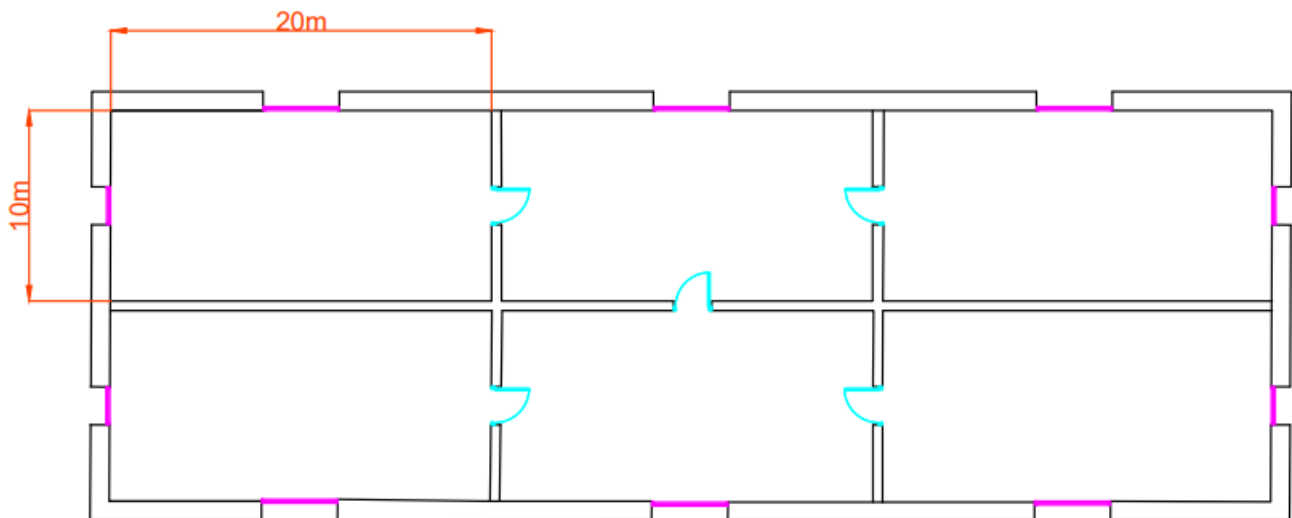


Fig. 18. Floor plan of the first building of the microgrid (6 thermal zones)

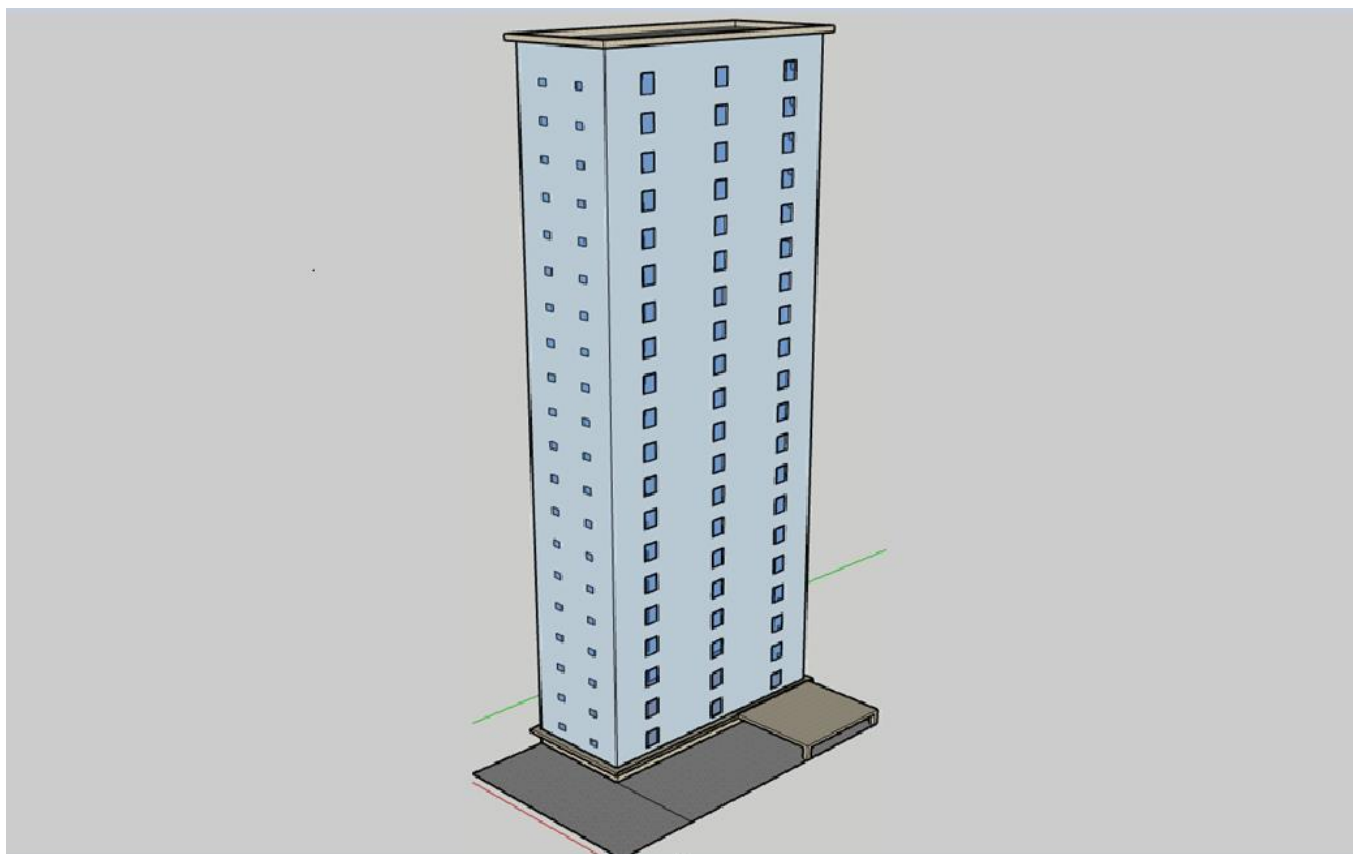


Fig. 19. Structure of the first building of the microgrid (20 floors)

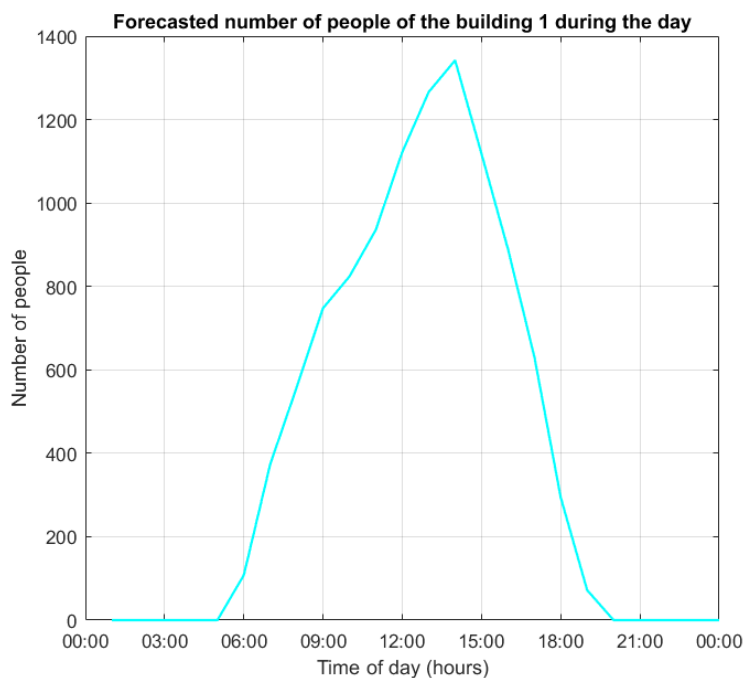


Fig. 20. Forecasted number of people in building 1

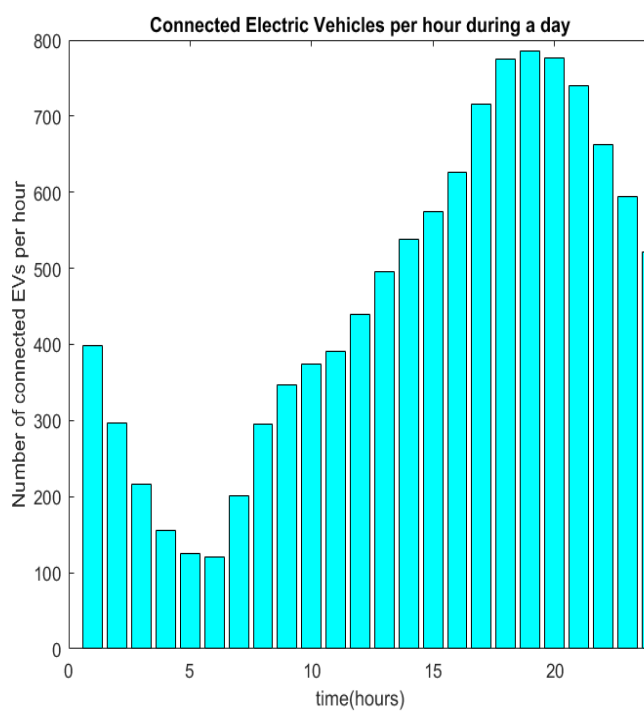


Fig. 21. Forecasted number of connected PEVs to the 1<sup>st</sup> building's parking garage

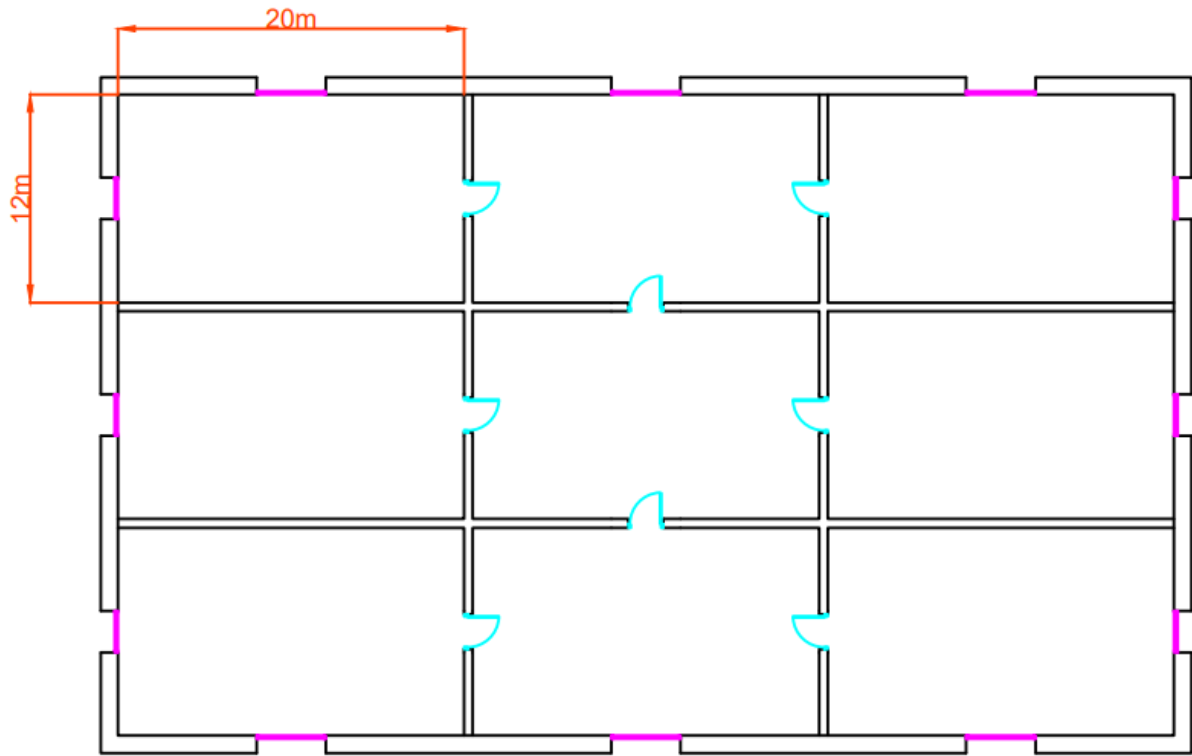


Fig. 22. Floor plan of the second building of the microgrid (9 thermal zones)

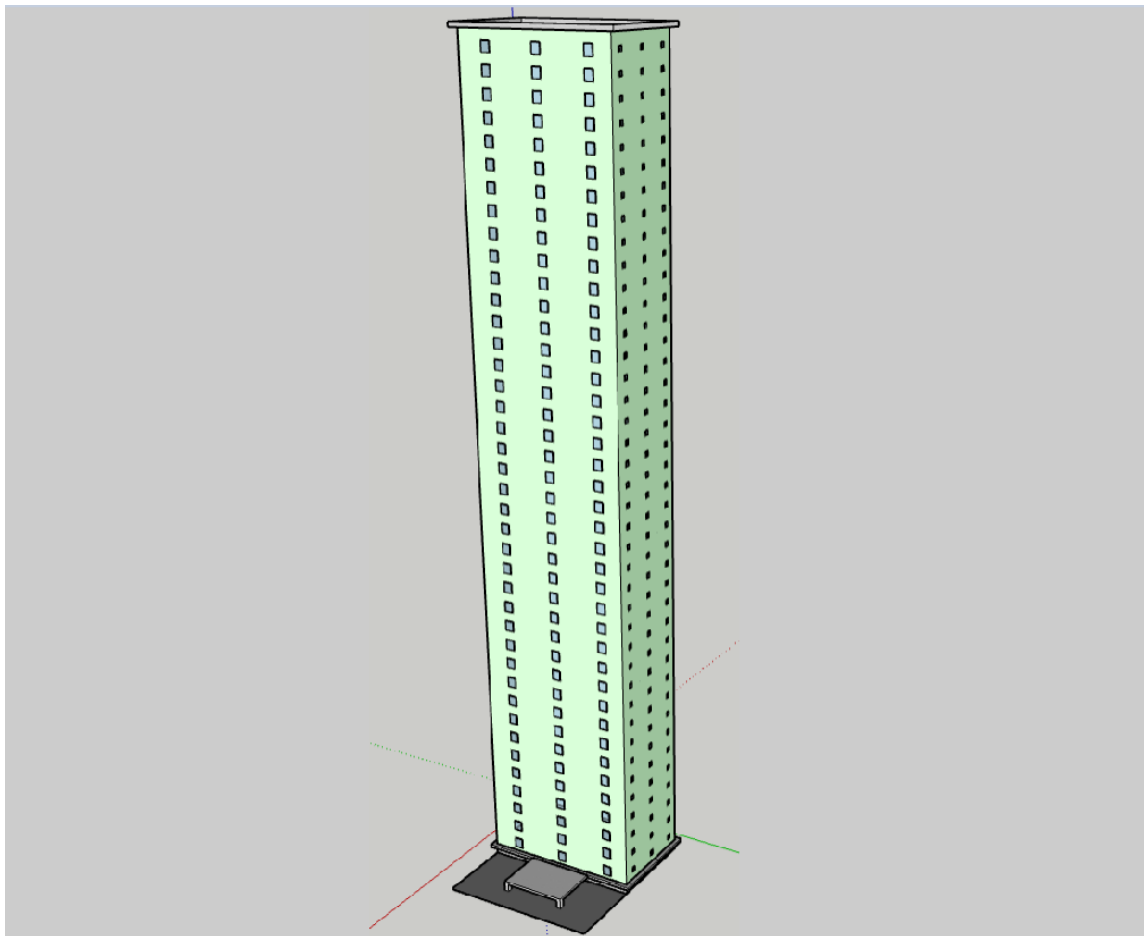


Fig. 23. Structure of the second building of the microgrid (40 floors)

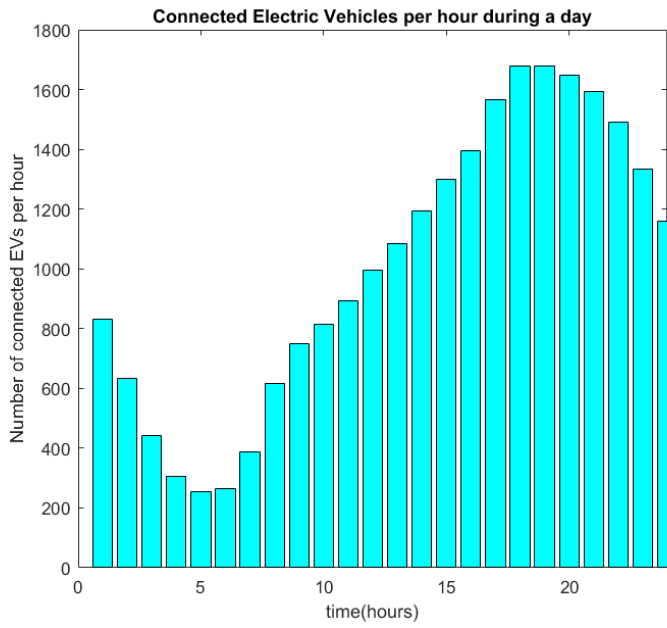


Fig. 24. Forecasted number of connected PEVs to the 2nd building's parking garage

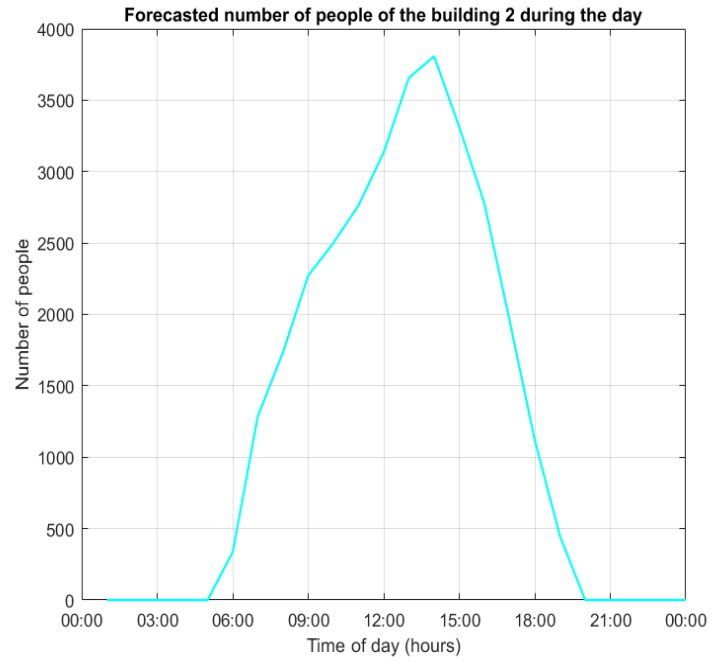


Fig. 25. Forecasted number of people in building 2

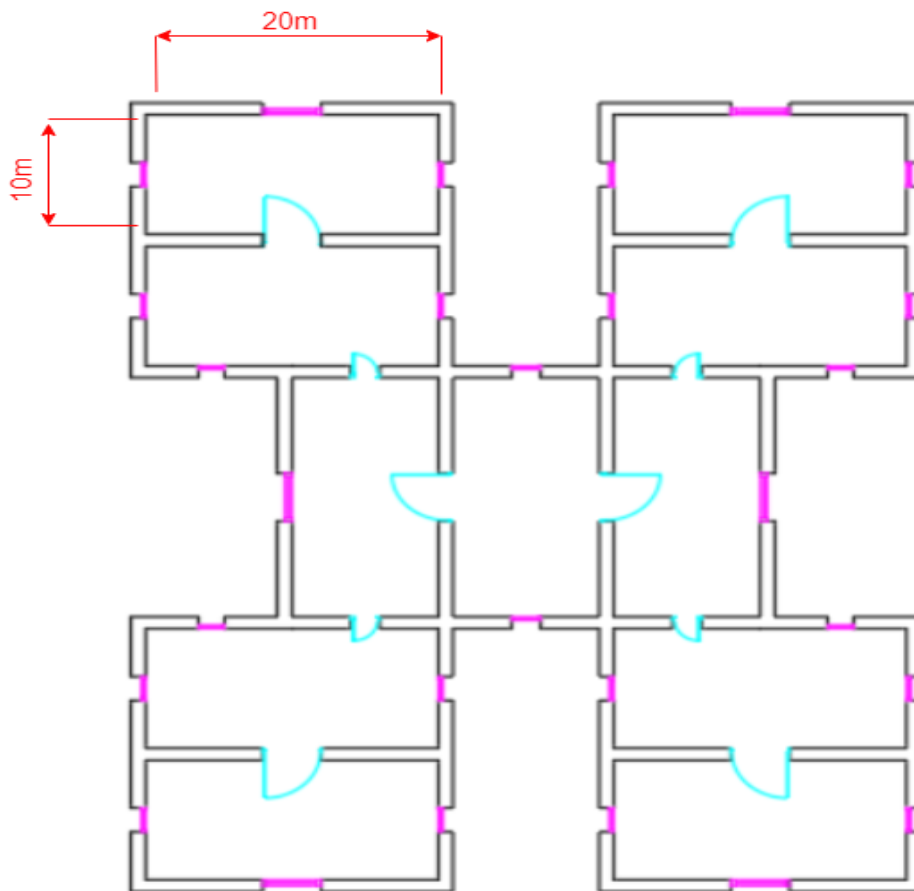


Fig. 26. Floor plan of the third building of the microgrid (11 thermal zones)

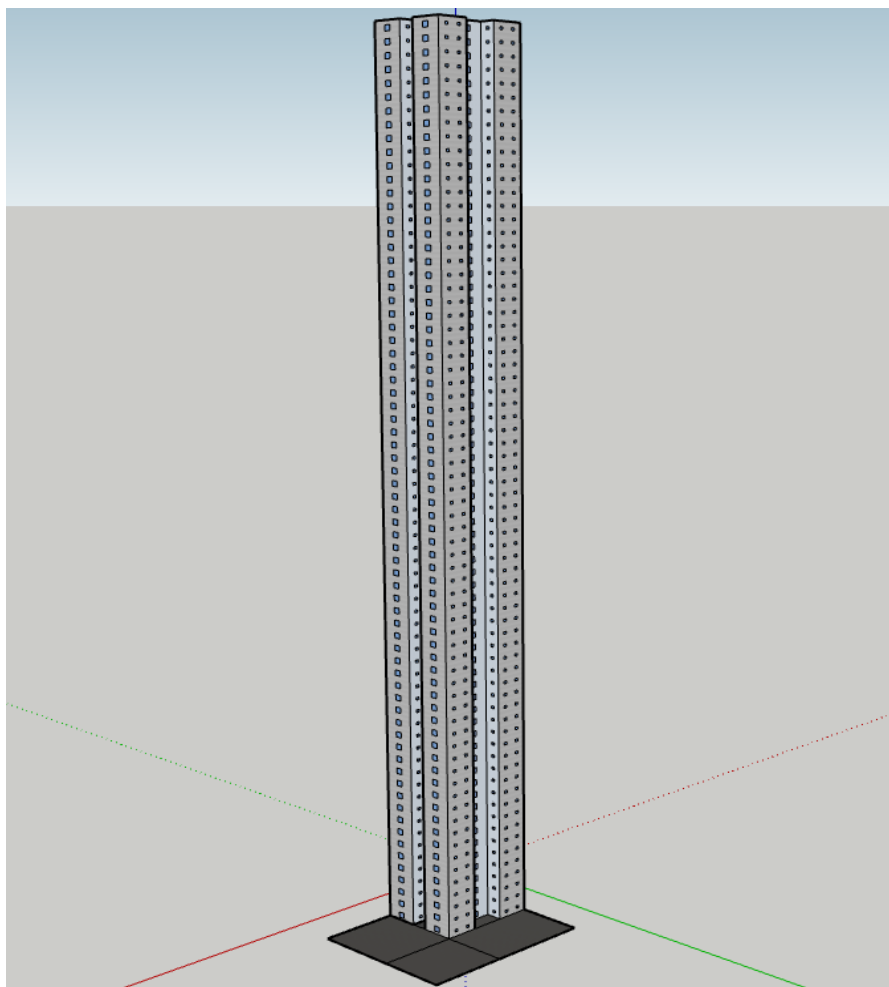


Fig. 27. Structure of the third building of the microgrid (70 floors)

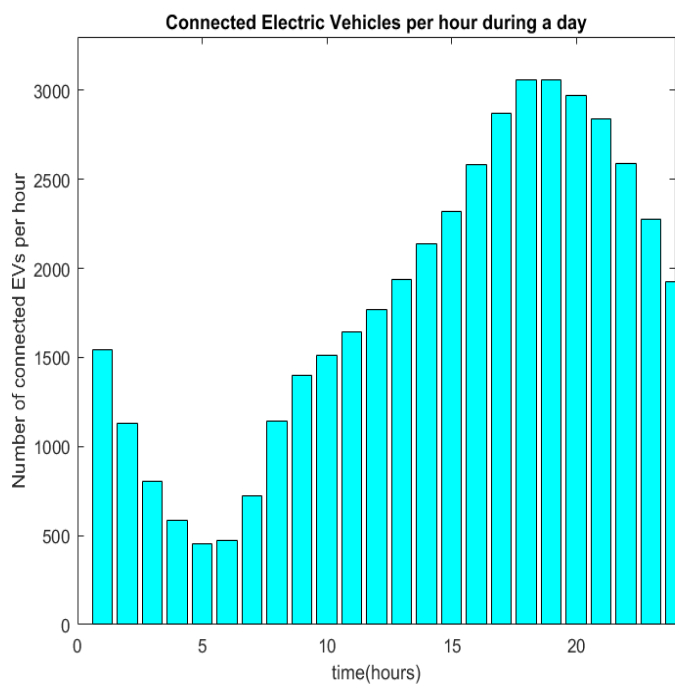


Fig. 28. Forecasted number of connected PEVs to the 3<sup>rd</sup> building's parking garage

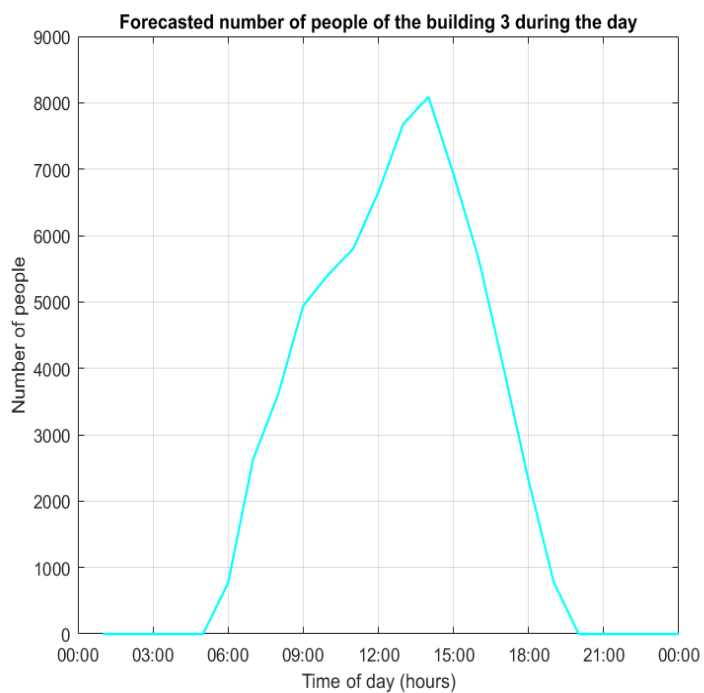


Fig. 29. Forecasted number of people in building 3

BUILDING PARAMETERS							
	Building 1		Building 2		Building 3		
Number of floors	20		40		70		
Total number of thermal zones	120		360		770		
Side_1 (m)	10		12		10		
Side_2 (m)	20		20		20		
Height (m)	3		3		3		
$V_j$ (m <sup>3</sup> )	600		720		600		
$T_{min}$ (°C)	18		19		17		
$T_{max}$ (°C)	26		27		27		

THERMAL ZONE PARAMETERS				NON-CRITICAL ELECTRICAL LOADS' PARAMETERS			
				Building 1	Building 2	Building 3	
$\rho_j$ (kg/m <sup>3</sup> )	1.2	$R_{se,j}$ ((m <sup>2</sup> °C)/W)	0.04	$n_{non\ cr}$	0.25	0.25	0.25
$C_j$ (kWh/(kg · °C))	1/3600	$SC_j$	0.54	$n_{shift}$	0.75	0.75	0.65
$U_{wall,i}$ (kW/(m <sup>2</sup> °C))	$0.48 \cdot 10^{-3}$	$p_E$	0.2	$\bar{n}_{shift}$	1.25	1.25	1.35
$U_{win,j}$ (kW/(m <sup>2</sup> °C))	$2.9 \cdot 10^{-3}$	$\beta_j$ (°)	90	$T_{shift}$	7:00	7:00	7:00
$\tau_{win,j}$	$1.1 \cdot 10^{-3}$	$\theta$ (°)	11.9	$\bar{T}_{shift}$	17:00	17:00	17:00
$a_{w,j}$	$18.63 \cdot 10^{-3}$	$\theta_j$ (°)	39.9				

THERMAL AND ELECTRICAL LOADS PARAMETERS		
	Thermal loads (W)	Electrical loads (W)
PC	70	500
Printer	40	100
Display	60	100
Charger	20	100
Scanner	30	80
Lighting	37	120
Human Body	150	-

ELECTRIC VEHICLE PARKING GARAGE PARAMETERS	Parking 1	Parking 2	Parking 3
Number of charging points	1000	3000	6500

ELECTRIC VEHICLE PARAMETERS	EV Type 1	EV Type 2	EV Type 3	EV Type 4
Battery Capacity(kWh)	77	45	26.8	66.5
$SoC_{max}$ (kWh)	69.3	40.5	24.12	59.85
$SoC_{min}$ (kWh)	7.7	4.5	2.68	6.65
$P_{max}$ (kW)	11	7.2	6.6	11
$P_{min}$ (kW)	-11	-7.2	-6.6	-11

TABLE I : MICROGRID PARAMETERS

## 6.2. Microgrid Operation Scenarios

Three different operation scenarios were examined for a 24-hour time period, in order to showcase the effectiveness of the proposed algorithm. The results of the examined scenarios are given next.

### 6.2.1. Scenario I

In Scenario I, the proposed energy management method described above is applied. The goal of this scenario is to minimize the overall operating cost of the microgrid.

The internal temperature of all building thermal zones for scenario I with their upper and lower limits of the temperature set-points are shown in Fig. 30, Fig. 31 and Fig. 32.

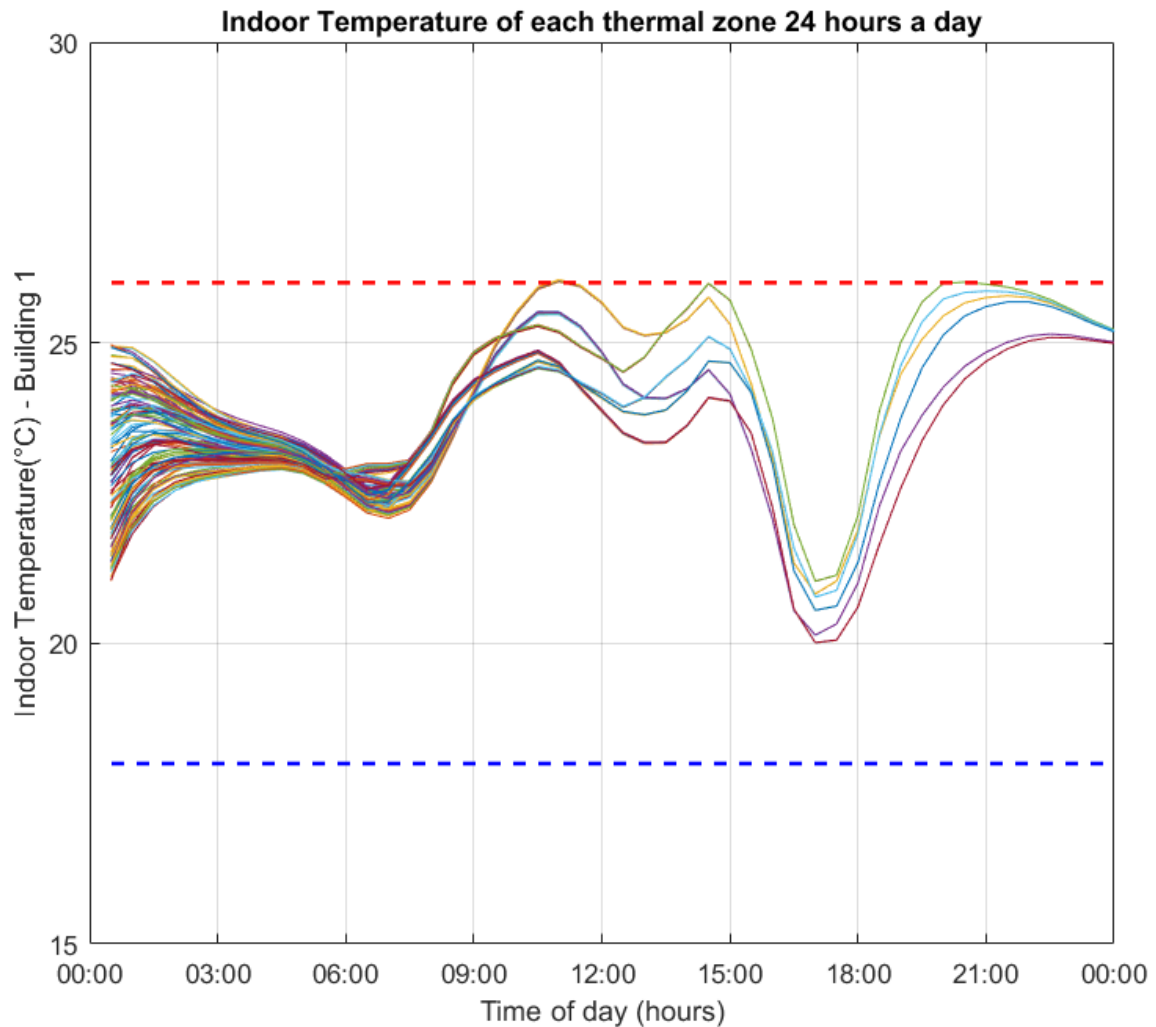


Fig. 30. Indoor temperature of 1<sup>st</sup> building's thermal zones

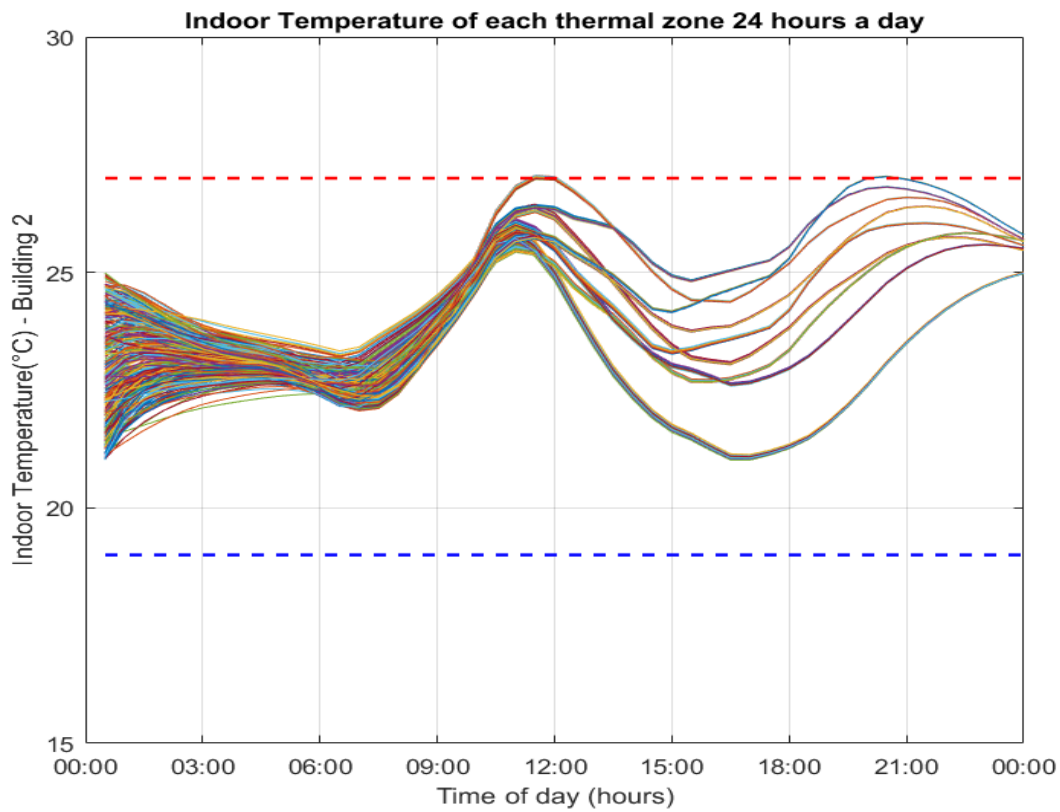


Fig. 31. Indoor temperature of 2<sup>nd</sup> building's thermal zones

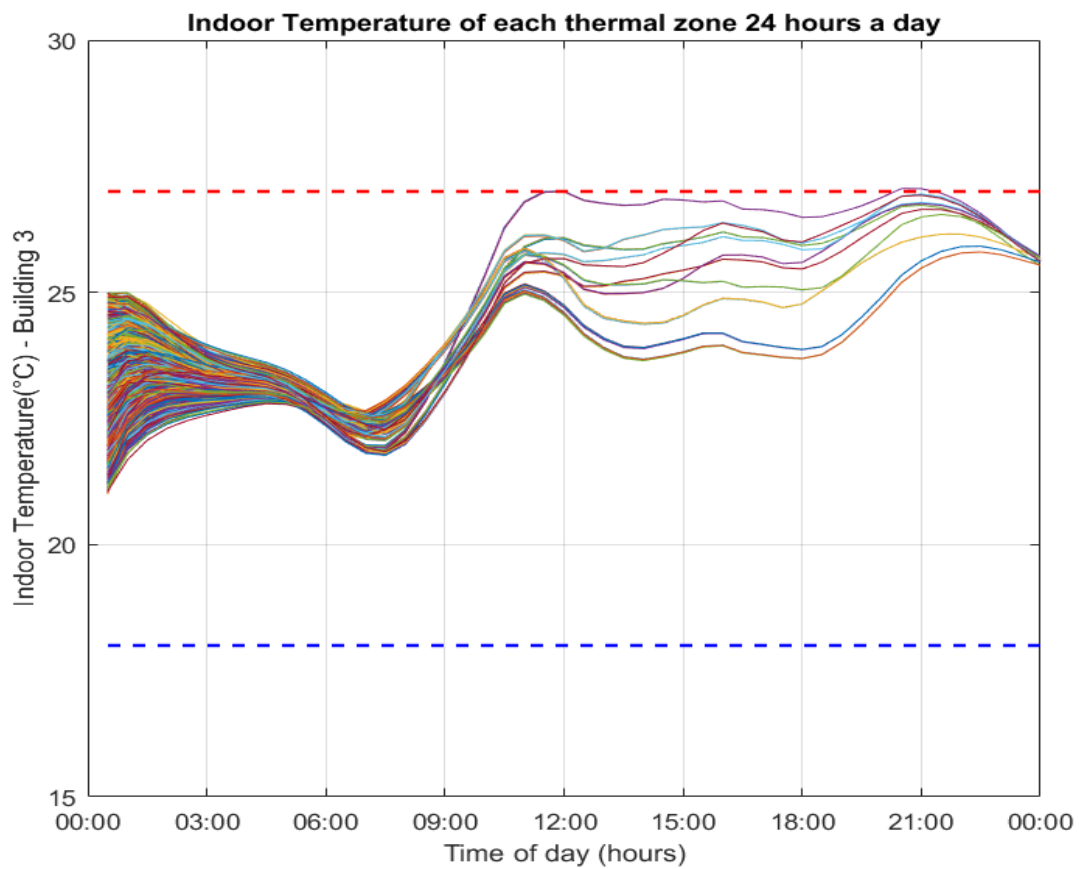


Fig. 32. Indoor temperature of 3<sup>rd</sup> building's thermal zones

It can be observed that the indoor temperatures of the thermal zones are adjusted within the comfort range of each building and they all tend to have the same behavior pattern.

The total cooling power consumption for every building of the microgrid, shown in the following figures, results from the execution of the first level of optimization. In all cases, the cooling power is following the outdoor temperature and the forecasted number of people having activity in the buildings, as it was expected. Moreover, the algorithm tries to decrease it at time periods of relatively high electrical price. Obviously, the largest building has the biggest cooling requirements.

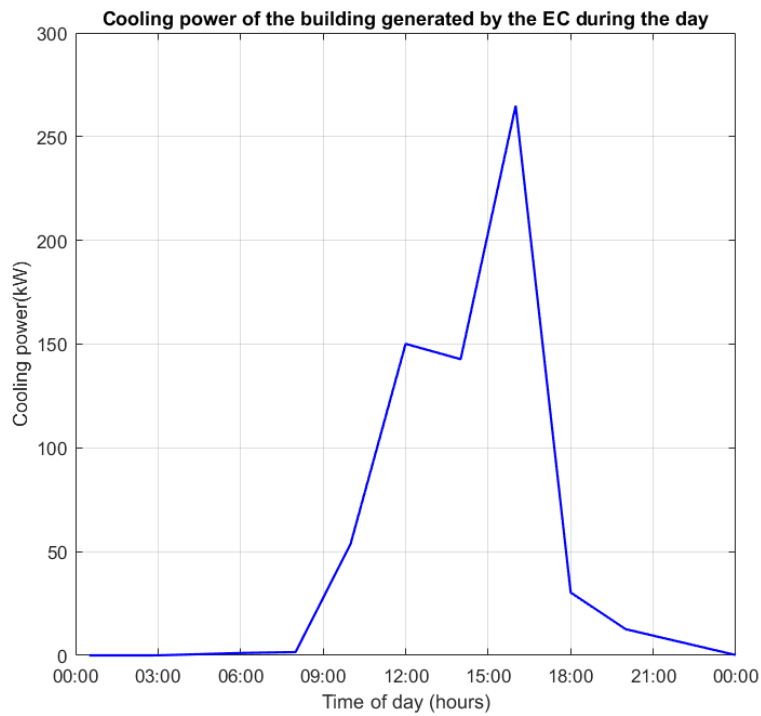


Fig. 33. Cooling power consumption of building 1

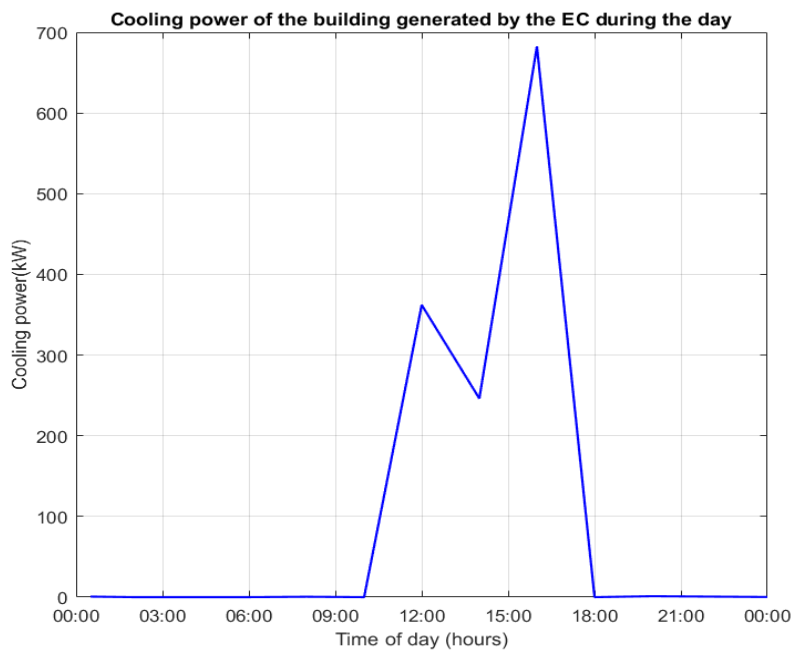


Fig. 34. Cooling power consumption of building 2

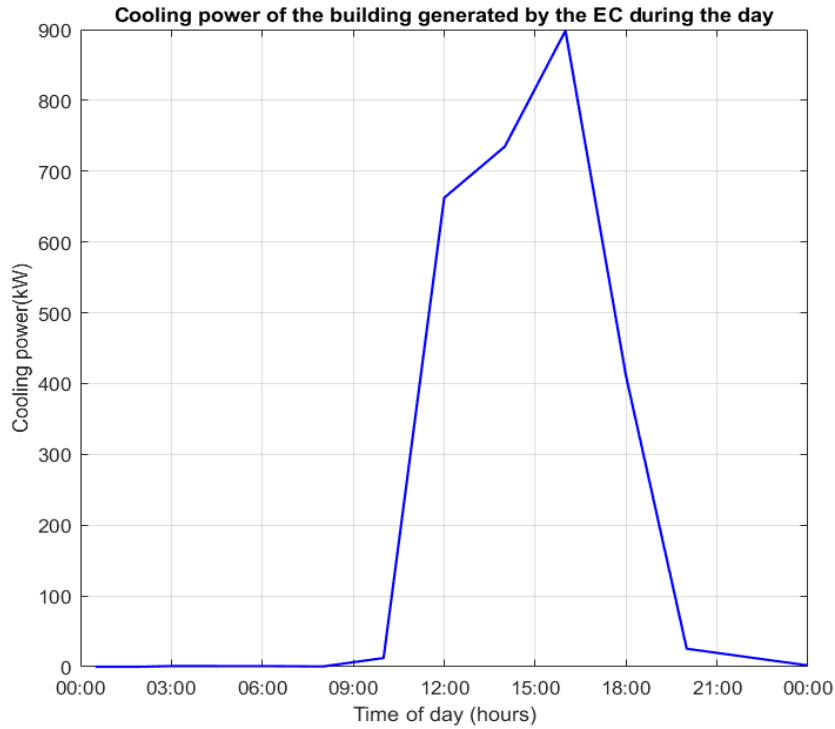


Fig. 35. Cooling power consumption of building 3

The electrical power demand of the above HVAC system of each building mainly follows the pattern of the forecasted number of people having activity in the buildings.

The following figures exhibit the non-critical building electrical loads of scenario I before and after the first level of optimization is applied, as well as the respective critical loads of each building of the microgrid.

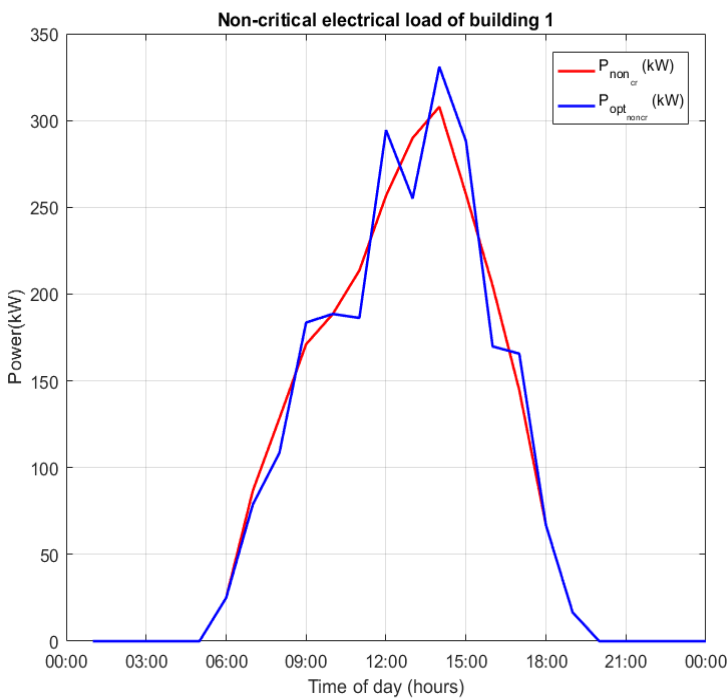


Fig. 36. Non critical electrical load of building 1

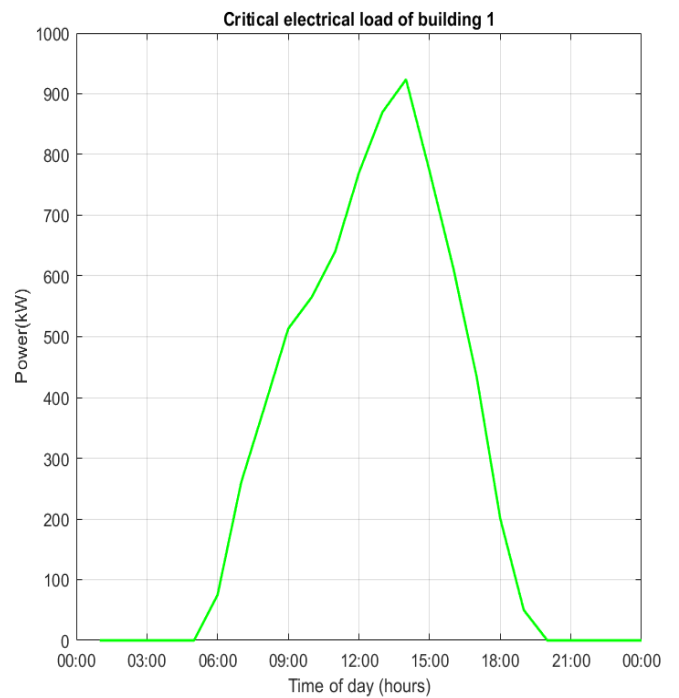


Fig. 37. Critical electrical load of building 1

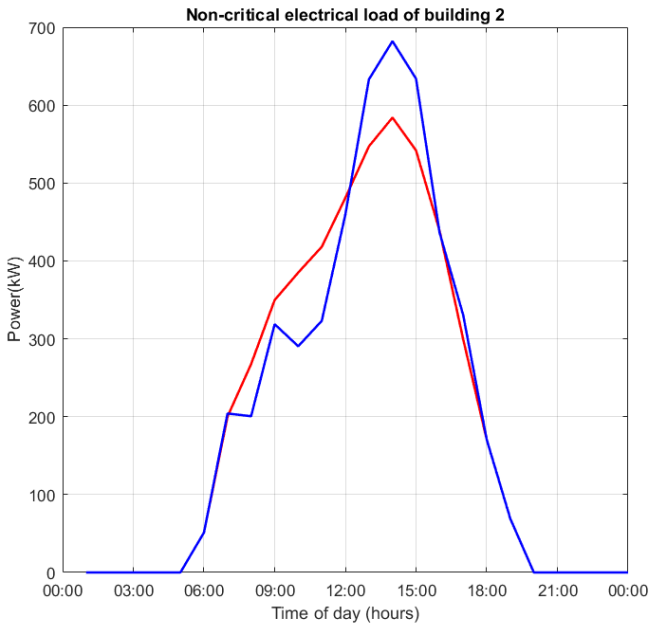


Fig. 38. Non critical electrical load of building 2

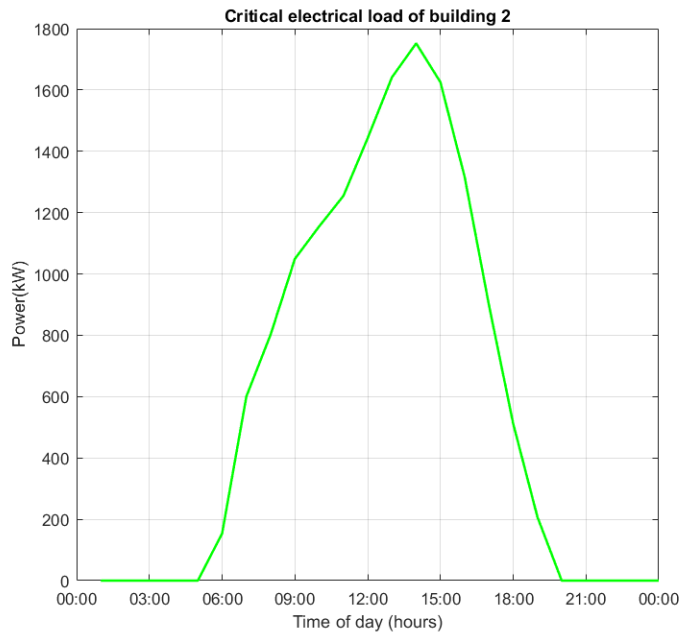


Fig. 39. Critical electrical load of building 2

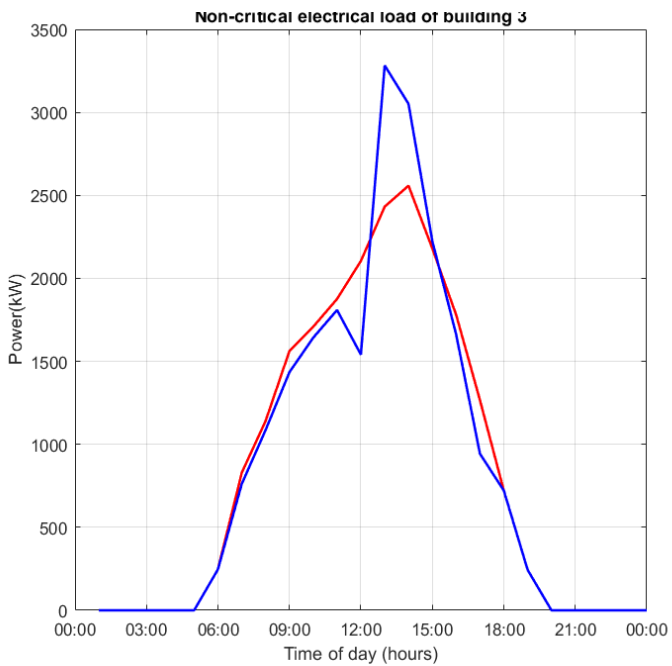


Fig. 41. Critical electrical load of building 3

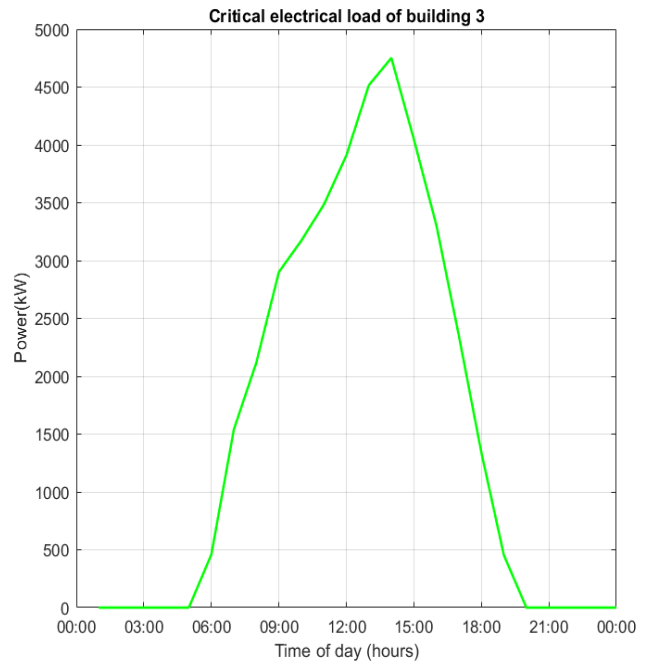


Fig. 40. Non critical electrical load of building 3

It is observed that non-critical electrical loads are shifted to time periods of low electricity price is low, in order to contribute to the minimization of microgrid's total operation cost while satisfying all the operational constraints, at the same time. Specifically, the algorithm shifts the electrical loads of the high electricity time period 07:00-09:00 to the low electricity price time period 13:00-15:00 of. This behavior is generally observed in all examined buildings.

The optimal power and the total energy exchange of each building electric vehicle parking lot are shown in the following figures. The results are obtained by the second level of optimization.

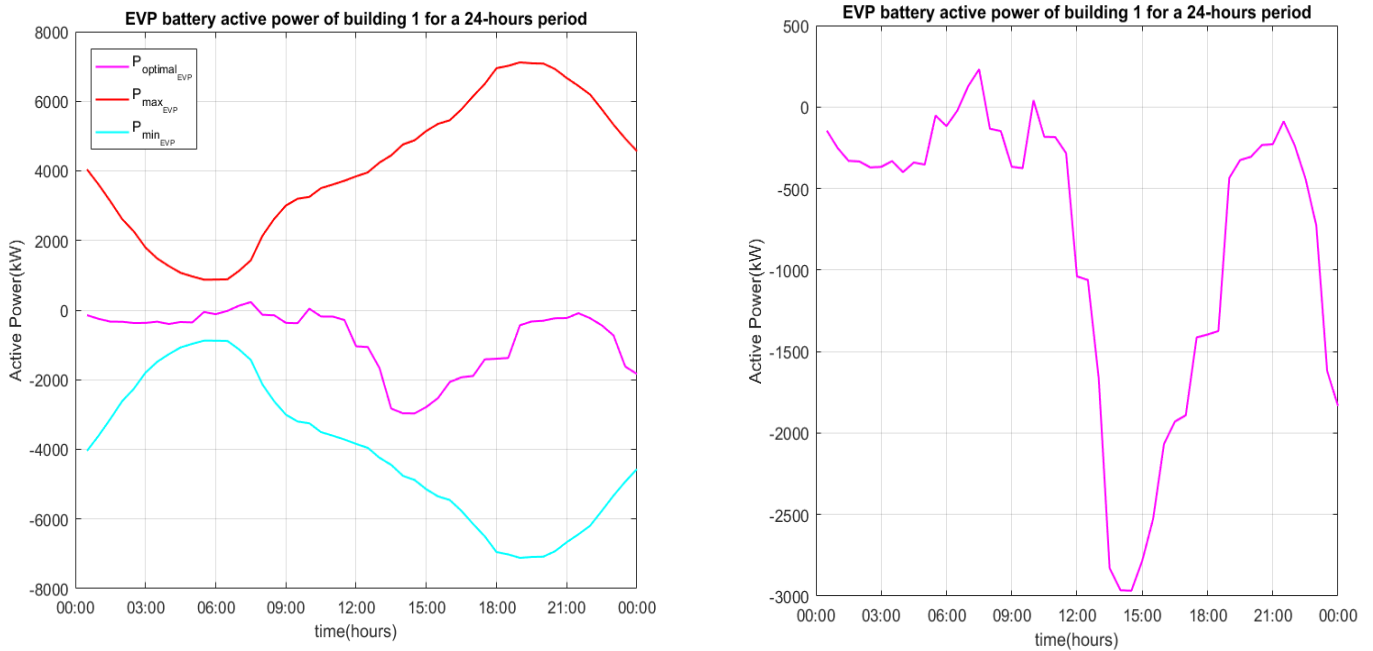


Fig. 42. Optimal active power of EVP battery of building 1

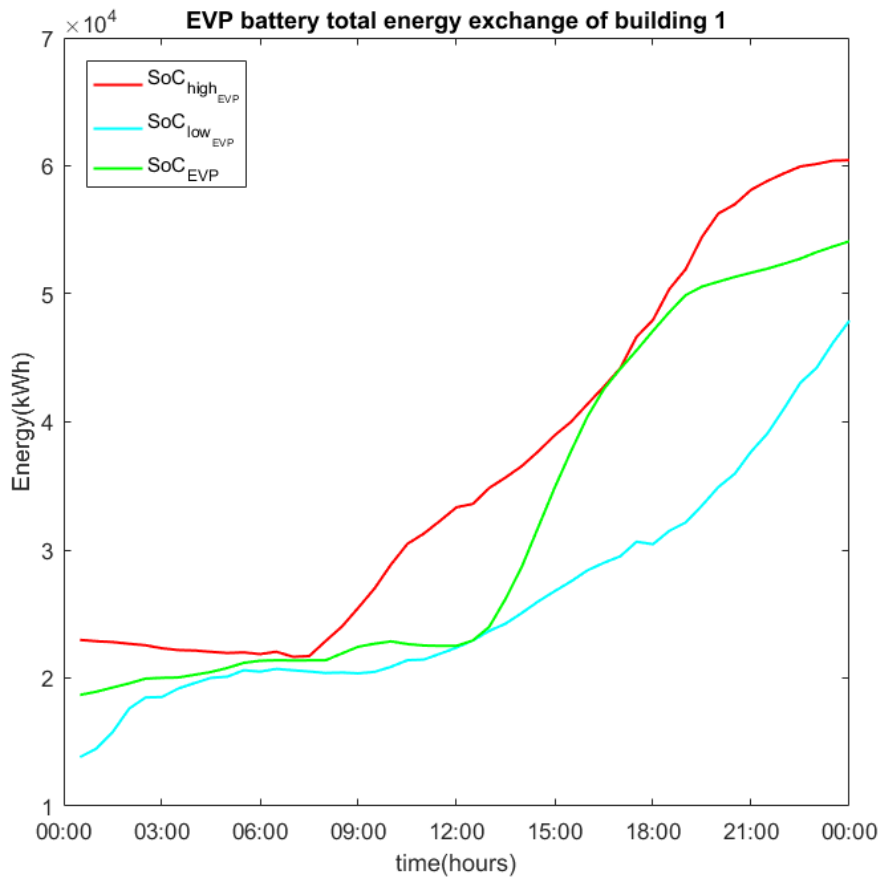


Fig. 43. EVP battery state of charge of building 1

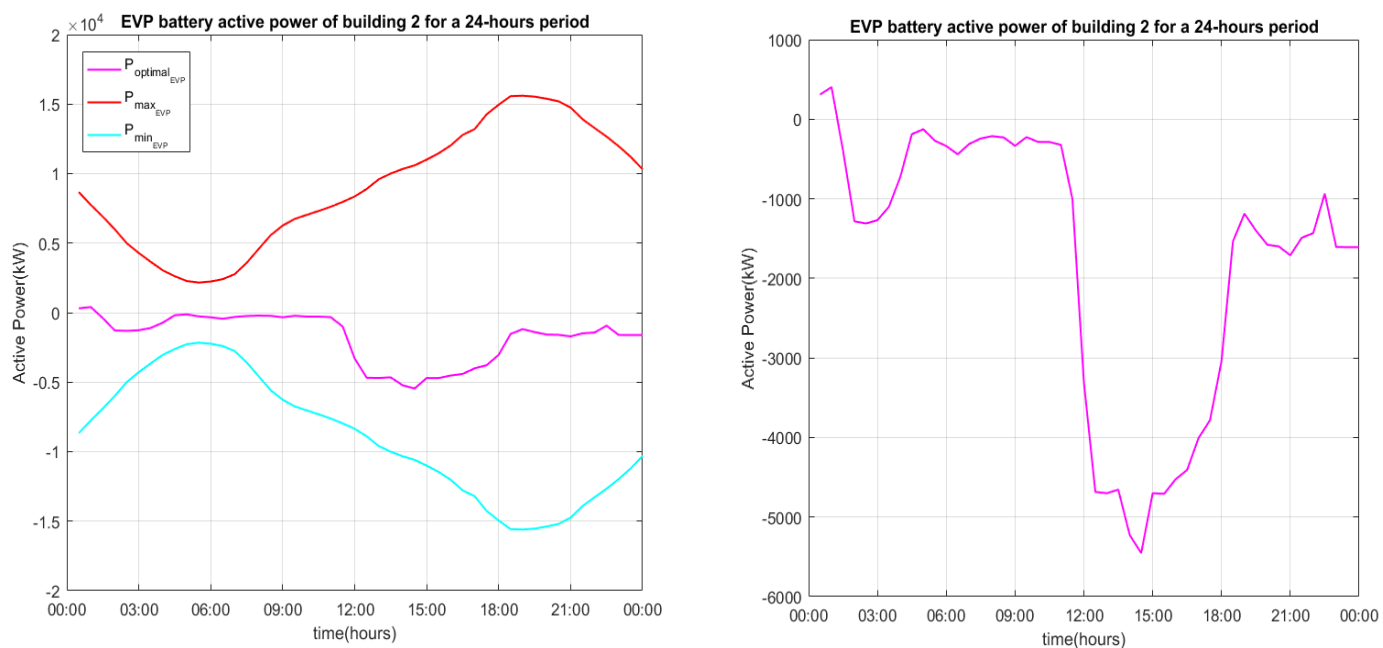


Fig. 44. Optimal active power of EVP battery of building 2

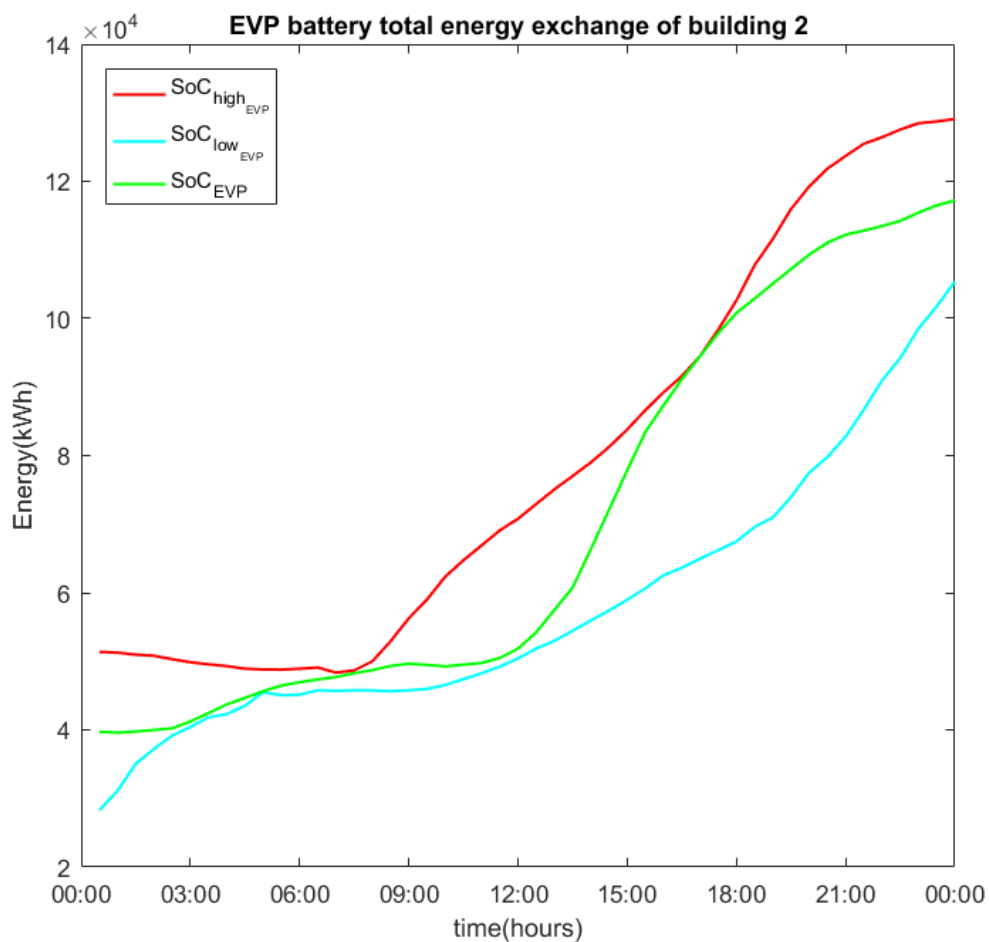


Fig. 45. EVP battery state of charge of building 2

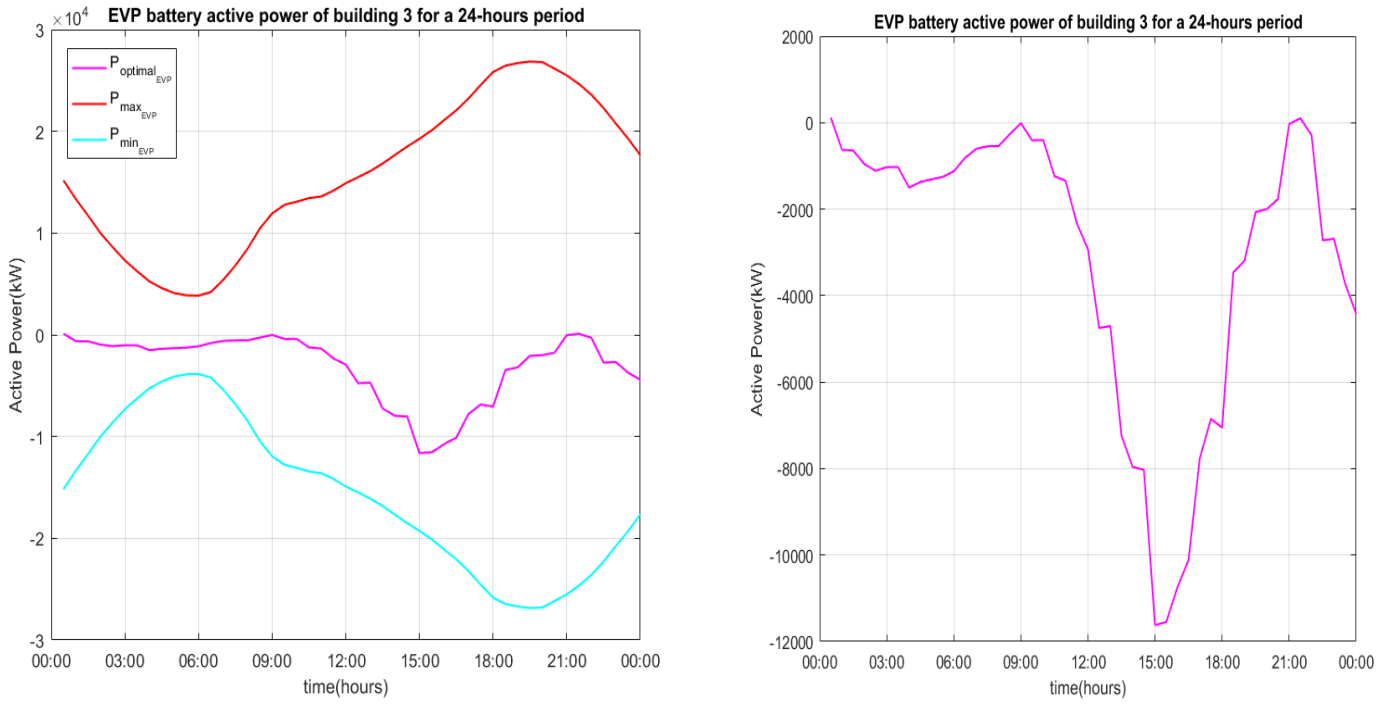


Fig. 46. Optimal active power of EVP battery of building 3

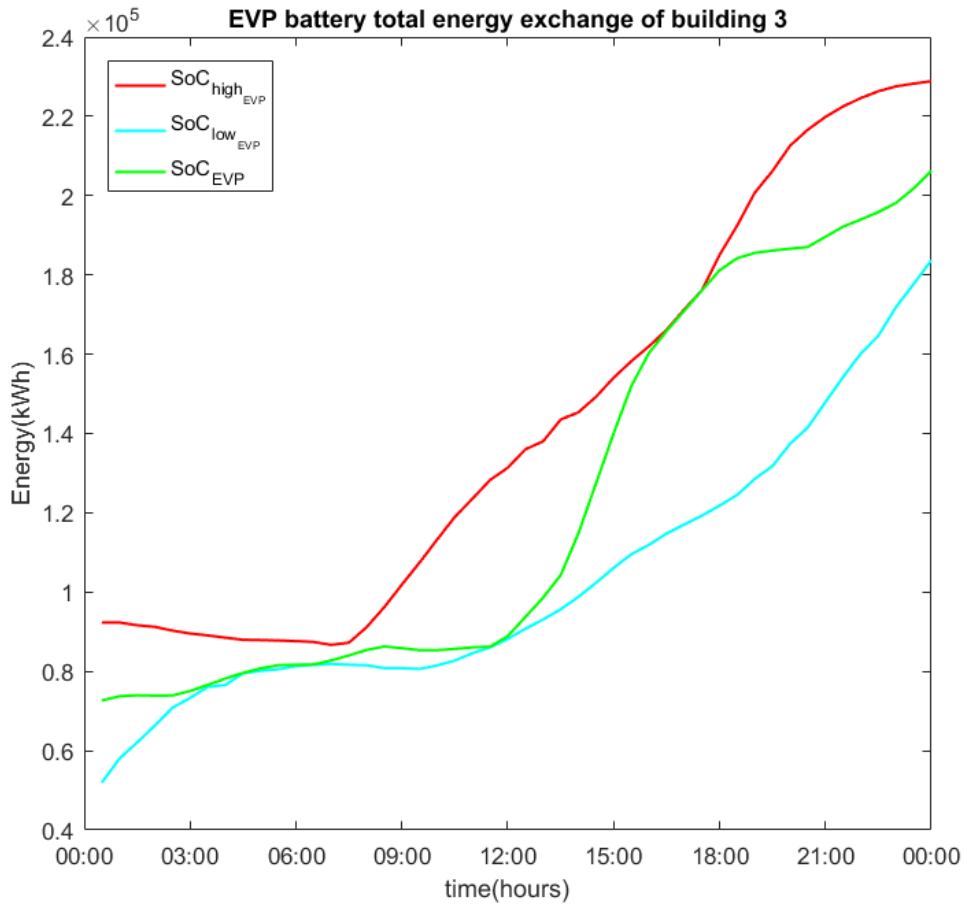


Fig. 47. EVP battery state of charge of building 3

Due to the modeling the equivalent battery using the generator convention, positive values mean that the battery is discharging (injects power to the grid), while negative values mean that the battery is charging (absorbs power from the grid).

The total energy exchange of the equivalent battery of each parking lot of the microgrid, as well as the respective upper and the lower limits vary with time because of the continuously changing number of connected EVs during the day and the change of the charging power according to electricity price variations. It is observed that in all examined cases for each one of the three buildings, the proposed algorithm intensively stores energy in time periods of low electricity price e.g., at 15:00 and injects power to the electric grid when the electricity price is high e.g., at 07:00 – 08:00, as the goal of the applied optimization strategy is to minimize the daily microgrid operation cost while satisfying all the constraints of the PEVs.

The total microgrid operation cost obtained for Scenario I is 19605(*m. u.*).

### 6.2.2. Scenario II

Scenario II includes the microgrid autonomous operation capability in addition to the characteristics of scenario I. It is assumed a power supply interruption from the electric grid takes place during 15:00 – 18:00. At this specific time period of the day, the microgrid should cover the total cooling power consumption and at least 70% of its total electric power demand, so as the crucial microgrid processes are allowed to take place. More specifically, at the time periods of the day that the microgrid operates autonomously, each electric vehicle parking lot supplies the respective predefined building loads.

The optimal power consumption and the total energy exchange of each building electric vehicle parking lot are shown in the following figures. The results obtained by the second level of optimization taking into consideration the microgrids autonomous capability.

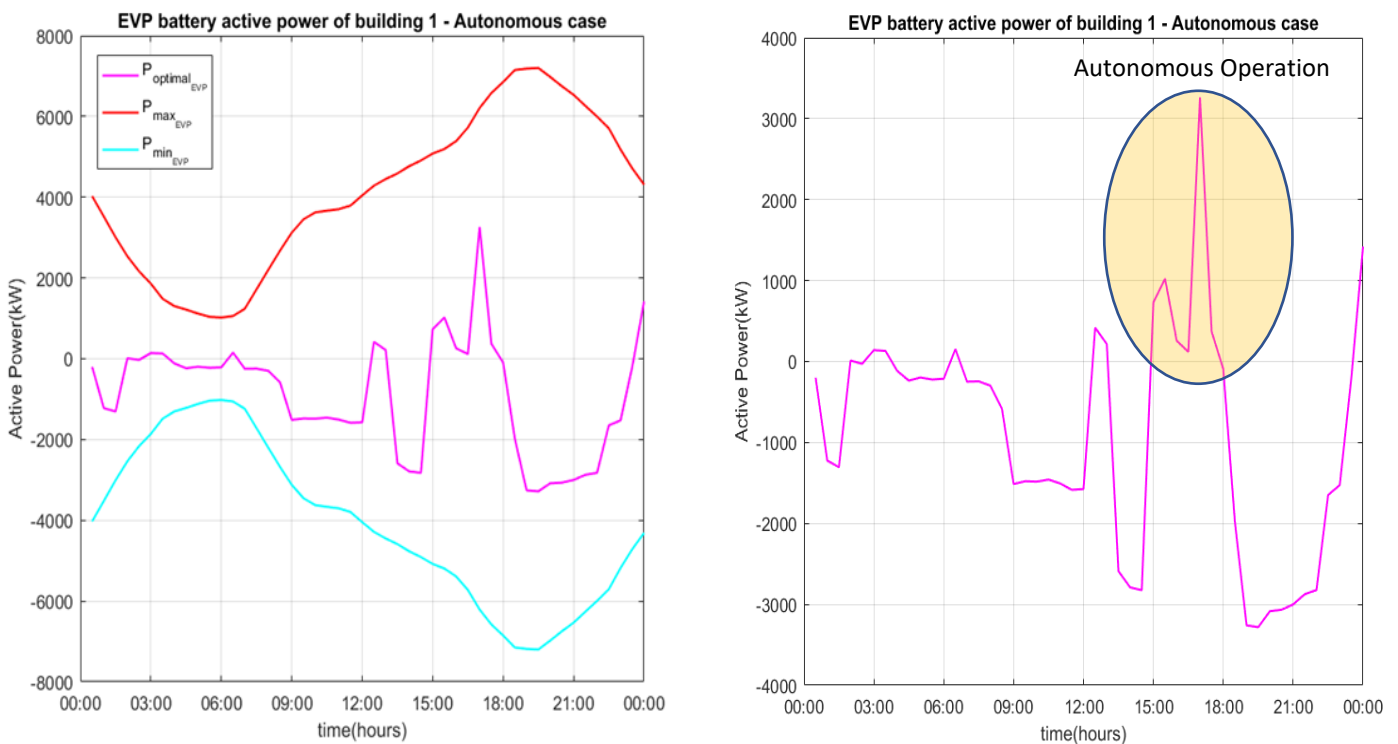


Fig. 48. Optimal active power of EVP battery of building 1-Scenario II

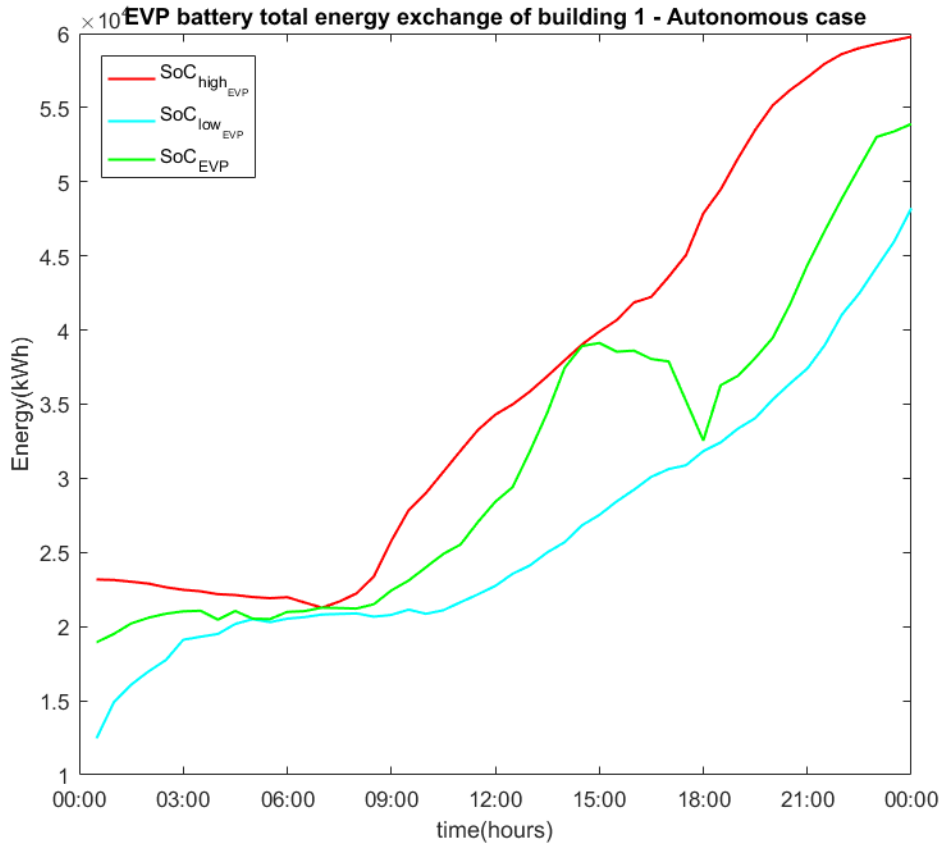


Fig. 49. EVP battery state of charge of building 1-Scenario II

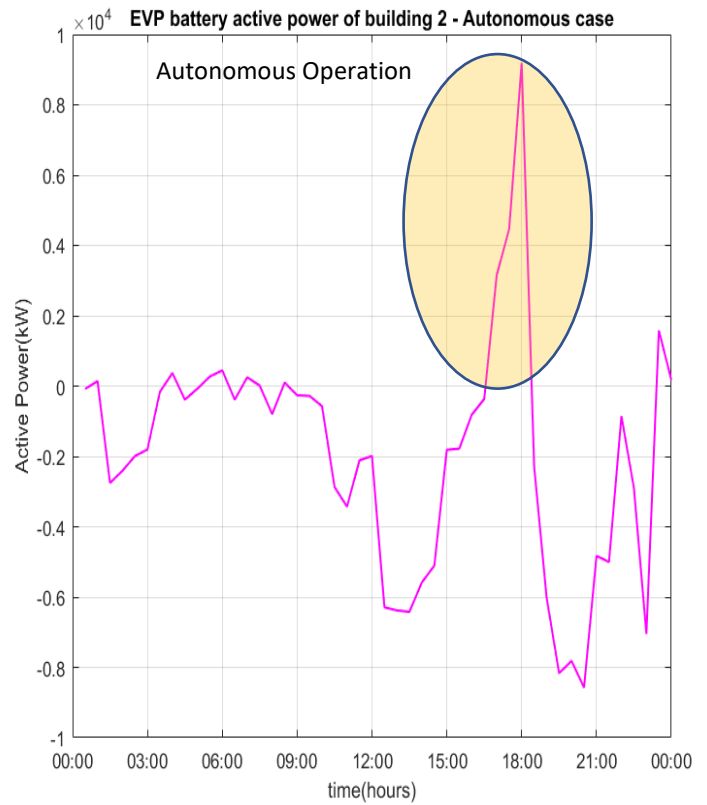
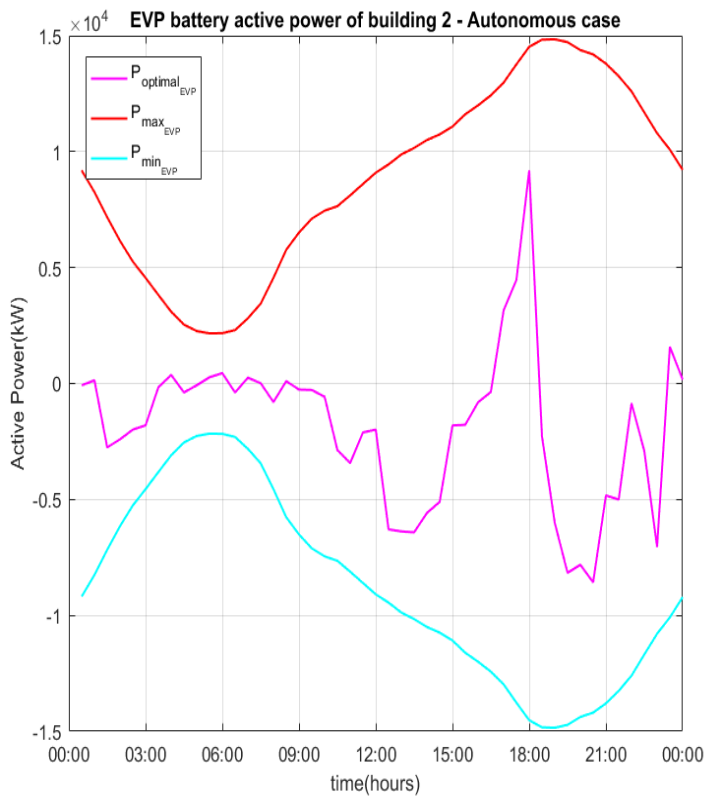


Fig. 50. Optimal active power of EVP battery of building 2-Scenario II

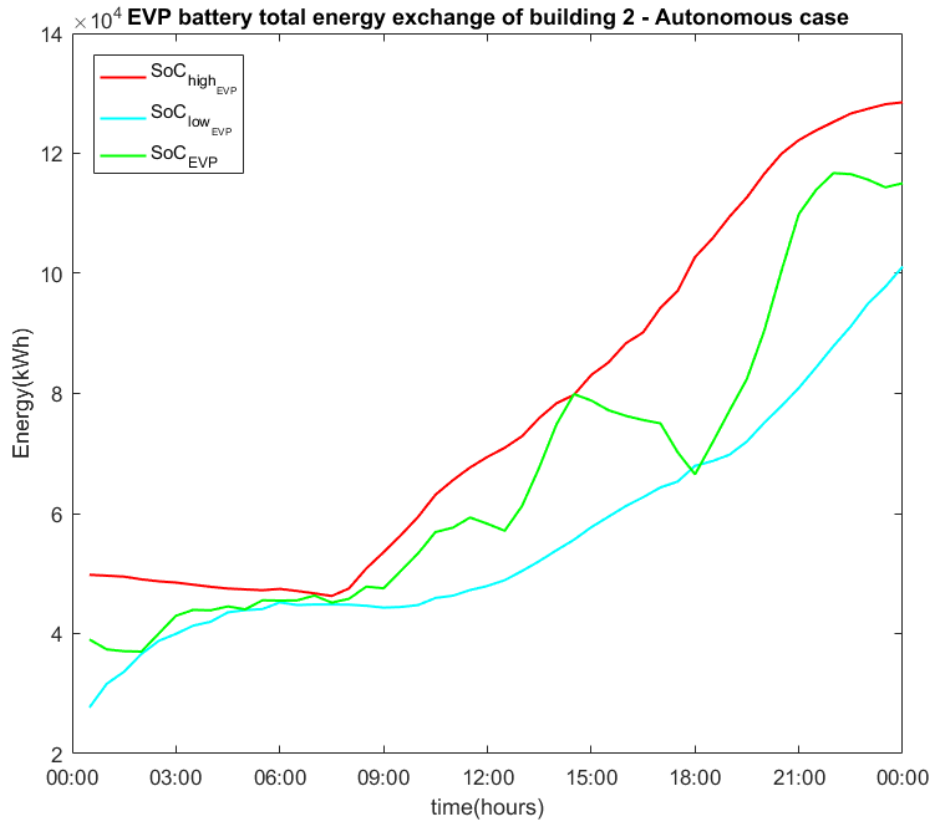


Fig. 51. EVP battery state of charge of building 2-Scenario II

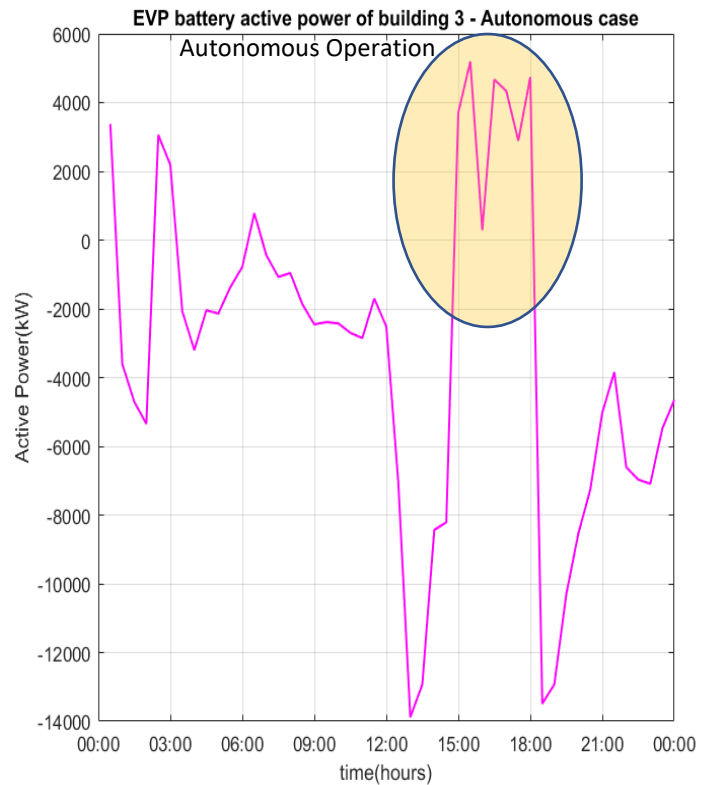
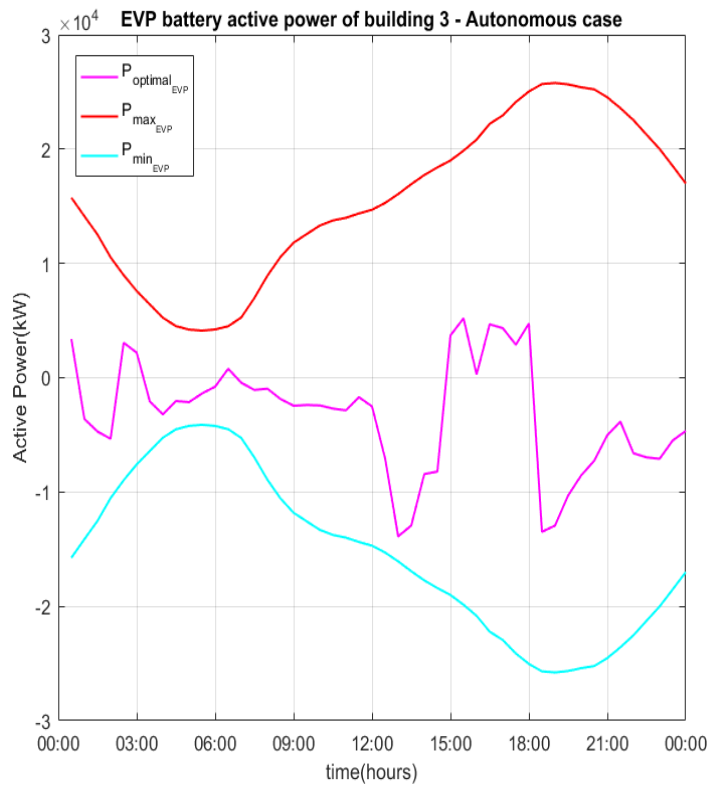


Fig. 52. Optimal active power of EVP battery of building 3-Scenario II

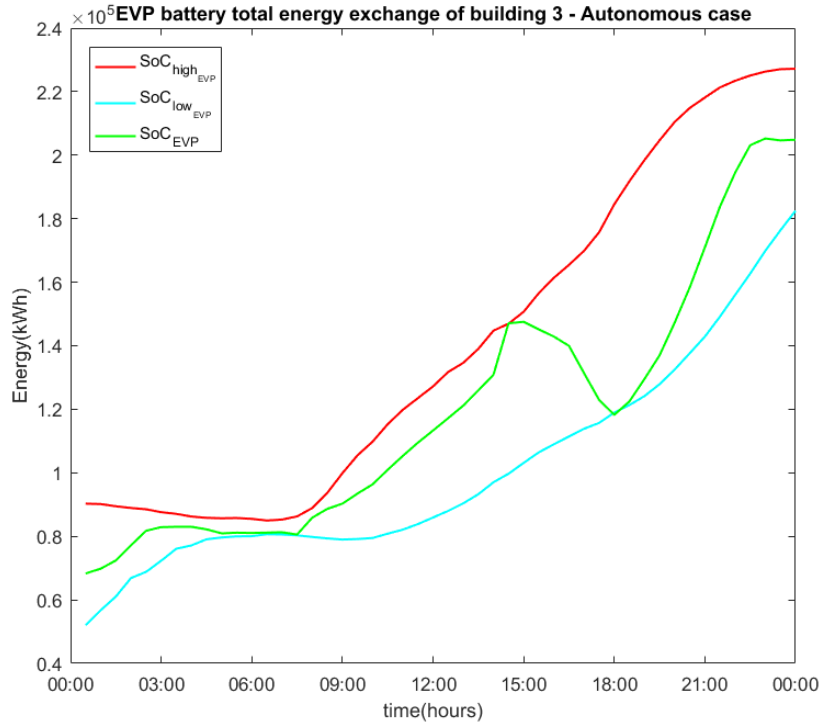


Fig. 53. EVP battery state of charge of building 3-Scenario II

From the figures above, it is observed that the lower limit of the total energy exchange has been increased at the time period by the proposed energy management algorithm in scenario II compared to scenario I so that the microgrid can operate autonomously. It is obvious that the main goal of the algorithm in Scenario II is to cover the microgrid’s energy demand and then to minimize its operation cost. This is necessary to ensure that the microgrid receives the electric energy it requires at the least for its essential operations, during grid power supply outage at the time period 15:00 – 18:00. The microgrid’s energy storage systems are forced to purchase excess energy from the electric grid prior to the grid power supply interruption in order to ensure the necessary energy is stored during the grid outage. Obtained results shown that all PEVs managed to reach their energy target without violating any operation or technical constraint. In Scenario II, there is an increase in microgrid’s operation cost with regard to Scenario I, as it was expected. The total operation cost for Scenario II is 24052(*m. u.*).

### 6.2.3. Scenario III

In scenario III, optimal operation of building HVAC systems, electrical loads and electrical vehicles parking lots are not considered. The goal of the algorithm in Scenario I and II was the minimization of HVAC system operation cost provided that the indoor temperature of all thermal zones is maintain between minimum and maximum values. However, the internal temperature of the thermal zones is maintained close to a constant set-point in Scenario III. This set point corresponds to the median internal temperature obtained in Scenario I in order to fairly compare the two operation scenarios. Furthermore, the non-critical electrical loads are not shifted optimally in time.

The differential equation of the PI controller used for each thermal zone to stabilize the internal temperature at the predetermined reference temperature is the following:

$$Q_{EC,j}(t) = K_P \cdot e(t) + K_I \cdot \int e(t) \cdot dt \tag{61}$$

$$e(t) = T_{in,j}(t) - T_{ref} \tag{62}$$

Electric Vehicles’ parking lots are also considered in this Scenario. In contrast with Scenarios I and II where the EVs are optimally charged/discharged depending on the forecasted values of electricity price, in Scenario III, they are in a “dump” charging mode. The PEVs absorb the constant amount of active power required to reach the SoC target at the time it is scheduled to be unplugged from the electric network. The constant power absorbed by the EVs is calculated as it follows:

$$P_{dump}(i) = \frac{SoC_0(i) - SoC_{target}(i)}{t_f(i) - t_0(i)} \tag{63}$$

This scenario was examined in order to calculate the cost of a common microgrid today not applying sophisticated energy management techniques as the proposed and compare it to the results obtained by the proposed energy management method.

The internal temperatures of the thermal zones and the total cooling electric power demand of each building of the microgrid are shown in Figs. (54)-(56) and Figs. (57)-(59), respectively. The electrical critical and non-critical electrical loads are shown in Fig. (60) for building 1, Fig. (61) for building 2 and Fig. (63) for building 3.

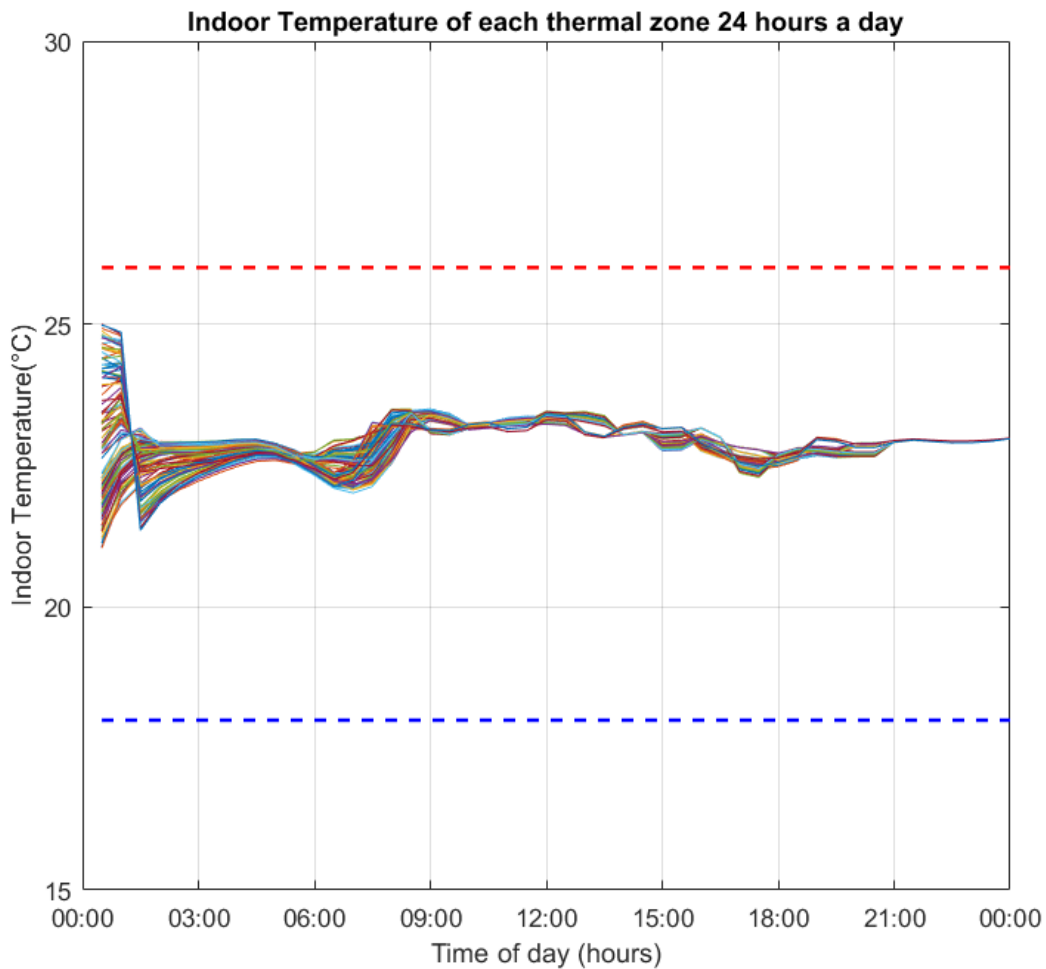


Fig. 54. Indoor temperature of 1<sup>st</sup> building’s thermal zones

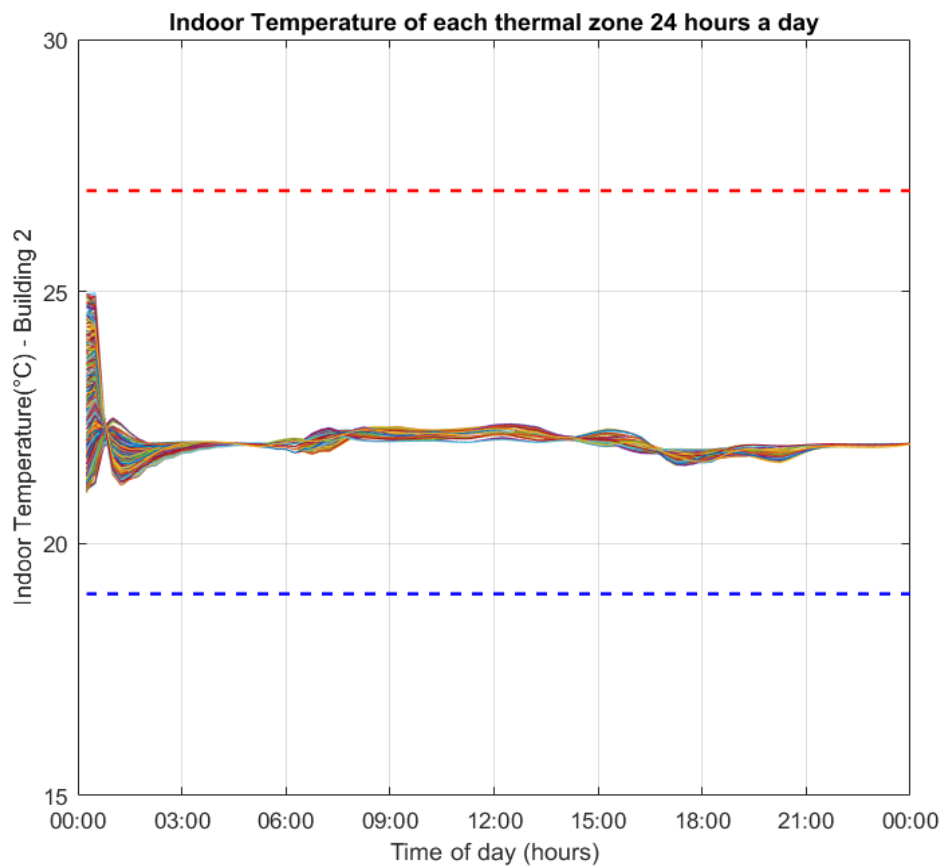


Fig. 55. Indoor temperature of 2<sup>nd</sup> building's thermal zones

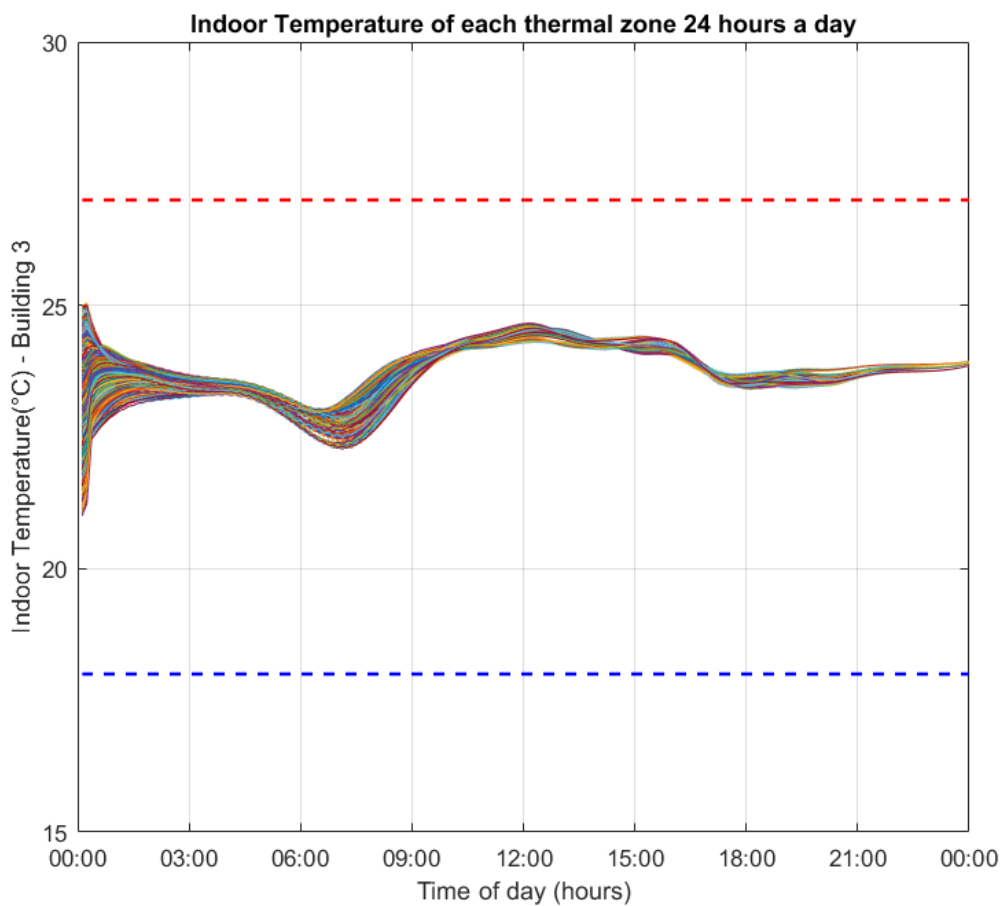


Fig. 56. Indoor temperature of 3<sup>rd</sup> building's thermal zones

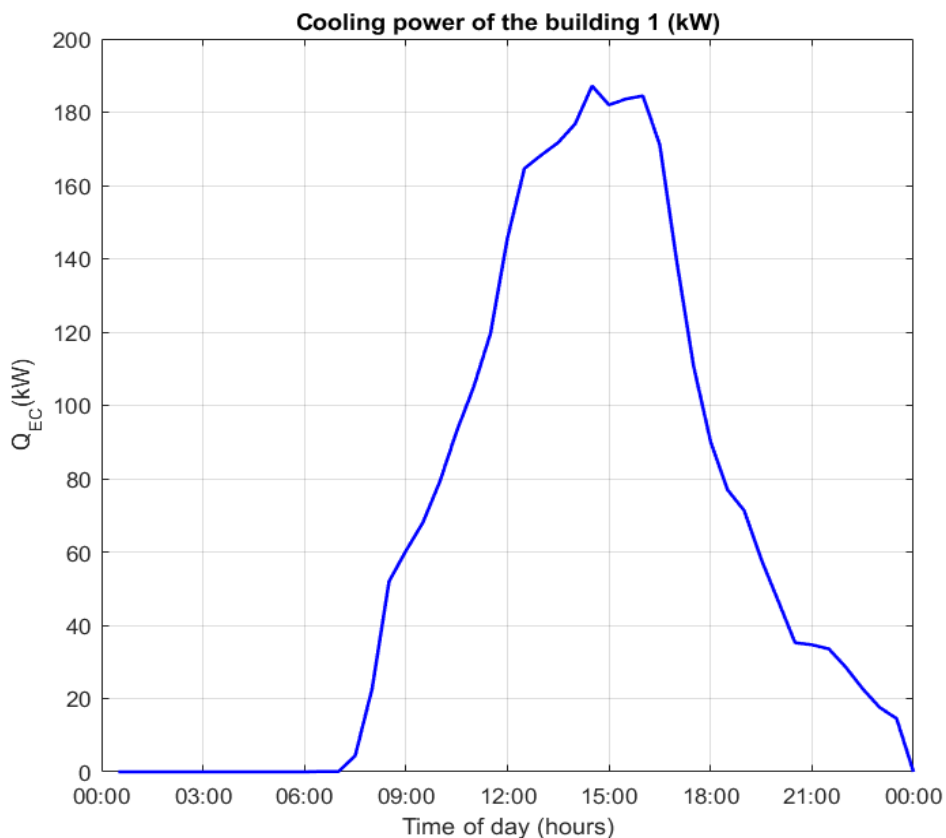


Fig. 57. Cooling power consumption of building 1

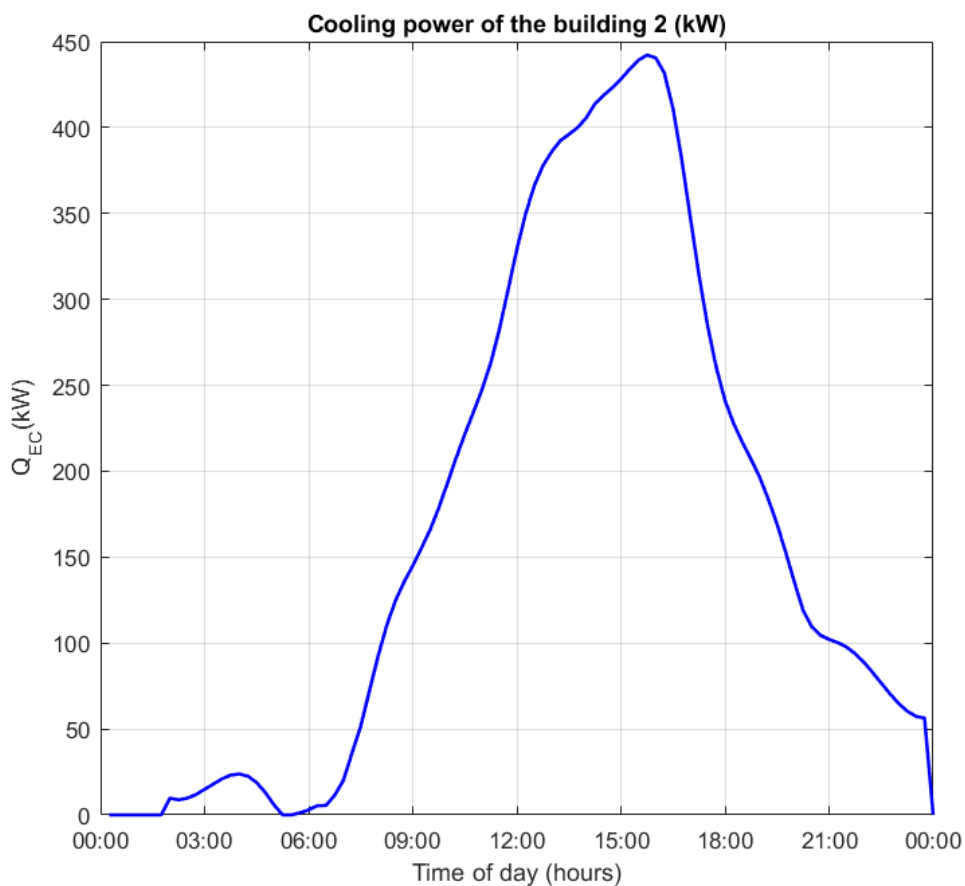


Fig. 58. Cooling power consumption of building 2

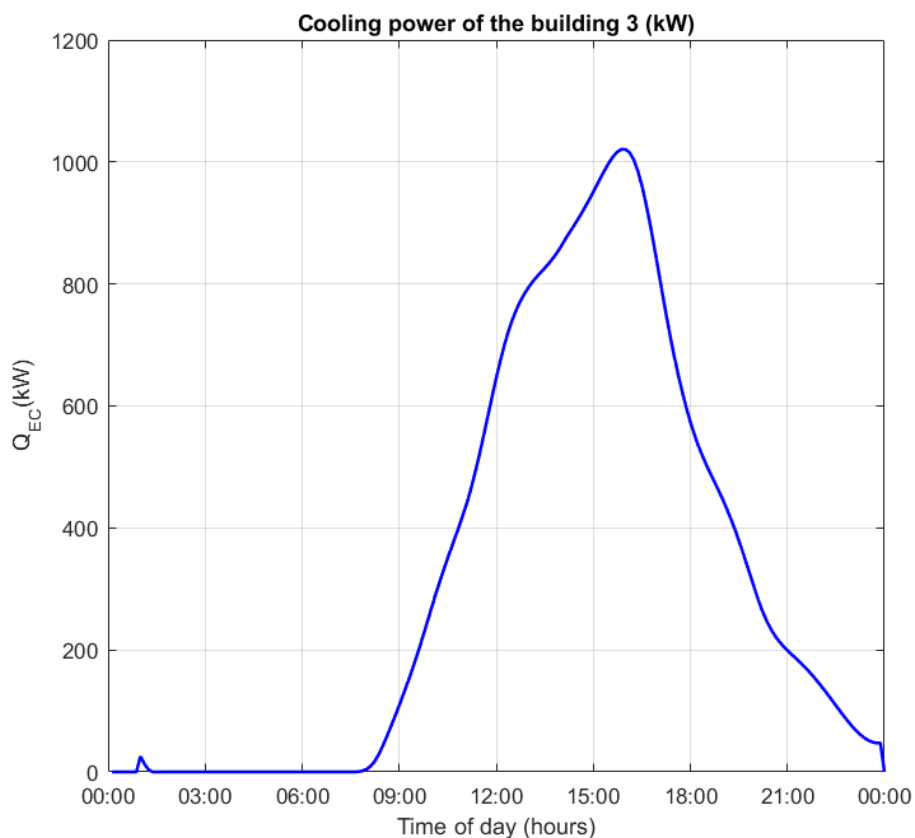


Fig. 59. Cooling power consumption of building 3

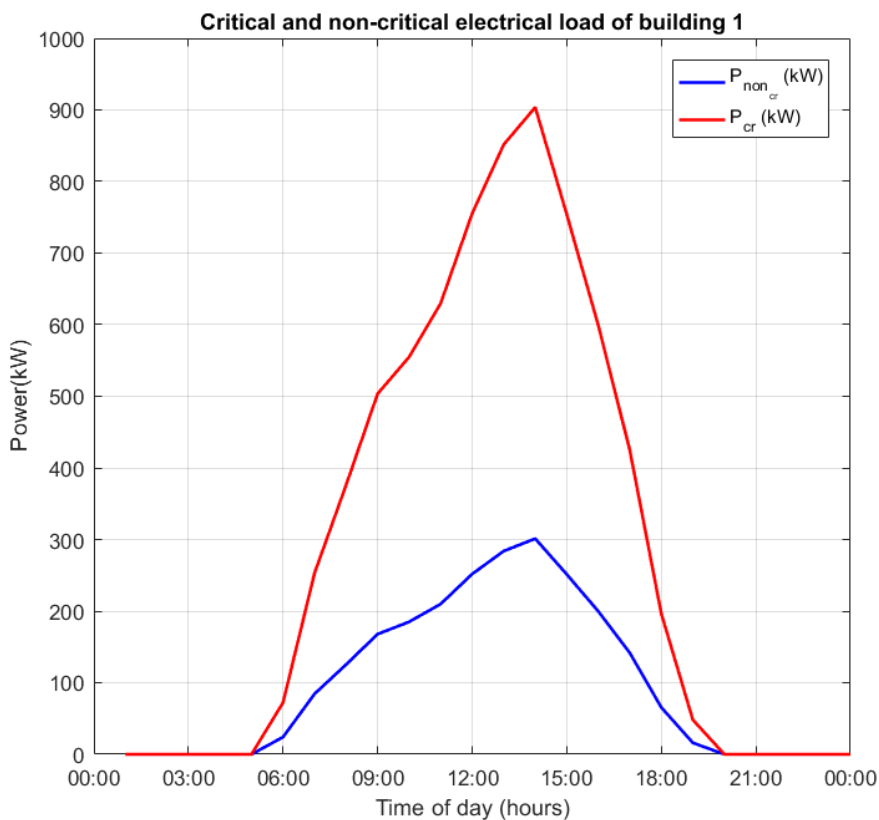


Fig. 60. Critical and non-critical electrical loads of building 1

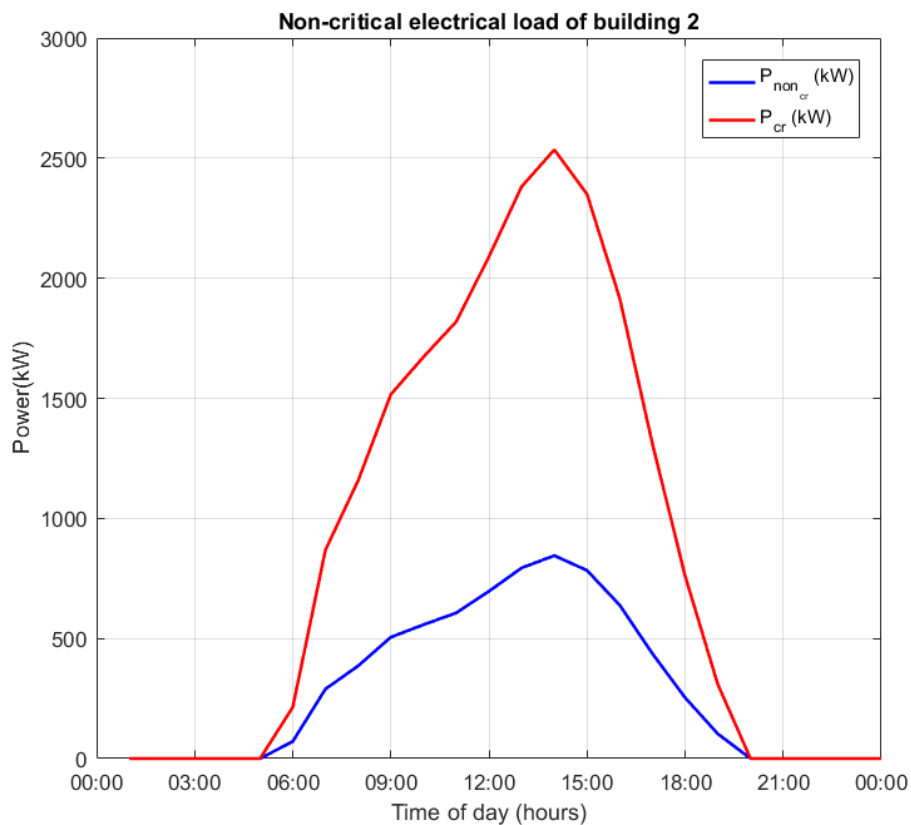


Fig. 61. Critical and non-critical electrical loads of building 2

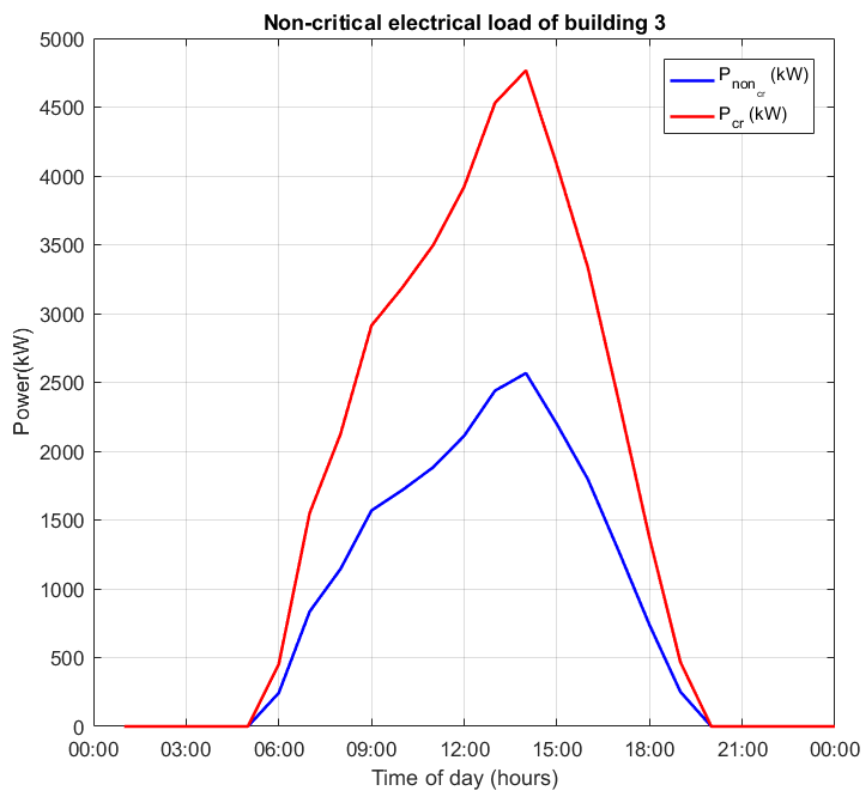


Fig. 62. Critical and non-critical electrical loads of building 3

The power consumption and the total energy exchange of each building electric vehicle parking lot are shown in the following figures.

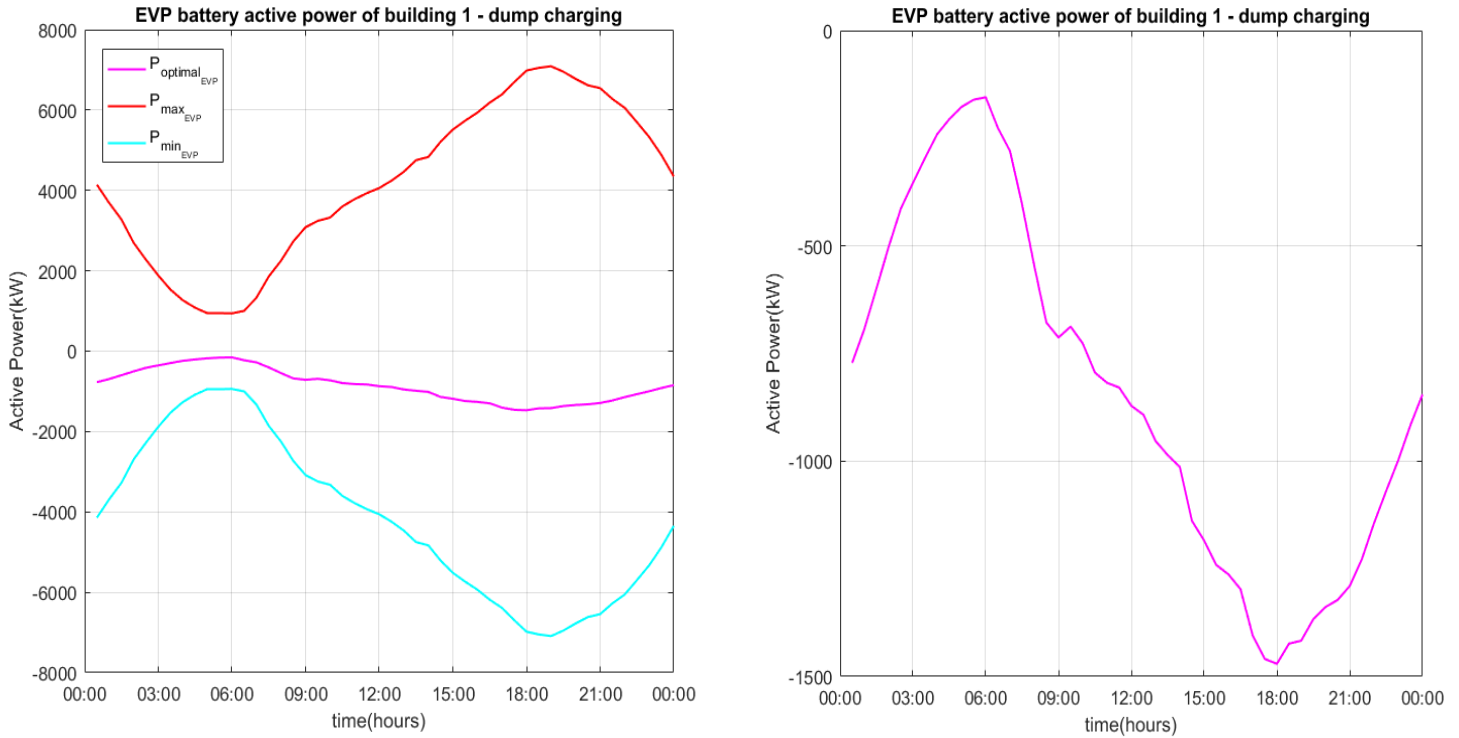


Fig. 63. Active power of EVP battery of building 1 - "dump" charging

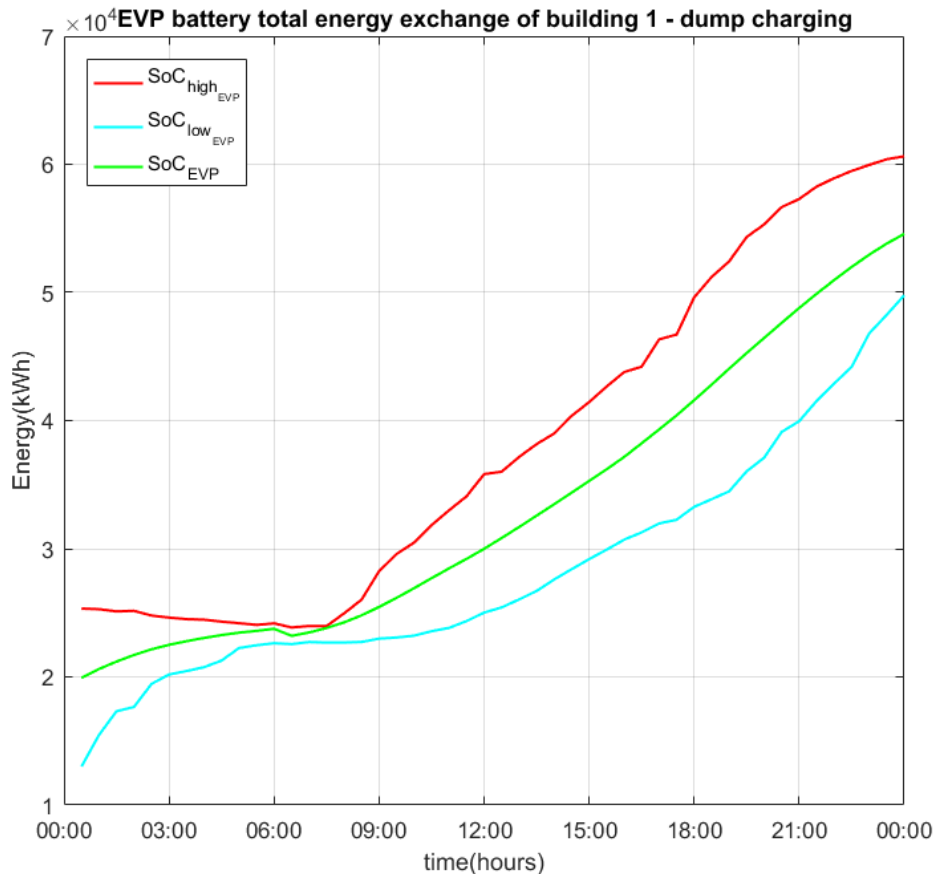


Fig. 64. EVP battery state of charge of building 1-Scenario III

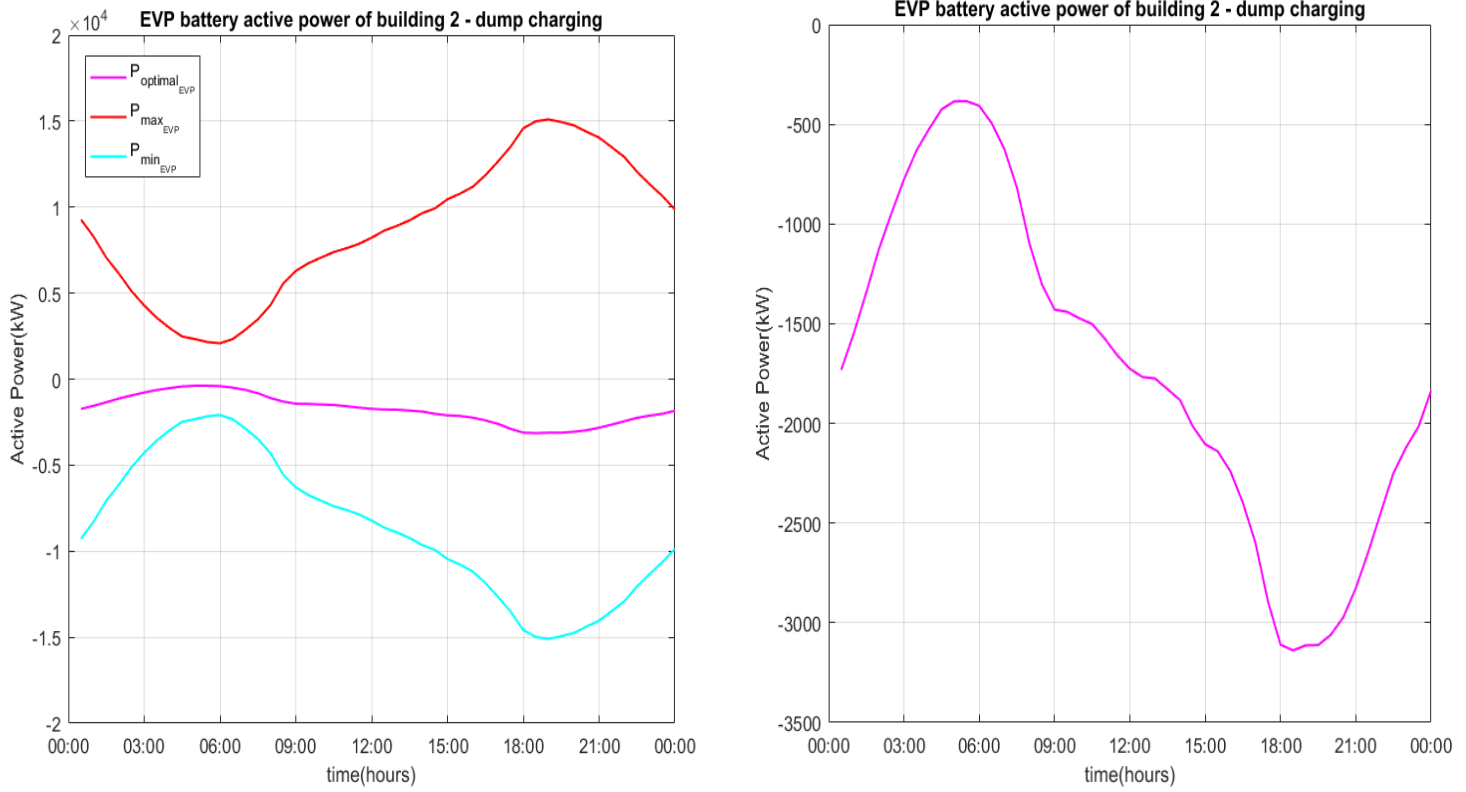


Fig. 65. Active power of EVP battery of building 2 - "dump" charging

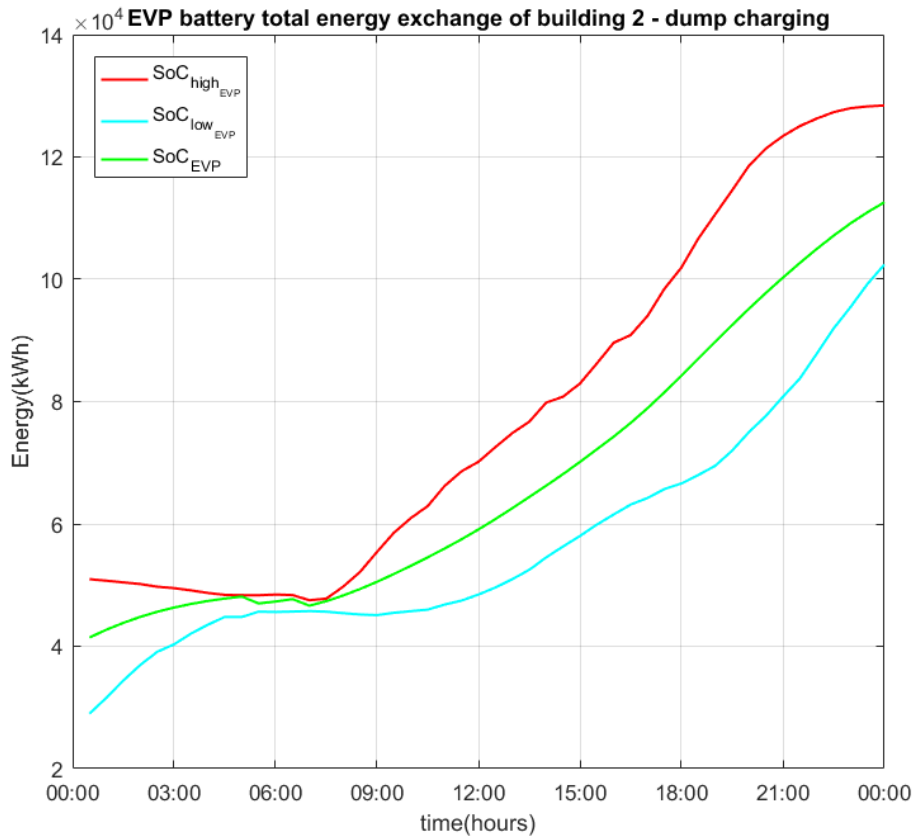


Fig. 66. EVP battery state of charge of building 2-Scenario III

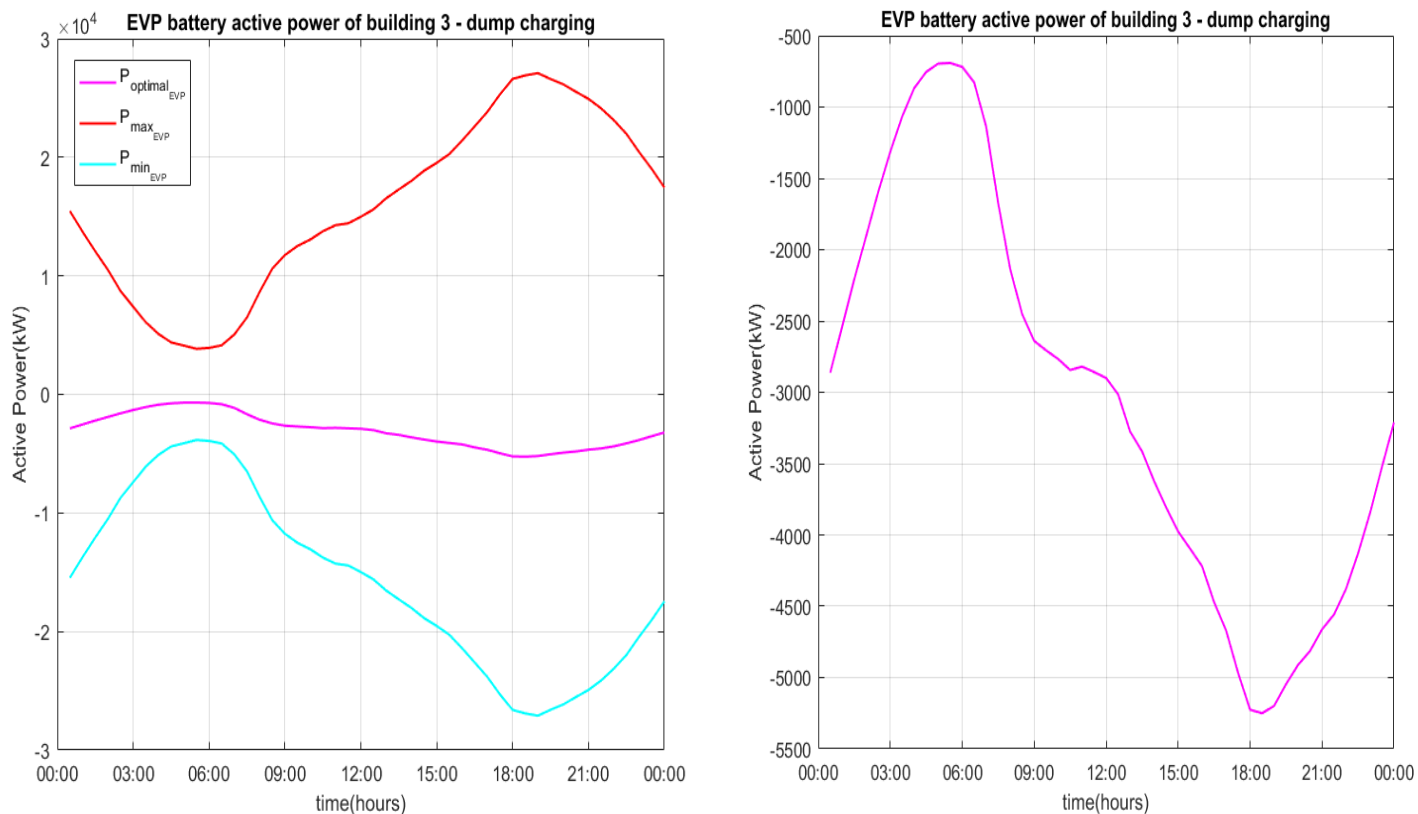


Fig. 67. Active power of EVP battery of building 3 - "dump" charging

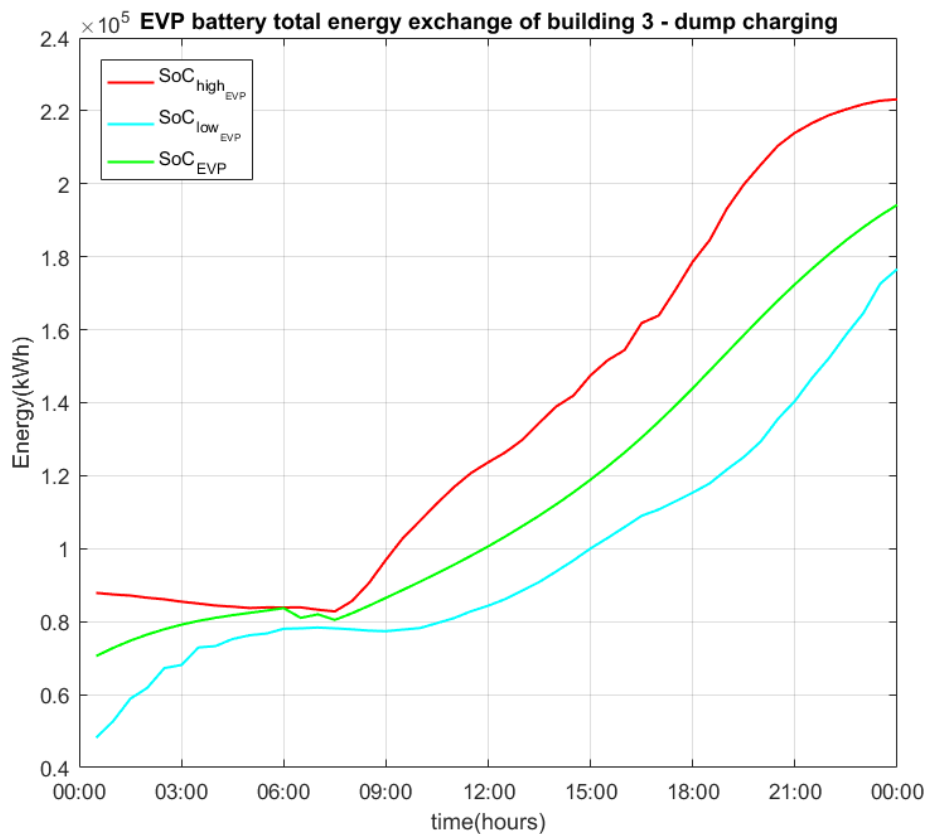


Fig. 68. EVP battery state of charge of building 3-Scenario III

In scenario III, PEV's operation does not depend on electricity price variations. They absorb a constant amount of power from the electric grid in order to reach their SoC target. This means that the total power of each parking lot takes only negative values (generator convention) as it can be easily observed from the previous figures. The total microgrid operation cost obtained for Scenario III is 26028(m.u.). It is obvious that the microgrid's operation cost is significantly increased with regard to Scenario I.

TABLE II: MICROGRID OPERATION COST

<b>Scenario</b>	<b>I</b>	<b>II</b>	<b>III</b>
Daily operation cost (m.u.)	19605	24052	26028

We observe that the daily operation cost of Scenario II is close to the one of scenario III. This is due to the fact that the autonomous operation period of the microgrid in scenario II is 15:00-18:00, where the electricity price takes its lowest price during the day. In the case of the optimization in scenario I, the electric vehicles parking lots absorb a large amount of power from the electric grid in this time period, while in scenario II, the electric vehicles parking lots inject power to the microgrid in order to cover its energy needs although the price of electricity is very low. Moreover, they absorb a large amount of energy during periods of high electricity price. If the autonomous microgrid operation period was different during the examined day and in which the price of electricity was high, a smaller increase of the microgrid's operation cost would be observed between scenarios I and II.

## **7. CONCLUSION**

---

In this thesis, a method that optimizes the operation of microgrids of complexes of large buildings is proposed. The proposed algorithm was applied to a microgrid consisting of large office buildings using realistic input data. Optimal operation of building HVAC systems, optimal time-shifting of non-critical electrical loads and optimal scheduling of the power exchanged by the PEVs with the electric grid are performed. At the same time, all technical and operation constraints of all microgrid's components are satisfied. The obtained simulation results prove that a significant reduction in total daily microgrid's operation cost of about 27% with regard to the typical operation of a microgrid today is possible.

To extend the scope of this thesis in the future, a real-time HVAC operation method could be integrated to the proposed one in order to efficiently deal with the uncertainties that arise from the forecasts of stochastic quantities such as electricity price, human and electric vehicle activity. Furthermore, except for large office buildings considered in this work, large residential buildings could also be modeled, as the characteristics of the thermal zones and the energy needs differ. More specifically, in the office buildings the thermal zones have large dimensions and dense presence and activity of people during the day, while the dimensions of the residential buildings are smaller and the presence of people is generally sparse. Also, the electrical devices used in these two types of buildings differ from each other and as a result the thermal and electrical loads differ, respectively. In future work, reactive power management could also be considered. Finally, instead of considering the large electric vehicle parking lots as the only power source during grid outages, additional production units could be included, such as microturbines, diesel generators, PV panels and wind generators.

## 8. REFERENCES

---

- [1] G. K. Farinis and F. D. Kanellos, "Integrated energy management system for Microgrids of," *Electric Power Systems Research*, vol. 198, September 2021.
- [2] J. Xiaolong, W. Jianzhong, M. Yunfei, W. Mingshen, X. Xiandong and J. Hongjie, "Hierarchical microgrid energy management in an office building," *Applied Energy*, vol. 208, pp. 480-494, December 2017.
- [3] J. Xiaolong, M. Yunfei, J. Hongjie, W. Jianzhong, T. Jiang and Y. Xiaodan, "Dynamic economic dispatch of a hybrid energy microgrid considering," *Applied Energy*, vol. 194, pp. 386-398, May 2017.
- [4] F. D. Kanellos, "Optimal Scheduling and Real-Time Operation of Distribution Networks With High Penetration of Plug-In Electric Vehicles," *IEEE SYSTEMS JOURNAL*, vol. 15, no. 3, pp. 3938 - 3947, September 2021.
- [5] "Why the Future of Driving is Electric. Available online: <https://evolveetfs.com/2018/11/why-the-future-of-driving-is-electric/>".
- [6] "A. Santos et al., "Summary of travel trends: 2009 National Household Travel Survey," U.S. Dept. Transp., Federal Highway Admin., Washington, DC, USA, Tech. Rep. FHWA-PL-11-022, 2011. [Online]. Available:<http://nhts.ornl.gov/2009/pub/stt.pdf>".
- [7] "TYPES OF ELECTRIC VEHICLES. Available Online: <https://www.acecwi.com/types-of-electric-vehicles/>".
- [8] "Advantages of electric cars – top benefits of EVs. Available Online : <https://www.energysage.com/electric-vehicles/advantages-of-evs/>".
- [9] "LITHIUM-ION BATTERY. Available online: <https://www.cei.washington.edu/education/science-of-solar/battery-technology/>".
- [10] "Lead Acid Batteries. Available Online: <https://www.pveducation.org/pvcdrom/batteries/lead-acid-batteries>".
- [11] "Flow Batteries. Available Online: <https://flowbatteryforum.com/what-is-a-flow-battery/>".
- [12] "Hydrogen Fuel Cells. Available Online: <https://www.energy.gov/eere/fuelcells/fuel-cells>".

- [13] "High-power ultracapacitor energy storage solutions based on breakthrough graphene material. Available Online: <https://www.skeletontech.com/ultracapacitor-technology>".
- [14] "Challenges Faced during Microgrid Implementation. Available online: <https://www.phoenixenergygroup.com/blog/challenges-faced-during-microgrid-implementation>".
- [15] "Features and Benefits About Microgrids. Available Online: <https://www.districtenergy.org/microgrids/about-microgrids97/features>".
- [16] "Microgrids. Available Online: <https://www.c2es.org/content/microgrids/>".
- [17] Y. E. G. Vera, R. Dufo-López and J. L. Bernal-Agustín, "Energy Management in Microgrids with Renewable Energy Sources: A Literature Review," *Applied Sciences*, vol. 9, no. 18, 2019.
- [18] A. Elmouatamid, R. Ouladsine, M. Bakhouya, N. E. Kamoun, M. Khaidar and K. Zine-Dine, "Review of Control and Energy Management Approaches in Micro-Grid Systems," *Energies*, vol. 14, no. 1, 2021.
- [19] L. I. Dulau, M. Abrudean and D. Bica, "Distributed Generation and Virtual Power Plants," *Conference: 2014 49th International Universities Power Engineering Conference (UPEC)*, September 2014.
- [20] S. A. Roosa, "Microgrid Architecture," *International Journal of Strategic Energy and Environmental Planning*, vol. 2, no. 5, 2020.